

**Feasibility Study of Human Lumbar Motion using Variability Techniques**

by

Yuvraj M. Pawar

A thesis submitted to the Graduate Faculty of  
Auburn University  
in partial fulfillment of the  
requirements for the Degree of  
Master of Science

Auburn, Alabama  
May 9, 2011

Copyright 2011 by Yuvraj M. Pawar

Approved by

P. K Raju, Chair, Thomas Walter Professor of Mechanical Engineering  
Maruti Ram Gudavalli, Associate Professor, Palmer Center for Chiropractic research, IA  
Dan Marghitu, Professor of Mechanical Engineering

## Abstract

More than 80 percent of people suffer from low back pain at some point in their lifetime. It is one of the most prevalent musculoskeletal disorders in the United States. The pain can be short-lived or long-lasting. In either case, low back pain can make many daily activities difficult to perform. Even though it is one of the most studied disorders, the etiology of low back pain is still unknown. Kinematics and kinetics of body movements can be affected by low back pain and may result in spinal instability. Previous studies have quantified this spinal stability using linear and nonlinear motion analysis techniques. The purpose of this study was to obtain the variation in kinematics of healthy volunteer subjects using these two techniques while the volunteer subjects are performing the lumbar movement during flexion-extension while sitting on an unstable surface. In addition, a second objective was to study the variation on a cadaveric specimen during flexion and extension motions.

Five healthy volunteers performed repetitive trunk flexion and extension movements while sitting on an unstable surface with different starting positions (forward, neutral, and backward) and two different movement initiation (forward and backward) directions. The cadaveric specimen was subjected to flexion-extension movements at different speeds. Traditional linear techniques such as mean, standard deviation, and coefficient of variation, along with nonlinear technique such as approximate entropy, were calculated from measured trunk kinematics to estimate the variability of the human motions.

The average values for the motions had a range from 10.556 degrees to 26.101 degrees. The standard deviation values had a range from 1.941 to 3.278. The coefficients of variation had a range from 7.258 to 26.597. The Approximate Entropy values had a range from 0.209 to 0.274.

To the best of the authors' knowledge this is the first study to determine the variability of sitting motions on an unstable surface using approximate entropy. Linear and nonlinear dynamic systems analyses were successfully applied to trunk flexion-extension data, which can serve as control data for further studies and understanding kinematics and kinetics of low back pain patients.

## Acknowledgments

I would like to express my sincere gratitude to my research advisors, Dr. P. K. Raju and Dr. Maruti Ram Gudavalli, for their invaluable guidance and help during the course of this study. I would like to specially thank Dr. Dan Marghitu for helping me with nonlinear techniques and being part of my committee.

I would like to acknowledge and extend my gratitude for the financial support received from Palmer Center for Chiropractic Research in Davenport, Iowa. I would like to thank my research group at Palmer Center for useful discussions and enjoyable moments in the lab. Special thanks to Dr. Ting Xia for his excellent technical assistance. This investigation was conducted in a facility constructed with support from Research Facilities Improvement Program Grant Number C06 RR15433-01 from the National Center for Research Resources, National Institute for Health.

My research assistantship during my studies supported by Award Number U19AT004137 from the National Center for Complementary & Alternative Medicine, National Institute of Health, is highly appreciated.

I would like to thank my family for unconditional love and support throughout my graduate studies. Finally, I am thankful to all my friends and colleagues for their unconditional friendship and support.

## Table of Contents

Abstract.....	ii
Acknowledgments .....	iv
List of Tables.....	vii
List of Figures .....	viii
List of Abbreviations .....	xv
1. Introduction.....	1
1.1 Background.....	1
1.2 Traditional Linear Methods to Quantify Variability.....	4
1.3 Nonlinear Methods to Quantify Variability.....	8
1.4 Specific Objective .....	13
2. Anatomy of Lumbar Spine.....	14
2.1 Vertebral Column.....	14
2.2 Vertebrae .....	17
3. Tools and Techniques .....	19
3.1 State of System .....	19
3.2 Time Series .....	19
3.3 State Space.....	20
3.4 Phase Space.....	20
3.5 Noise in Biomechanical Data .....	33
3.6 Filters.....	33
3.7 Sample Size .....	40
4. Methodology .....	41

4.1 Instrumentations for Tests on Human Subjects .....	41
4.2 Experimental Set-up.....	43
4.3 Human Subjects .....	44
4.4 Data Acquisition .....	44
4.5 Data Analysis .....	47
4.6 Calculation of ApEn.....	51
4.7 Instrumentation for Test on Cadaver Spine .....	52
4.8 Potting the Specimen.....	56
4.9 Digitization .....	56
4.10 Data Acquisition.....	57
4.11 Data Analysis .....	58
5. Results.....	60
5.1 Human Volunteer Study.....	60
5.2 Cadaver Study.....	115
6. Discussions.....	133
7. Conclusions .....	138
References.....	141
Appendices.....	148
A. Technical Specifications .....	148
B. MATLAB Programs .....	153
C. Documentation.....	157

## List of Tables

Table 3. 1 Linear and Nonlinear Measures .....	30
Table 4. 1 Subtests.....	47
Table 5. 1 Linear and Nonlinear Measures .....	72
Table 5. 2 Linear and Nonlinear Measures .....	81
Table 5. 3 Linear and Nonlinear Measures .....	89
Table 5. 4 Linear and Nonlinear Measures .....	98
Table 5. 5 Linear and Nonlinear Measures .....	106
Table 5. 6 Linear and Nonlinear Measures .....	125
Table A. 1 Technical Specification of Polhemus Unit .....	148
Table A. 2 Technical Specifications of Optotrak 3020 Unit .....	150
Table A. 3 Technical Specifications of System Control Unit.....	151

## List of Figures

Figure 2. 1 Normal Disc .....	15
Figure 2. 2 Human Lumbar Spine .....	16
Figure 2. 3 Vertebra.....	17
Figure 2. 4 Ligaments of Spine .....	18
Figure 3. 1 Sine Wave .....	21
Figure 3. 2 Phase Plane Plot.....	21
Figure 3. 3 3-D Phase Plane Plot.....	22
Figure 3. 4 Random Data .....	22
Figure 3. 5 Phase Plane Plot.....	23
Figure 3. 6 3-D Phase Plane Plot.....	23
Figure 3. 7 Foam Strip .....	24
Figure 3. 8 Displacement, Velocity, Acceleration Diagram .....	25
Figure 3. 9 Phase Plane Plot.....	26
Figure 3. 10 3-D Phase Plane Plot.....	26
Figure 3. 11 Displacement, Velocity, Acceleration Diagram .....	27
Figure 3. 12 Phase Plane Plot.....	27
Figure 3. 13 3-D Phase Plane Plot.....	28
Figure 3. 14 Displacement, Velocity, Acceleration Diagram .....	28
Figure 3. 15 Phase Plane Plot.....	29
Figure 3. 16 3-D Phase Plane Diagram .....	29



Figure 3. 17 Mean for Foam Test.....	31
Figure 3. 18 Standard Deviation for Foam Test.....	31
Figure 3. 19 Coefficient of Variation for Foam Test.....	32
Figure 3. 20 Approximate Entropy for Foam Test.....	32
Figure 3. 21 Step Response.....	35
Figure 3. 22 Frequency Response .....	36
Figure 3. 23 Frequency Response .....	37
Figure 3. 24 Filter Frequency Response .....	38
Figure 3. 25 Acceleration using Accelerometer and Filter .....	39
Figure 4. 1 Polhemus Unit .....	42
Figure 4. 2 Subject in Test Position.....	46
Figure 4. 3 Data Export.....	48
Figure 4. 4 Optotrak SCU and Stober Units with Markers on Sensors .....	53
Figure 4. 5 Optotrak 3020 Unit .....	54
Figure 4. 6 Schematic Diagram of the Set-up.....	55
Figure 4. 7 Cadaver Test Set-up and Stylus with Markers .....	56
Figure 5. 1 Displacement Time Series with Velocity and Acceleration .....	61
Figure 5. 2 Phase Plane Plot.....	61
Figure 5. 3 3-D Phase Plane Plot.....	62
Figure 5. 4 Displacement Time Series with Velocity and Acceleration .....	62
Figure 5. 5 Phase Plane Plot.....	63
Figure 5. 6 3-D Phase Plane Plot.....	63
Figure 5. 7 Displacement Time Series with Velocity and Acceleration .....	64

Figure 5. 8 Phase Plane Plot.....	64
Figure 5. 9 3-D Phase Plane Plot.....	65
Figure 5. 10 Displacement Time Series with Velocity and Acceleration.....	65
Figure 5. 11 Phase Plane Plot.....	66
Figure 5. 12 3-D Phase Plane Plot.....	66
Figure 5. 13 Displacement Time Series with Velocity and Acceleration.....	67
Figure 5. 14 Phase Plane Plot.....	67
Figure 5. 15 3-D Phase Plane Plot.....	68
Figure 5. 16 Displacement Time Series with Velocity and Acceleration.....	68
Figure 5. 17 Phase Plane Plot.....	69
Figure 5. 18 3-D Phase Plane Plot.....	69
Figure 5. 19 Displacement Time Series with Velocity and Acceleration.....	70
Figure 5. 20 Phase Plane Plot.....	70
Figure 5. 21 3-D Phase Plane Plot.....	71
Figure 5. 22 Mean Values for Subtests.....	75
Figure 5. 23 Standard Deviation for Subtests .....	75
Figure 5. 24 Coefficient of Variation for Subtests .....	76
Figure 5. 25 Approximate Entropy for Subtests .....	76
Figure 5. 26 Variations in Angular Velocity.....	77
Figure 5. 27 Variations in Angular Velocity.....	78
Figure 5. 28 Variations in Angular Velocity.....	78
Figure 5. 29 Variations in Angular Velocity.....	79
Figure 5. 30 Variations in Angular velocity .....	79

Figure 5. 31 Variations in Angular Velocity.....	80
Figure 5. 32 Variations in Angular Velocity.....	80
Figure 5. 33 Mean Values for Subtests.....	84
Figure 5. 34 Standard Deviation for Subtests .....	84
Figure 5. 35 Coefficient of Variation for Subtests .....	85
Figure 5. 36 Approximate Entropy for Subtests .....	85
Figure 5. 37 Variations in Angular Velocity.....	86
Figure 5. 38 Variations in Angular Velocity.....	86
Figure 5. 39 Variations in Angular Velocity.....	87
Figure 5. 40 Variations in Angular Velocity.....	87
Figure 5. 41 Variations in Angular Velocity.....	88
Figure 5. 42 Variations in Angular Velocity.....	88
Figure 5. 43 Variations in Angular Velocity.....	89
Figure 5. 44 Mean Values for Subtests.....	92
Figure 5. 45 Standard Deviation for Subtests .....	93
Figure 5. 46 Coefficient of Variation for Subtests .....	93
Figure 5. 47 Approximate Entropy for Subtests .....	94
Figure 5. 48 Variations in Angular Velocity.....	94
Figure 5. 49 Variations in Angular Velocity.....	95
Figure 5. 50 Variations in Angular Velocity.....	95
Figure 5. 51 Variations in Angular Velocity.....	96
Figure 5. 52 Variations in Angular Velocity.....	96
Figure 5. 53 Variations in Angular Velocity.....	97

Figure 5. 54 Variations in Angular Velocity.....	97
Figure 5. 55 Mean Values for Subtests.....	101
Figure 5. 56 Standard Deviation for Subtests .....	101
Figure 5. 57 Coefficient of Variation for Subtests .....	102
Figure 5. 58 Approximate Entropy for Subtests .....	102
Figure 5. 59 Variations in Angular Velocity.....	103
Figure 5. 60 Variations in Angular Velocity.....	103
Figure 5. 61 Variations in Angular Velocity.....	104
Figure 5. 62 Variations in Angular Velocity.....	104
Figure 5. 63 Variations in Angular Velocity.....	105
Figure 5. 64 Variations in Angular Velocity.....	105
Figure 5. 65 Variations in Angular Velocity.....	106
Figure 5. 66 Mean Values for Subtests.....	109
Figure 5. 67 Standard Deviation for Subtests .....	110
Figure 5. 68 Coefficient of Variation for Subtests .....	110
Figure 5. 69 Approximate Entropy for Subtests .....	111
Figure 5. 70 Variations in Angular Velocity.....	111
Figure 5. 71 Variations in Angular Velocity.....	112
Figure 5. 72 Variations in Angular Velocity.....	112
Figure 5. 73 Variations in Angular Velocity.....	113
Figure 5. 74 Variations in Angular Velocity.....	113
Figure 5. 75 Variations in Angular Velocity.....	114
Figure 5. 76 Variations in Angular Velocity.....	114

Figure 5. 77 Displacement Time Series with Velocity and Acceleration.....	116
Figure 5. 78 Phase Plane Plot.....	116
Figure 5. 79 3D Phase Plane Plot .....	117
Figure 5. 80 Displacement Time Series with Velocity and Acceleration.....	117
Figure 5. 81 Phase Plane Plot.....	118
Figure 5. 82 3D Phase Plane Plot .....	118
Figure 5. 83 Displacement Time Series with Velocity and Acceleration.....	119
Figure 5. 84 Phase Plane Plot.....	119
Figure 5. 85 3-D phase Plane Plot.....	120
Figure 5. 86 Displacement Time Series with Velocity and Acceleration.....	120
Figure 5. 87 Phase Plane Plot.....	121
Figure 5. 88 3-D Phase Plane Plot.....	121
Figure 5. 89 Displacement Time Series with Velocity and Acceleration.....	122
Figure 5. 90 Phase Plane Plot.....	122
Figure 5. 91 3-D Phase Plane Plot.....	123
Figure 5. 92 Displacement Time Series with Velocity and Acceleration.....	123
Figure 5. 93 Phase Plane Plot.....	124
Figure 5. 94 3-D Phase Plane Plot.....	124
Figure 5. 95 Mean for Tests .....	127
Figure 5. 96 Standard Deviation for Tests .....	127
Figure 5. 97 Coefficient of Variation for Tests.....	128
Figure 5. 98 Approximate Entropy for Tests .....	128
Figure 5. 99 Variations in Velocity .....	129

Figure 5. 100 Variations in Velocity .....	129
Figure 5. 101 Variations in Velocity .....	130
Figure 5. 102 Variations in Velocity .....	130
Figure 5. 103 Variations in Velocity .....	131
Figure 5. 104 Variations in Velocity .....	131
Figure A. 1 Liberty Polhemus Unit .....	148
Figure A. 2 Magnetic Source Diagram.....	149
Figure A. 3 Sensor Diagram .....	150
Figure A. 4 Optotrak Data Acquisition Unit II .....	152

## List of Abbreviations

ApEn	Approximate Entropy
CV	Coefficient of Variance
SD	Standard Deviation

## **1. Introduction**

### **1.1 Background**

Low back pain (LBP) is the second most prevalent work-related musculoskeletal disorder in the United States. Nearly everyone suffers from LBP at some point in his or her lifetime. In the United States alone, 85% of the population suffers from low back disorder. Of all cases of LBP, 70% are due to lumbar strain or sprain, 10% are due to age-related degenerative changes, 4% are due to osteoporotic compression fractures, and 3% are due to spinal stenosis (eMedicine Mechanical Low Back Pain Hills, 2010). A 2009 National Health Interview Survey (NHIS) reported that 28.2% of respondents had visited physicians within the last three months for LBP.

The costs of LBP can be very expensive both to society and to the individual. In 1998, the total cost attributable to LBP in the U.S. was estimated to be \$26.3 billion (Lou et al., 2004). Moreover, indirect costs incurred due to lost work days are substantial, with approximately 2% of the U.S. workforce compensated for back injuries each year (Andersson G.B., 1999).

The majority of LBP is non-specific and is based on conditions where no clear cause can be found. However, despite this lack of understanding, biomechanical or physiological components can reveal the initiation and resolution of the condition (Hoogendoorn et al., 2000; Hartvigsen et al. 2003; Mulholland 2008). Acute pain is a short-term low back pain that generally lasts from a few days to a few weeks. It is



generally caused by trauma to the lower back such as a sports injury, daily work, etc., or by a disorder such as arthritis. Chronic pain, on other hand, is measured by duration. Generally, pain lasting longer than 3 months is considered chronic. It is often progressive and the cause can be difficult to determine. Even though acute pain is diagnosed by short duration, a small percentage of sufferers go on to develop more long-term conditions (Melloh et al., 2009). A large number of studies have focused on chronic LP, but they have not revealed a complete understanding of this condition (Bergman, 2007).

In order to apprehend this condition, researchers are now focusing on the effect of LBP on trunk movements. Kinematic and kinetic quantities are assumed to be periodic or pseudo periodic based on body characteristics and personal ability to control the lumbar spine. With neuromuscular and musculoskeletal pathologies or injuries, these movements may not be periodic and may result in increased instability of the lumbar spine (Papadakis et al., 2009).

Many researchers have employed linear and nonlinear techniques to gait parameters to develop an understanding of physiological stability. Techniques of gait analyses have revealed long correlations in degrees of variability, and these have been related to maturation and degeneration of gait stability with age and central nervous system pathologies (Hausdorff, 2007). Such studies have played a vital role in understanding the conditions of normal and unhealthy movements, and in diagnosing patients with motor deficiencies. Motor learning is a nonlinear process, exhibiting nonlinear learning curves depending on the task, conditions, and characteristics of the learner. Normal variations that occur in motor performance across multiple repetitions of

a task over time are the main reason for human movement variability (Stergiou et al. 2004).

Many investigations have linked variability with the health of the biological system. Specifically, one could find thousands of research articles that have shown that heart rate variability is affected by changes in the autonomic nervous system's regulation of the heart rate (Goldberger et al., 2002; Ho et al., 1997). However, there was not a complete understanding of how human movements affect these heart rate dynamics. Later, some studies revealed that in certain populations, gait instability is related to cardiovascular health (Hausdorff et al., 2003). Moreover, these studies proposed that, similar to heart rate studies investigating heart rate dynamics, investigating lumbar spine dynamics may provide insight into locomotor control and may have clinical applications. Traditionally, random error or noise within the system was considered the etiology of variability. Motor learning textbooks usually describe movement variability as error and skilled movement as movement with decreased variability. For example, if one is tossing a bean bag, sometimes someone may toss it into the hole on the wooden plank, but the bean bag doesn't always go into the hole because of variability. This leads some to conclude that there is some problem with the motor program and that it is not executed correctly when the bean bag fails to go in the hole. From this viewpoint, variability is considered to be an error in the motor control system.

However, there is mounting evidence that the variability in normal movement reveals variation not as error but as a necessary condition for function. In fact, there is growing understanding that the phenomena previously described as noisy are actually the result of nonlinear interactions and have deterministic origins (Stergiou et al. 2004).

Hence, studying the noisy component of the measured signal can yield important information about the system under study.

Variability can be defined in behavioral, biological and statistical senses. Behavioral variability can be defined as differences in observed behavior when the entity is placed in the exactly same situation. Biological variability is the power possessed by living organisms, both animal and vegetable, of adapting themselves to modifications or changes in their environment, thus possibly giving rise to ultimate variation of structure or function. Statistical variability refers to measures of centrality around a mean or an average and includes measures such as standard deviation, range and variance. All these definitions contribute to an understanding of human variability (Harbourne and Stergiou, 2009).

## **1.2 Traditional Linear Methods to Quantify Variability**

There are numerous studies that have shown the methods and quantities to determine the variability in systems. Traditional and nontraditional approaches have been used to identify the variability in kinetic, kinematic, and temporal variables. Traditional methods originating from statistical dispersion theory have been effectively applied in many investigations, and are considered to be appropriate to quantify the total variability patterns in human movements. Statistical dispersion is spread in a system. Range, standard deviation, variance, coefficient of variance are commonly used measures of statistical dispersion for variability analysis. Range is the difference between the largest and smallest observations. Probably the most common measures of variability used by researchers are variance and standard deviation. Variance is the mean of the squared deviations of a set of measurements, while standard deviation is the square root of the

variance. Although variance and standard deviation are computed similarly, variance is used less often in variability studies because units of variance are squared, making the interpretation of variability somewhat harder than the interpretation of standard deviation (Stergiou, 2004). Coefficient of variation is a normalized measure of dispersion that is defined as the ratio of the standard deviation to the mean and is given as a percentage. Standard deviation of data must always be understood in context of the mean of the data. Hence, when comparing two different sets of data with different means and units, coefficient of variation is more useful than standard deviation.

Of the all linear techniques used to determine variability, standard deviation and coefficient of variation are the most popular methods. These techniques have been used for a long time. Fitzgerald and colleagues (1983) presented an assessment method in conjunction with age-related normal values for the lumbar spinal range of motion. 172 volunteers participated in the study, which were divided into 6 age groups. Lumbar spinal flexion, right and left lateral thoracolumbar spinal flexion, and spinal extension were observed, and the coefficient of variation was calculated for each measurement. From the results the author showed that the variability in the normal range of motion increased with the age. In a similar kind of study related to effect of age on the gait variability, Buzzi et al. (2003) tried to understand the difference in the variability in two different age groups. Subjects were asked to walk on the treadmill, and gait parameters were recorded and analyzed using standard deviation and coefficient of variation. The authors suggested that the linear measures distinguished between the groups by indicating significantly high variability, but that they could not distinguish between the increase in noise within the system and the inherent variability associated with it. In the study carried out by Jackson

et al. (2010), the authors evaluated the normative lumbar flexion-extension values for different ages and racial groups. Mean and standard deviations were calculated for lumbar flexion-extension. It was evident from the result of standard deviation that the normative values of lumbar flexion and extension are different for different ages and racial groups.

The lumbar spine has also been studied in terms of postural variability. Specifically, Herp et al. (2000) assessed the three-dimensional range of movement in non-pathological subjects. 100 subjects (50 males and 50 females) with no recent back pain history were recruited. Each subject performed lumbar flexion-extension, side flexion to the left and right, and axial rotation to the left and right. There was significant difference in range of motion observed in younger and older age groups. The results revealed greater flexibility in women than in men. Along the same lines, Buchanan et al. (2001) tried to examine the upper trunk variation in space for instabilities. Subjects stood on support surfaces and the variability of upper trunk anterior posterior position in space was computed. Each subject performed the experiment with and without open eyes. The results showed very little evidence of variability with open eyes, while more variability was observed when eyes were closed. The authors thus concluded that postural patterns are influenced by mechanical and neural constraints. Changes in postural patterns are closely associated with visual information. Some investigators (Garcia-Alsina et al., 2005) have also concentrated on normal range, velocity, and consistency of the movement of active arm elevation using coefficient of variation technique; they have shown that analysis of arm elevation repeatability in angular position and the velocity and repeatability of motion can give picture of overall performance of shoulder.

Stride-to-stride variability during gait is one of the most widely researched movement analyses. Hausdorff et al. (1999) characterized the development of mature stride dynamics. 50 boys and girls were recruited in the study and were classified in 3 age groups: 3–4 years old, 6–7 years old and 11–14 years old. Two force-sensitive switches were placed inside the subject's right foot to record force applied to floor at the time when foot struck the floor. Each subject was asked to walk on a running track at his or her self-selected speed. The authors suggested that variations in the stride were significantly larger for 3–4-year-old children than that of 6–7-year-olds and 11–14-year-olds. They also concluded that temporal structure of gait fluctuations is not fully developed until 7 years of age. Dingwell and Marin (2006) tried to understand the kinematic variability and local dynamic stability across the range of walking speed. 6 healthy males and females participated in the study. Standard deviation was calculated for each of the gait time series recorded. The results showed an increase in standard deviation for both faster and slower preferred walking speeds, which made the authors conclude that variability increases at both slower and faster walking speeds. In another stride variability study, Dingwell et al. (2001) characterized the local dynamic stability properties of locomotor behavior using standard deviation measurement and suggested that treadmill walking was associated with significant changes in variability and local stability as compared to walking over ground. Thus the motorized treadmill walking may produce misleading results in situations where changes in neuromuscular control are likely to affect the variability of locomotion. In 2004, Kurz et al. used a relative phase dynamics to evaluate gait in subjects who had undergone anterior cruciate ligament (ACL) reconstruction. The large standard deviation values indicated a considerable

amount of variability in shank-thigh relative phase dynamics within each group during running conditions.

Some researchers have also used linear techniques to study questions related to human cadaveric movement. Brown et al. (2002) quantified instability of the lumbar spine using vertebrate distractor to measure motion segment stiffness by applying defined load at constant rate. They used mean, standard deviation, and range of stiffness as the measure of variability of motion stiffness and found out that motion segment stiffness is dependent on disc morphology. In another human cadaveric study, Hitchon et al. (2005) compared the biomechanical performance of human cadaveric spines implanted with artificial discs at the L4-L5 levels with spines in an intact state and after anterior discectomy. They concluded that the artificial disc stabilized the spine after discectomy, comparable to that of the intact spine.

### **1.3 Nonlinear Methods to Quantify Variability**

Physicians in the medical field use linear models for prediction and problem solving (Harbourne et al., 2009). However, biological systems, including humans, are complex adaptive systems, characterized by multiple interconnected and interdependent parts (Harbourne et al., 2009). These are highly non-linear systems with inherent variability in all healthy organisms. There is growing understanding that linear models are limited in many cases and are certainly not the best models for understanding the nonlinear human system (Stergiou, 2004). Professionals in different medical fields such as biomechanics, epidemiology, etc. are now turning to nonlinear tools for solving such complex systems.

Although a large number of studies use linear tools as a measure of variability, they may not be truly representative of the variability. They ignore the viewpoint that variability may have a structure that can be useful and provide information about the strategies used to control the body's degree of freedom (Harbourne et al., 2003). Structure in human movement data may not be visibly clear and it may become difficult to distinguish the data sets. Hence, many researchers are now focusing on nonlinear techniques that can lead to a better understanding of the holistic behavior of the motor system. The structure of the time series can reveal important information regarding properties of posture that evolve during human movement. Hence, it is advantageous to have variability in movement. The theory of optimal variability concentrates on the advantages of having a balance between rigid control and randomness in movement, i.e. complexity (Stergiou et al., 2006). Complexity can indicate spatial variation in movements (Mijna Hadders-Algra, 2007). Currently the most commonly used method to determine the complexity is approximate entropy (ApEn) (Karmakar et al., 2006; Khandoker et al., 2008). Approximate entropy is a method that quantifies the regularity or predictability of a time series. Pincus and Goldberger (1994) and Pincus (1995) suggested that in order to calculate ApEn two main parameters are required:  $m$ , the number of observation windows to be compared and  $r$ , the tolerance factor. Generally  $m=2$  for all ApEn calculations while  $r$  ranges from 0.1 to 0.25 SD of the  $u(i)$  data (Pincus and Goldberger 1994; Pincus 1995).

Vast number of studies has been conducted in trying to understand deterministic dynamical systems through reconstructed dynamics. Techniques such as correlation dimension, K-S entropy, and the Lyapunov Exponent have been extensively studied.



ApEn has been compared with correlation dimension (Grassberger and Procaccia 1983) and the Lyapunov Exponent (Pincus 1997). Most of these techniques effectively employ embedding dimensions larger than  $m=2$  (Pincus and Goldberger, 1994). As a result these techniques are superior in deterministic dynamical system environment as compared to ApEn. However, in biological settings we encounter mixed (stochastic and deterministic) systems, and those parameters and techniques produce poor results (Stergiou, 2004). There are many advantages of ApEn over the aforementioned nonlinear techniques that are explained by Pincus (1997) as:

1. ApEn is unaffected by the noise below the tolerance factor 'r'.
2. ApEn is unaffected by outliers (such as a spike in the time series).
3. ApEn requires a small amount data to quantify complexity.
4. ApEn is finite for random, noisy deterministic and mixed data sets, which are observed in biological environments.
5. Increased complexity in the data is associated with an increase in ApEn.

Because of these advantages, ApEn technique is more widely used in biological environments than other nonlinear techniques. Pincus and Goldberger (1994) studied the utility of ApEn over other nonlinear tools. They studied the heart rate data of aborted sudden infant death syndrome (aborted-SIDS) infants compared to normal infants, which showed the ApEn values for aborted-SIDS infant was significantly higher than normal infants. The authors concluded that abnormal physiology is associated with more regularity while normal physiology is linked with greater complexity. In another study ApEn was utilized to examine the effect of age on luteinizing hormone and follicular

stimulating hormone serum concentrations in men and women. In a similar kind of study Veldhuis et al. (1998) studied the orderliness of hormone release patterns.

Several human studies have also used ApEn measures for postural analysis. In 2003 Harbourne et al. examined the lumbar postural control during various stages of development in independent sitting. Five infants of age 4 were categorized into 3 groups based on their ability to maintain posture. The result suggested that infants dynamically assume the sitting posture by increasing the stability and regularity of their strategy and by controlling the degree of freedom, first to approximate the skill, then to explore adaptations to function in the environment. Justin et al. (2009) tried to understand the effect of speed on the trunk motion during overground walking. The acceleration time series of the lower trunk was used to calculate the ApEn values. The result showed lack of regularity and repeatability difference, indicating that trunk motion was preserved between same conditions. Khandoker et al. (2008) examined the variability indexes in minimum foot clearance that would correlate with balance impairments. The results showed that ApEn is effective in quantifying gait dynamics in normal and pathological conditions and hence could be useful for early diagnosis of at-risk gait.

Nowadays nonlinear tools are gaining more attention as a way to examine the variability in human movement. There are several reasons for selection of nonlinear techniques as an alternative measure for variability, which are:

1. The use of linear tools can mask the true structure of variability in the movement pattern. These techniques generally average the kinematic data to produce a mean picture of the subject's movement, which completely ignores the temporal variation.

2. Use of linear tools assumes the variability in movement to be random and independent, while studies have shown that they are not random and may have deterministic origin which can be revealed using nonlinear tools.
3. Deterministic movement dynamics offer a moving system the ability to be adaptable and flexible in a constantly changing environment. Nonlinear tools have the ability to understand these dynamics.

Although nonlinear tools have aforementioned advantages, they have some demerits as well (Harbourne et al. 2009):

1. Nonlinear measurement techniques require mathematical equations and software to evaluate time series data; as a result they must be carried out in a research environment.
2. There is a lack of understanding of variability and complexity in most medical fields.
3. Translation of nonlinear measures to clinical problems requires concurrent use of linear tools to make associations and determine clinical meaning.
4. Most of these measures require multiple repetitions or cycles of a movement.

The aforementioned limitations of nonlinear techniques and the simplicity of calculation using linear tools make linear tools the preferred methods for understanding variability even in most biomechanical settings today.

Searching the literature has revealed that both linear and nonlinear techniques can be effectively applied for motion analysis. Linear tools are useful but may ignore the hidden structure which can be determined by nonlinear techniques. The main objective of this study, which is a part of a bigger project investigating the effectiveness of

chiropractic adjustments on the vertebral column by understanding its postural stability and lumbar proprioception, is to identify the best method to quantify the variability in the human lumbar spine during sitting flexion-extension in healthy subjects and in human cadaveric spine movements.

#### **1.4 Specific Objective**

Specific goals that would be required to achieve this objective are:

1. To measure and record human lumbar movements and conduct in-vitro testing on the human cadaveric spine using the six-degree-of freedom-motion tracking system.
2. To denoise the displacement data and differentiate it to get velocity and acceleration values.
3. To quantify the effect of movement direction on the variability of human lumbar spine motion.
4. To quantify the effect of speed and incision on flexion-extension kinematics in the cadaveric lumbar spine.
5. To measure change in velocity while performing flexion-extension tasks.

## **2. Anatomy of Lumbar Spine**

The human spine is a complex structure that comprises the spinal cord and its protective and supportive coverings, known as the vertebral column or backbone. The spinal cord is a thin tubular bundle of nervous tissue that extends from the brain and makes up the central nervous system. It has a hollow center that is filled with fluid. The delicate tissues of the spinal cord are enclosed in and protected by the vertebral column.

### **2.1 Vertebral Column**

The vertebral column is a column that has series of 33 stacked bones known as vertebrae (including the 5 that are fused to form the sacrum). Each vertebra is separated by spongy cushioning material called intervertebral discs that help to avoid contact between the adjacent vertebrae (University of Maryland Medical Center). These discs consist of strong annulus fibers known as annulus fibrosus, which distribute pressure evenly across the disc, and a soft jelly-like center known as the nucleus pulposus. The nucleus pulposus contains loose fibers suspended in mucoprotein gel. This nucleus pulposus helps to absorb shock during daily activities and prevent intervertebral contact.

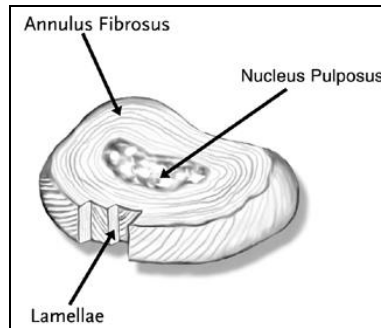


Figure 2. 1 Normal Disc

Each vertebra is connected to its adjacent vertebra by an intricate web of muscles, ligaments and connective tissue. The pair of vertebrae and their supporting structures contributes to the specific and limited range of motion. Together they create a movable spine structure with the spinal cord as the feedback system continuously monitoring motion by sending and receiving signals to and from the brain. The spine has 31 segments. The motor nerve roots branch out at each segment from the ventral side and sensory nerve roots enter from the dorsal side. The ventral and dorsal roots collectively form paired spinal nerves on each side of the spinal cord.

The vertebral column has several curves when viewed laterally. These curves represent various regions on the column: cervical, thoracic, lumbar and pelvic (Anatomy of Human Body, 1918).

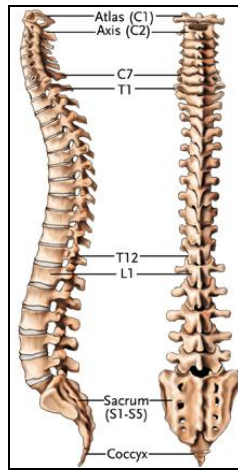


Figure 2. 2 Human Lumbar Spine

The cervical spine: This vertebral region curves convexly from the anterior and is the upper part of the spine. It is made up of 7 vertebrae (C1 to C7).

The thoracic spine: Below the cervical spine is the thoracic spine, which curves concavely from the front. It consists of 12 vertebrae (T1 to T12) and forms middle portion of the spine.

The lumbar spine: The lower part of spine is called the lumbar spine. It is convex anteriorly. It is made up of 5 vertebrae (L1 to L5); however, some people may have 6 of them. Since the lumbar region is a lower region and these vertebrae have to support more weight than the vertebrae above them, they have developed larger and stronger bodies.

The sacrum: The sacrum is a large triangular bone at the base of the lumbar spine. Its narrow lower part joins the coccyx. The sides are connected to the ilium (the largest bone forming pelvis).

The coccyx: It is the lowest part of the spine that is attached by ligaments to the margins of the sacral hiatus.

## 2.2 Vertebrae

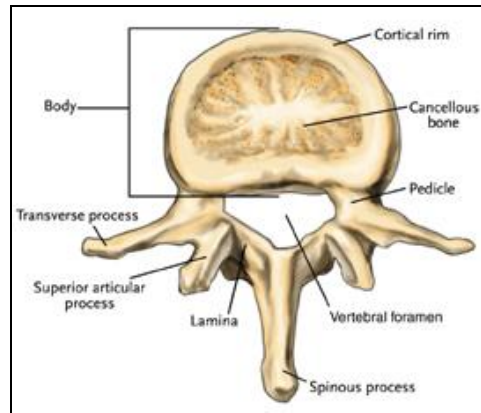


Figure 2. 3 Vertebra

An individual bone of the spine is called a vertebra. Together, the vertebrae make a freely mobile yet sturdy structure that enables human beings to perform various common tasks in daily routine. When the vertebrae are combined together the bodies form a strong pillar for the support of the head and trunk. The vertebral body is the main part, which bears about 80% of the load while standing and provides attachments for discs between the vertebrae. Both the vertebral body and the discs increase in size from the head to the sacrum. Each vertebra has two cylinder-shaped projections that stick out from the back of the vertebral body, providing side protection for the spinal cord and nerves. The lamina is the roof of the spinal canal that provides support and protection for the backside of the spinal cord. The bony projection that is felt on the back of any person is called the spinous process and is at a right angle to the midline of the lamina. These spinous processes are attached to each another by ligaments. The transverse processes are located at right angles to the junction of the pedicles and the lamina. They provide a place for the back muscles to attach to the spine. The spinal canal is the bony tunnel that surrounds the spinal cord. It is made up of vertebral bodies in front, the pedicles on the sides and the laminae on the back. Each vertebra has a paired joint on the left and right of



the spinous process that allows the connection between the vertebrae above and below it and is called the facet joints.

There is a complex web of infinitesimal muscle that controls the bony structure of the spine, known as the soft tissue. The paraspinal muscles are the muscles running along either side of the spine that mainly control the vertebral movement. These muscles and ligaments are covered by layers of skin and connective tissue (University of Maryland Medical Center).

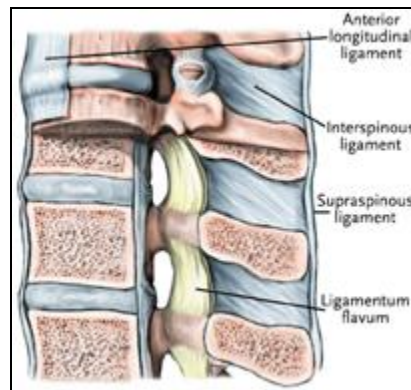


Figure 2. 4 Ligaments of Spine

### **3. Tools and Techniques**

#### **3.1 State of System**

Different methods of nonlinear techniques are based on the examination of structural characteristics of a time series that is embedded in an appropriately constructed state space. State space is the vector space where a dynamical system can be defined at any point. The characteristics of that state space then can be examined to gain insight into the motor control of posture. The phase space is a plot that represents the behavior of a dynamic system in state space. The phase plane plot is simply a representation of the state space.

#### **3.2 Time Series**

A time series is a sequence of data collected at regular intervals over a period of time. Time series data analysis can be very useful in understanding the variability of given parameters over a period of time. For example, if we record the distances from the center of bicycle to the edge of the road, we may categorize the rider's driving as learner or proficient. Time series can be analyzed in two ways: Time domain and Frequency domain. A discrete time series is one in which the data is collected at discrete time points. Discrete time series refers to fixed time intervals between two adjacent observations (Deng et al. 1997).

### **3.3 State Space**

The dynamic behavior of the system can be examined only if the structural characteristic of time series is studied. To understand the structural characteristic we need to reconstruct the state space where the behavior of the system is embedded. State space is a vector space where the dynamical system can be defined at any point. By examining the state space one can gain insight into the motor control of the posture (Stergiou, 2004).

### **3.4 Phase Space**

Phase space is the space in which all possible states of systems are represented, with each possible state of the system corresponding to one unique point in the phase space. The phase space usually comprises all possible values of position and momentum variables and the plot of it is sometimes called a phase plane plot. For every behavior of the dynamic system, a point is plotted in multidimensional space. The trajectory of the plotted points is analogous to the system's changing state.

Figure 3.1 below shows the time series and phase plots for sine curve and random data.

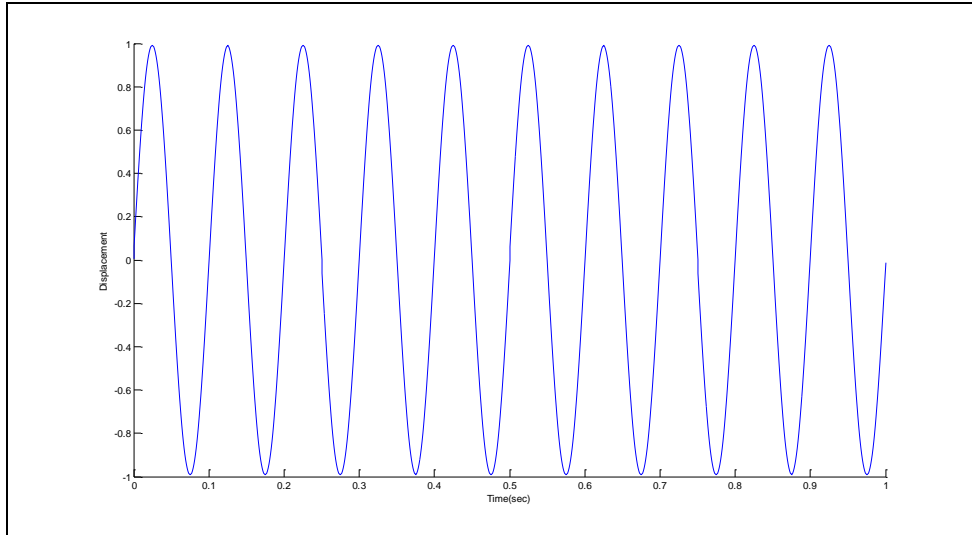


Figure 3. 1 Sine Wave

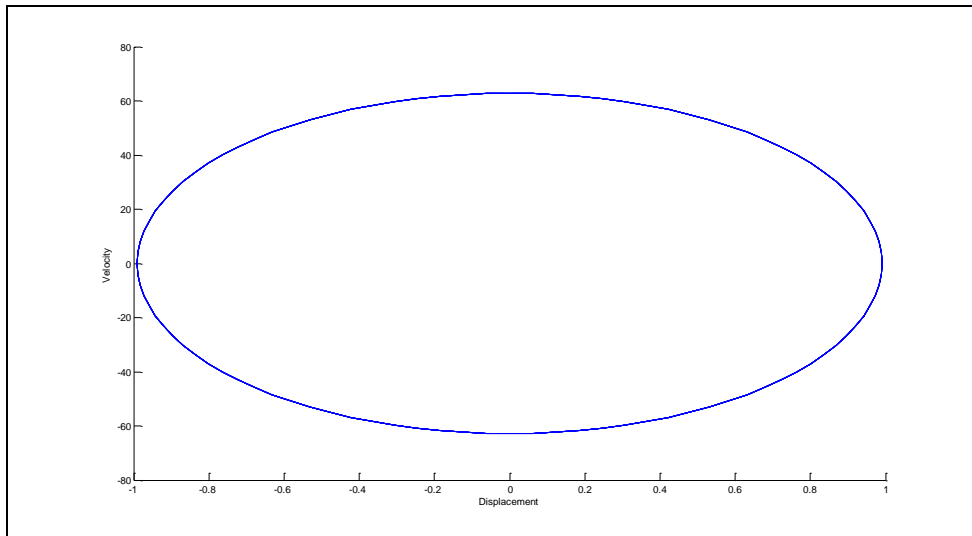


Figure 3. 2 Phase Plane Plot

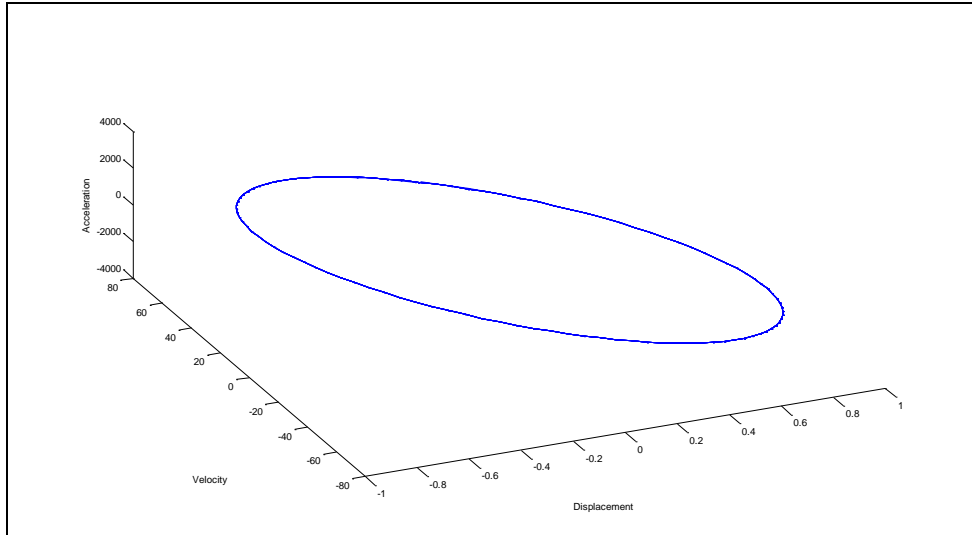


Figure 3. 3 3-D Phase Plane Plot

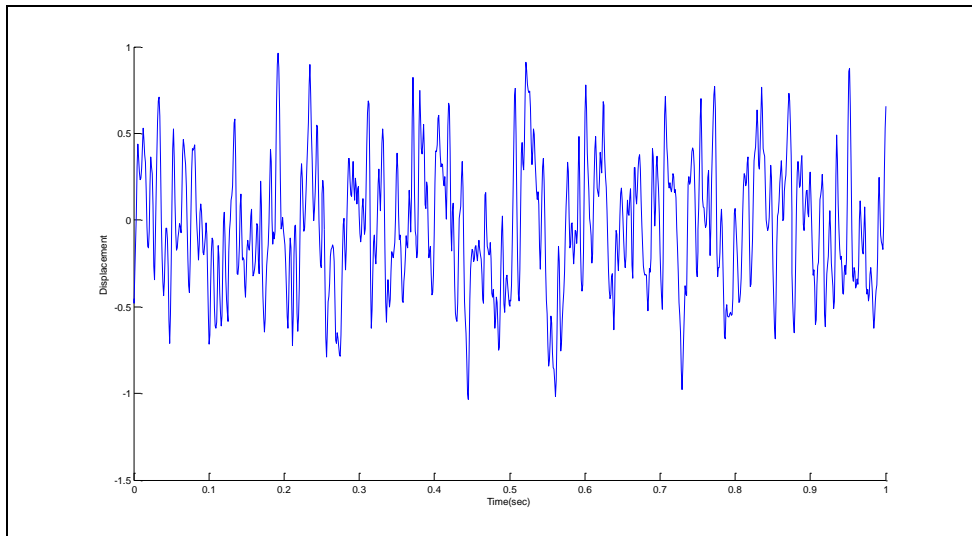


Figure 3. 4 Random Data

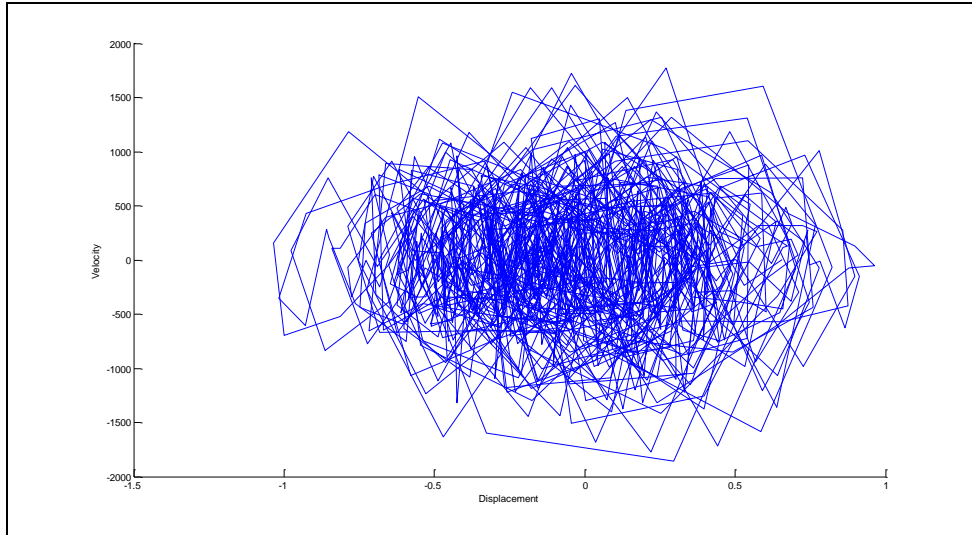


Figure 3. 5 Phase Plane Plot

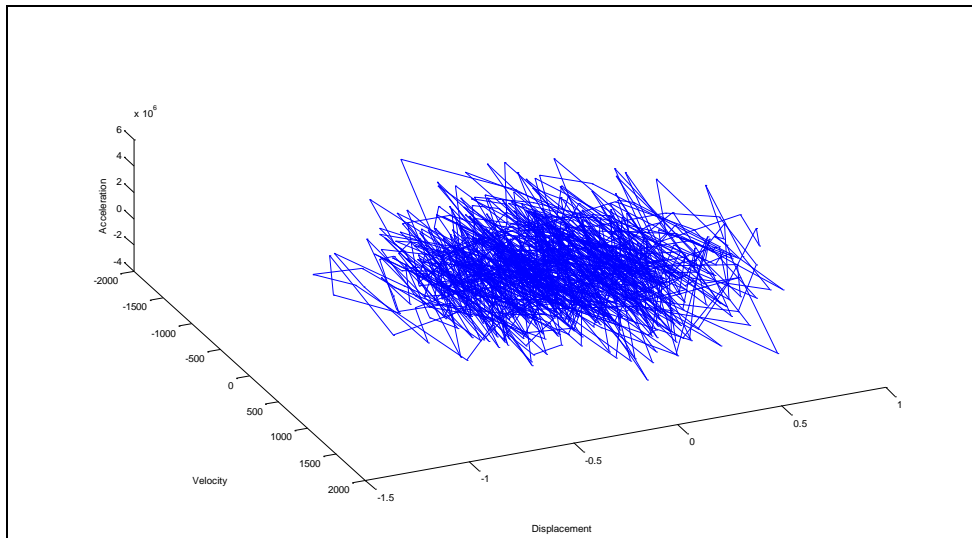


Figure 3. 6 3-D Phase Plane Plot

Figures 3.1 and 3.4 show time series from a simple periodic function (sine curve) and random data respectively. Figures 3.2 and 3.5 show phase plane plots of these time series. The phase plane plot of the periodic function gives a closed orbit with complete overlapping of the trajectories and no divergence at all. However, the phase plane plot for

random data has no order and the trajectories have no clear patterns. Hence, one can see that in a biomechanical setting, if the time series is perfectly periodic and repetitive, the phase plane plots will show clear patterns with no divergence, while the time series with some variability will show some divergence.

As mentioned previously, a phase plane plot is just a representation of state space and many times it is difficult to distinguish between the different time series data that we are comparing. In order to clarify this point, an experiment was carried out on a flexible foam strip (2 ft long) with 4 sensors attached at different levels spaced similarly to the T1, L1, L3, and S1 levels of the human spine (Figure 3.7). The motion data was recorded at the sampling rate of 120 fps.

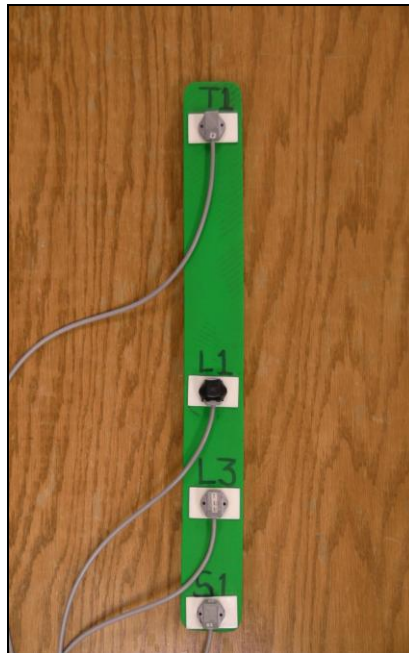


Figure 3. 7 Foam Strip

This foam strip was then placed on a fixed bottom and was moved to and fro smoothly, so that it replicated motions similar to human lumbar flexion-extension

movement. Three types of data were recorded: 1) Smooth and Controlled; 2) Smooth and Uncontrolled; 3) Unsmooth and Uncontrolled.

These data were filtered using a second-order Butterworth filter with a cut-off frequency of 10 Hz; Sample rate = 120 fps; Nyquist frequency = sample rate/2 = 60 Hz;  $W_n = \text{cut off freq}/\text{Nyquist freq} = 10/60 = 0.166 \text{ Hz}$  (England and Granata, 2006).

### 1) Smooth and Controlled Movement

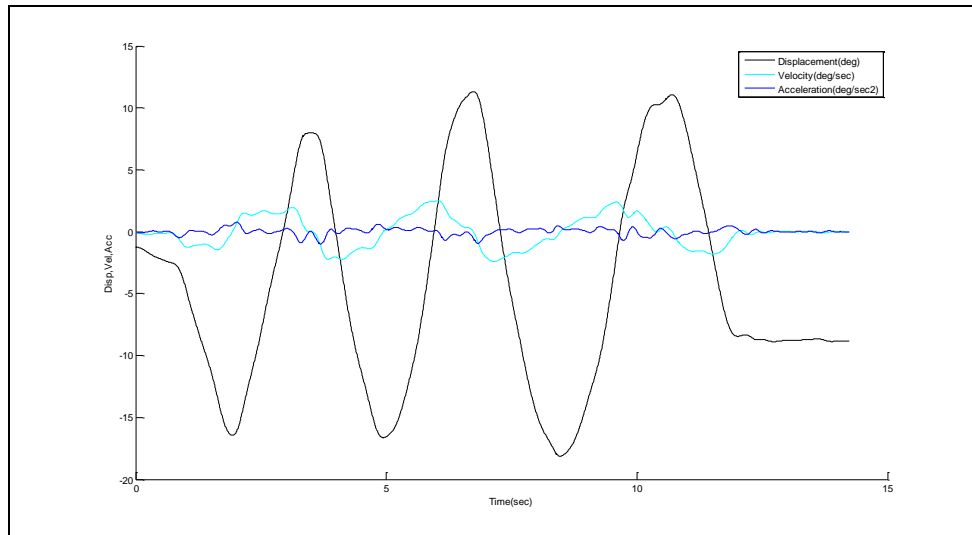


Figure 3. 8 Displacement, Velocity, Acceleration Diagram



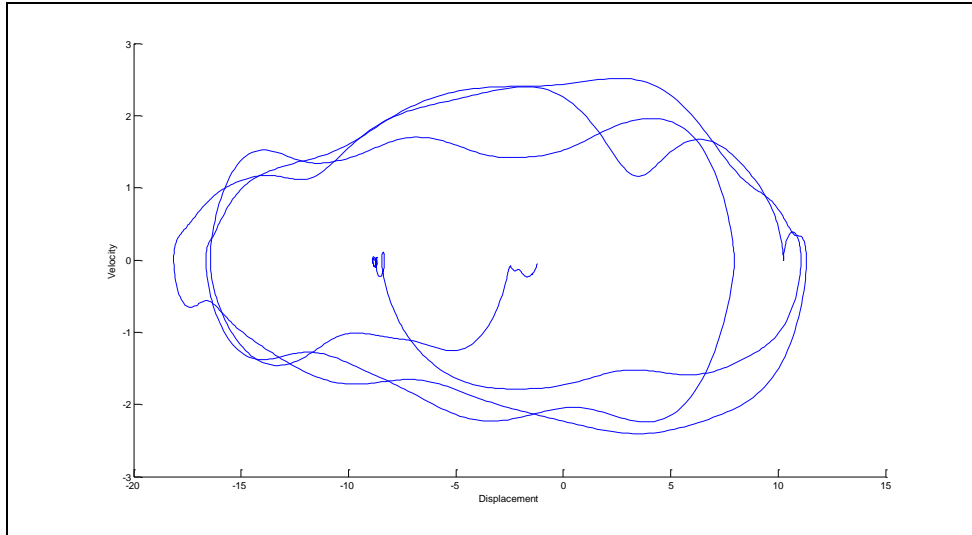


Figure 3. 9 Phase Plane Plot

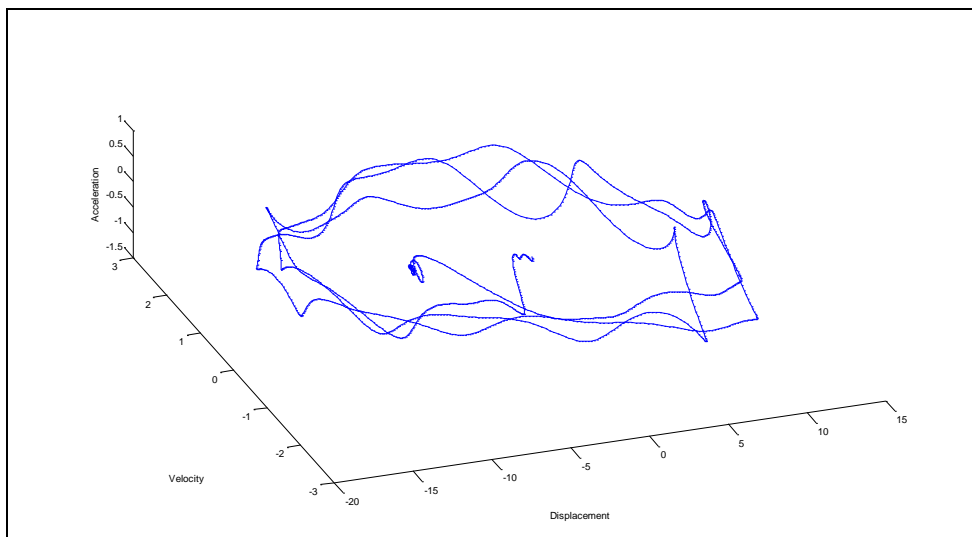


Figure 3. 10 3-D Phase Plane Plot

## 2) Smooth and Uncontrolled Movement

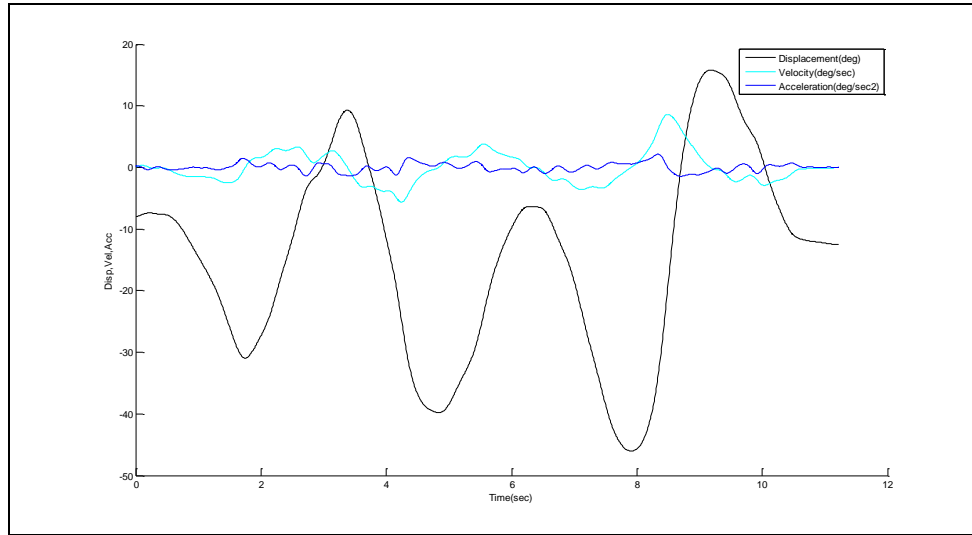


Figure 3. 11 Displacement, Velocity, Acceleration Diagram

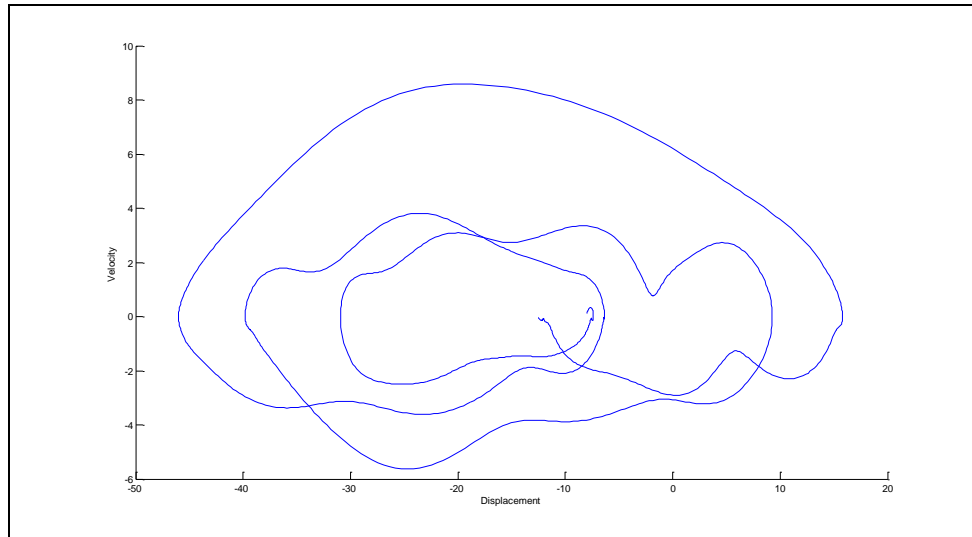


Figure 3. 12 Phase Plane Plot

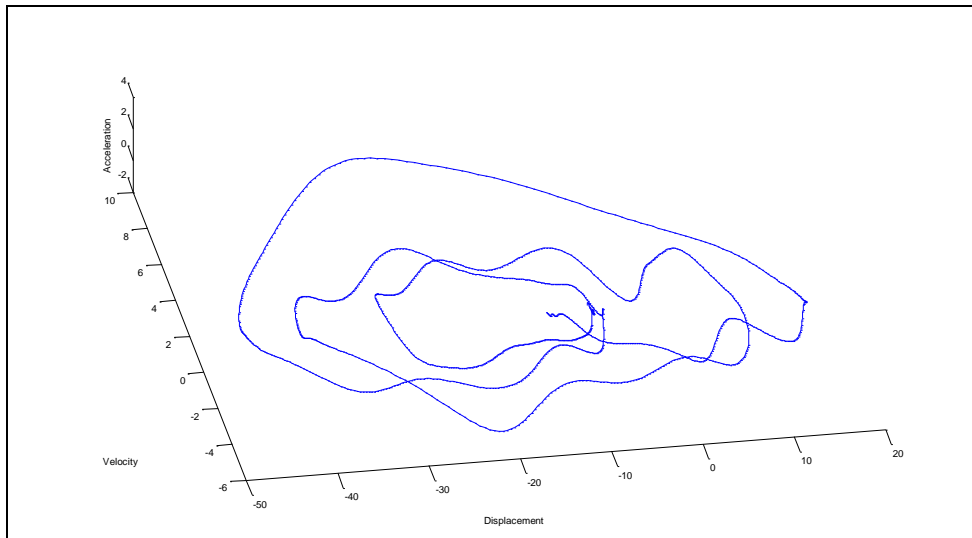


Figure 3. 13 3-D Phase Plane Plot

### 3) Unsmooth and Uncontrolled Movement

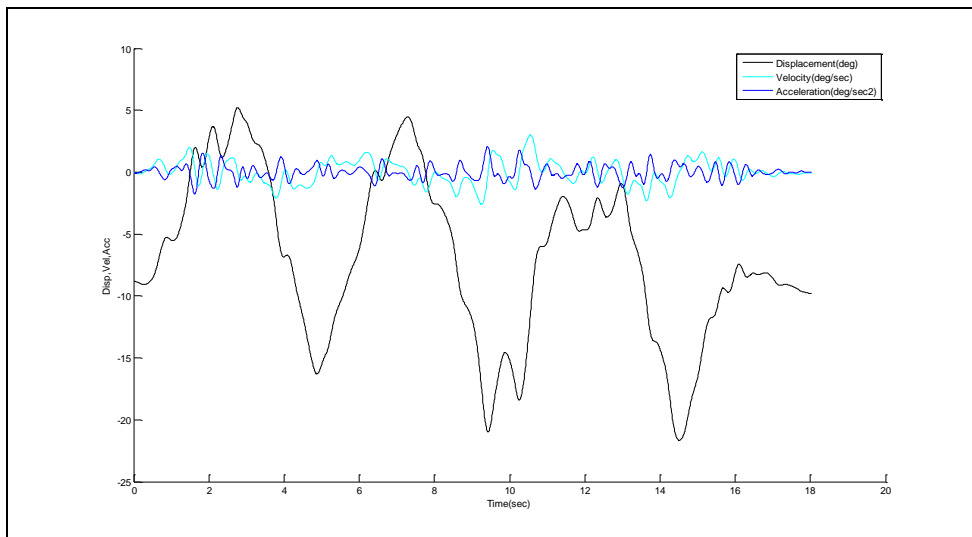


Figure 3. 14 Displacement, Velocity, Acceleration Diagram

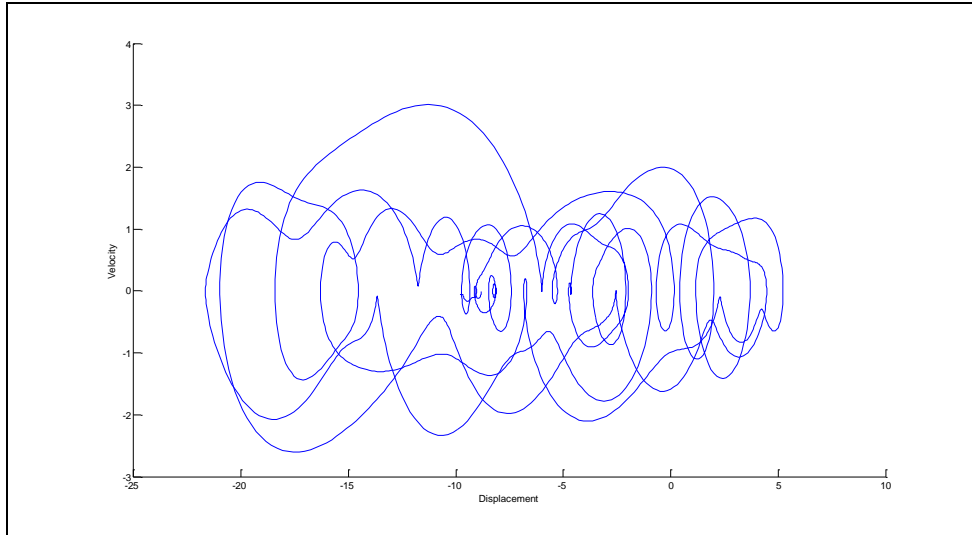


Figure 3. 15 Phase Plane Plot

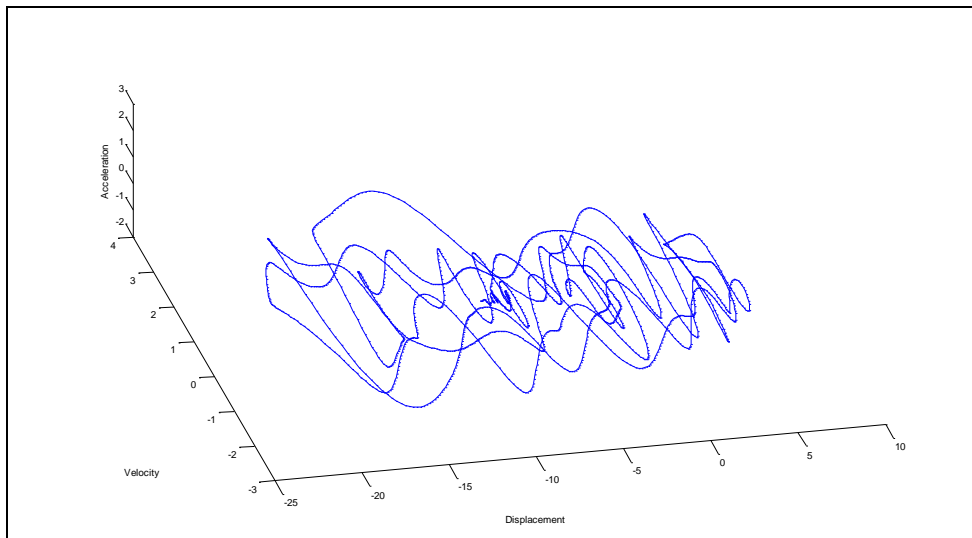


Figure 3. 16 3-D Phase Plane Diagram

As seen from the phase plane plots (Figures 3.9, 3.12, 3.15) we see that the smooth and controlled motions produce the trajectories that have some elegant pattern, while the unsmooth and uncontrolled movements showed no pattern in trajectories. The smooth and uncontrolled time series showed some pattern and was similar to that of the smooth and controlled. Hence, we can say that phase plane plots could be used to

distinguish between different conditions. But they do not quantify variability, and provide a visual means to distinguish between various movements. In general, phase plots should just be considered as a guideline and not the method to differentiate the variability in time series, which could be more effectively done by the linear and nonlinear techniques explained above.

Table 3. 1 Linear and Nonlinear Measures

<b>Test Condition</b>	<b>Total ROM</b>			
	<b>Mean</b>	<b>SD</b>	<b>CV (%)</b>	<b>ApEn</b>
Smooth and Controlled Movement	27.51279	2.660723	9.670858	0.117
Smooth and Uncontrolled Movement	46.67221	15.47123	33.14869	0.2269
Unsmooth and Uncontrolled Movement	23.02578	2.624542	11.39828	0.2757

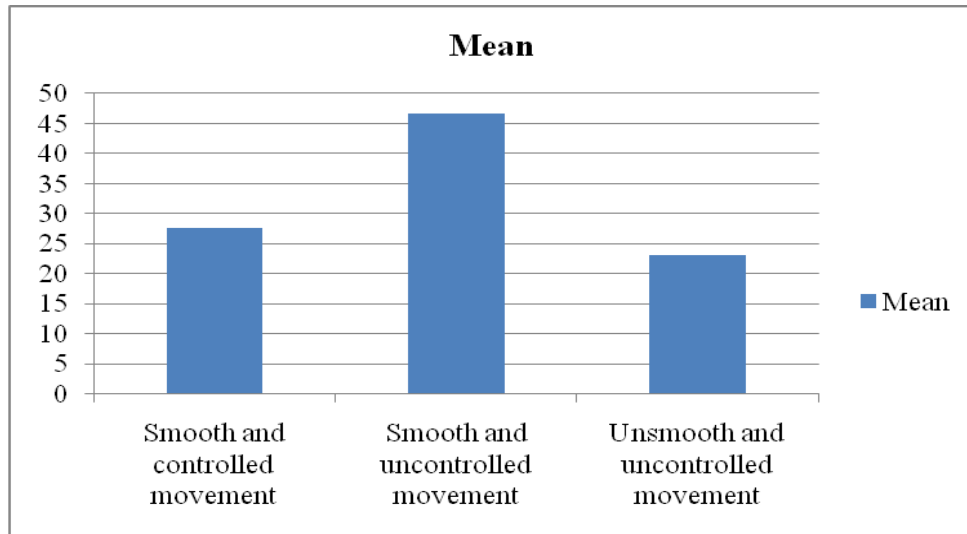


Figure 3. 17 Mean for Foam Test

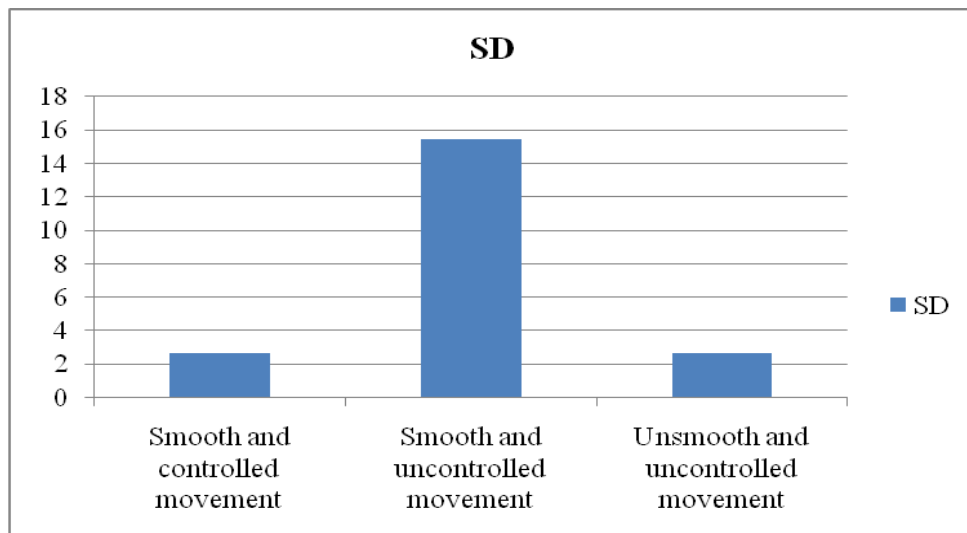


Figure 3. 18 Standard Deviation for Foam Test

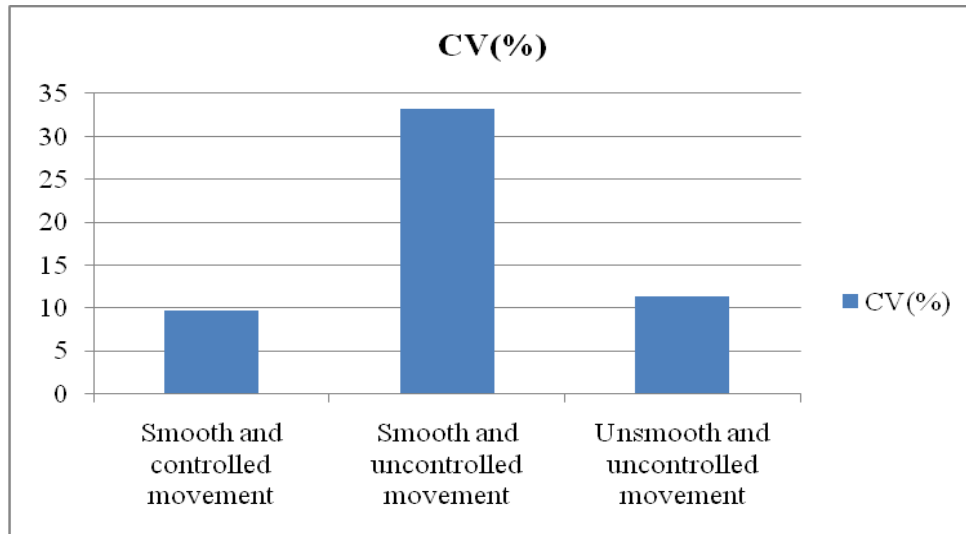


Figure 3. 19 Coefficient of Variation for Foam Test

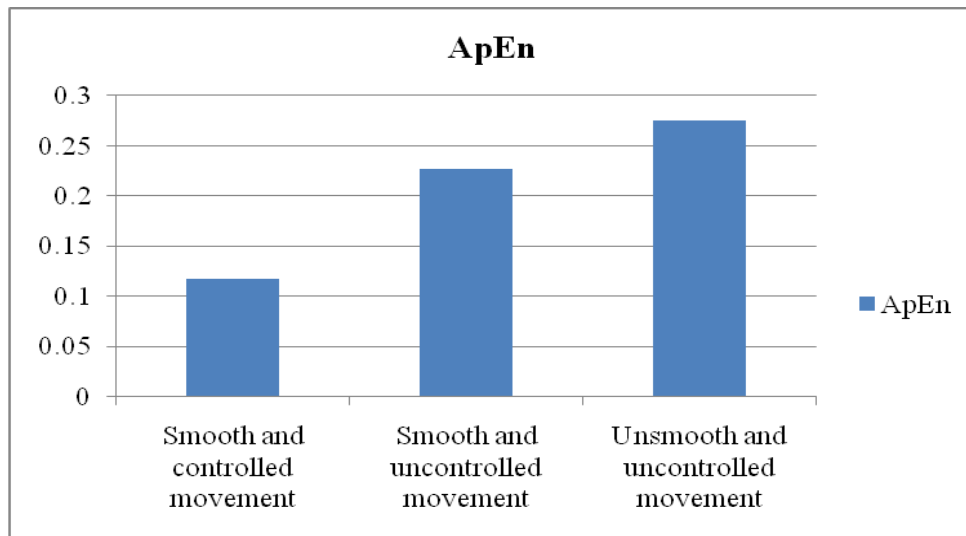


Figure 3. 20 Approximate Entropy for Foam Test

Linear and nonlinear techniques estimated and represented above in Figures 3.17–3.20 showed that linear techniques have higher variability for smooth and uncontrolled movement, which is unexpected since unsmooth and uncontrolled movement is more random than others. On other hand, approximate entropy (ApEn) showed higher variability for unsmooth and uncontrolled movement after smooth and uncontrolled movement. The linear techniques failed to account for the underlying structure of the

movement. ApEn showed an increasing trend as the randomness in the movement increased, which was in agreement with the phase plane plots.

### **3.5 Noise in Biomechanical Data**

As described previously, the data collected above was filtered before it was used to plot various graphs. The filter mainly removes the unwanted features from the signals. These unwanted signals, or noise, are inherent in all electronic devices. Noise can be generated for various reasons, the most common being the random thermal motion of electrons inside an electrical conductor, regardless of any applied voltage and random fluctuations of the electric current in an electrical conductor.

### **3.6 Filters**

The displacement data in most biomechanical studies are differentiated in order to get the velocity and acceleration. These signals are generally of more importance than the displacement data and may yield important clinical information. If a noise-contained signal is differentiated it results in more noisy velocity and acceleration data. To understand the severity of this problem, let us consider a time series  $x(t)$  consisting of a sum of  $N$  sinusoids of frequency  $\omega_i$ , amplitude of  $a_i$  and phase  $\Phi_i$ . This could be mathematically represented as:

$$x(t) = \sum_{i=1}^N a_i \cos(\omega_i t + \Phi_i)$$

The amplitude of velocity is expressed by  $\omega_i a_i$  and that of acceleration is defined as  $\omega_i^2 a_i$  (Wachowiak et al., 2000). Hence, as we can see from these expressions, if the displacement signal frequency has noise, then it would only be amplified by



differentiating the displacement signal twice. In order to avoid this, signals are de-noised using filters.

Filters are one of the crucial parameters of signal processing and mainly have two important roles: (a) separation of signals that have been combined and (b) restoration of signals that have been distorted in some way (Smith, 1999). Original signals may get adulterated with noise, interference, or other signals. They may even get distorted in some way. A good filter should have the ability to nullify these errors.

Every filter has various characteristics that give complete information of that particular filter. These are known as the responses of the filter. They are impulse, step, and frequency responses. All responses contains the same information but in different arrangements and can be calculated directly if any one response is known (Smith, 1999).

One of the important functions of the filter is to represent the information contained in the signal. This can be done in time domain or frequency domain. Information represented in time domain explains when something occurred and what the amplitude was, while the frequency domain representation is more indirect. In the frequency domain the information is represented by the relationship between many points in the signal (Smith, 1999).

The step response explains how the information represented in time domain is modified by the system, while the frequency response reveals how information represented in the frequency domain is being changed (Smith, 1999).

In order to measure the performance of a filter in time domain, certain parameters of step response should be considered.

These are:

- a) Risetime
- b) Overshoots
- c) Phase Linearity

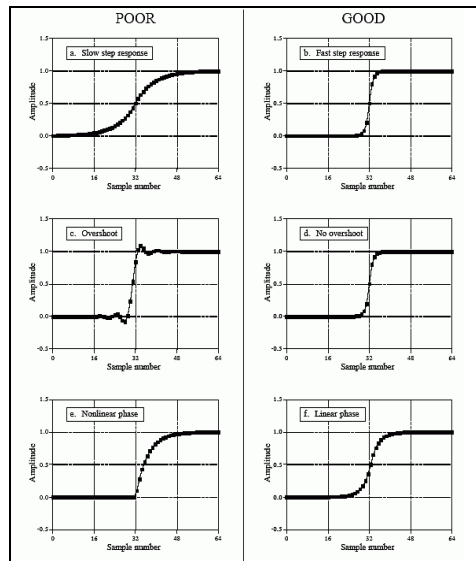


Figure 3. 21 Step Response

The filter design is poor if the designed filter has risetime as shown in Figure 3.21.a; however, the risetime in Figure 3.21.b is steep and short, making it an ideal response for time domain filter.

Figure 3.21.c shows overshoot in the step response. Overshoot is basically distortion of information in the signal and results in a change in the amplitude of the samples of the signals. Conversely, Figure 3.21.d shows the desired step response with no overshoot.

Phase linearity is the symmetry between the upper and lower halves of the step response. Figure 3.21.e shows unsymmetrical step response which is due to the faulty filter design and is undesirable.

The purpose of designing a filter in the frequency domain is to allow signals with certain frequencies to pass through while blocking some signals with other frequencies. Passbands are the frequencies that are passed untouched, while stopband refers to frequencies that are blocked. Between the two is the transition band. When this region is narrow it is called fast roll-off. The division between the passband and the transition band is called the cutoff frequency.

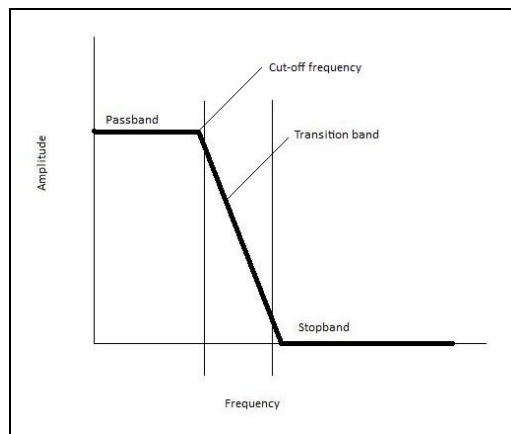


Figure 3. 22 Frequency Response

In order to estimate how well a filter performs in the frequency domain, three frequency response parameters should be considered:

- a) Roll-off
- b) Passband
- c) Stopband Attenuation

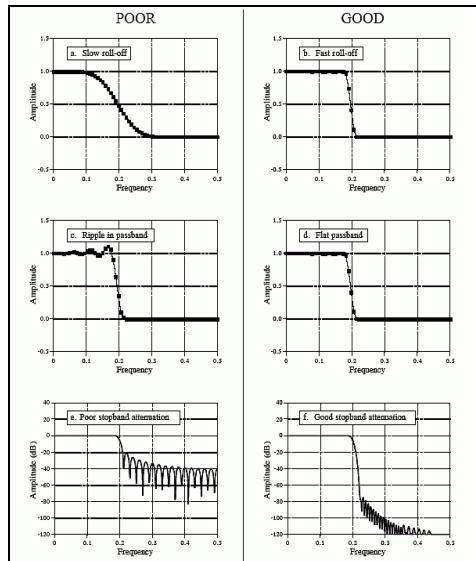


Figure 3. 23 Frequency Response

As shown in Figure 3.23, in order for the filter to be effective, it must have a fast roll-off. Figure 3.23.b shows faster roll-off as compared to Figure 3.23.a, which is desirable. The presence of a ripple in the passband adds distortion to the passband frequencies when moving through filter (Figure 3.23.c). In order to avoid this, no ripple should be present in the passband (Figure 3.23.d), and lastly, to completely block the stopband frequencies, the designed filter should represent good stopband attenuation in frequency response as shown in Figure 3.23.f.

Normally one has to trade off between the two responses as it is not possible to optimize a filter for both applications. A filter designed for step response may not yield good results for frequency response. In order to check our designed filter in the frequency domain, the frequency response of the filter was estimated using MATLAB R2008a; see Figure 3.24 below.

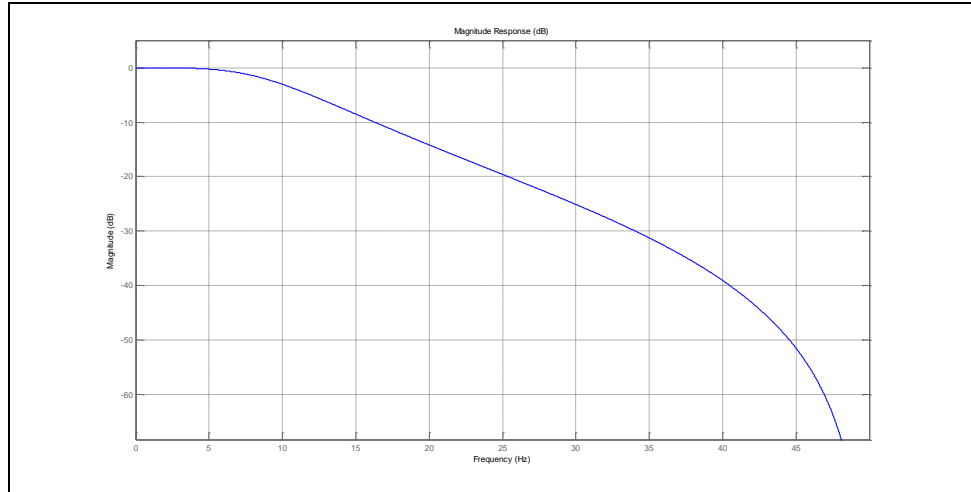


Figure 3. 24 Filter Frequency Response

The frequency response of the designed filter shows slow roll-off, but the passband is flat.

In order to calculate dynamic stability, the present study uses a 10 Hz low pass second-order Butterworth filter. The filter cut-off frequency was selected to assure sufficient bandwidth to represent torso dynamics—i.e. approximately ten times the natural frequency of the torso (Moorhouse and Granata 2005; Winter et al. 1998). The filter was designed in MATLAB R2008a, which also determined the velocity and acceleration from biomechanical displacement signals (See appendix for program).

In order to test this program, a small experiment was carried out using Optotrak 3020 (Northern Digital Inc.; Ontario, Canada) and an accelerometer CXL10HF3 (Crossbow Technology Inc.; California, USA). The Optotrak unit was stationed on a table and connected to the computer through ODAU II and a system control unit. First principal, motion analysis software, was used in conjunction with the Optotrak unit to record the data at 100 Hz. Three infrared markers were firmly attached on the surface of

the accelerometer facing the Optotrak unit using double-sided tape. These markers were supplied with the strober voltage of 9V.

On starting the recording in First principal, the accelerometer was given upward and downward motion for three complete cycles. The Optotrak unit recorded the motion data while the accelerometer simultaneously collected the acceleration data. This data was then exported and saved on the computer hard drive in Microsoft Excel spreadsheet format. The accelerometer data was collected in Volts. To convert this data into  $\text{m/sec}^2$ , zero-G volts of 2.5 V in each particular direction and for the particular accelerometer was subtracted from the available data values. This data was then divided by the sensitivity of 0.105 V/g for that particular direction and multiplied by 9.81 to get the value in  $\text{m/sec}^2$ . Both zero-G voltage and sensitivity values were given in a calibration sheet provided for that particular accelerometer (See Appendix C). Results of this test are shown below (Figure 3.25).

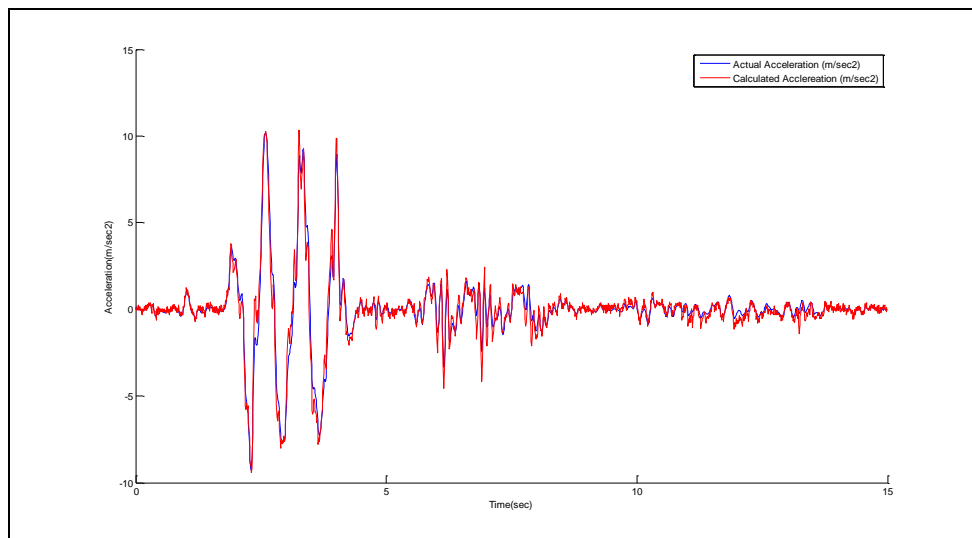


Figure 3. 25 Acceleration using Accelerometer and Filter

As we can see from the graph, values from actual acceleration data taken from accelerometer and values of calculated acceleration computed from the MATLAB R2008a program are in close agreement with each other. To estimate error in numerical value, the Root mean square error of the two signals was calculated using MATLAB R2008a and was found to be 0.4724. This value is very low and suggests that the designed filter is efficient in performance and gives accurate velocity and acceleration data.

### **3.7 Sample Size**

A biomedical study, to be successful, has to have a well-defined problem, appropriate population, a reliable procedure and instruments, among other resources. In addition to these, an adequate sample size is one of the most critical parameters to be considered. It must be “big enough” that it does not waste resources on an inconclusive study, and “short enough” that it can yield useful results in a timely manner. Sample size is of the utmost importance in experiments involving human or animal subjects for ethical issues. In an over-populated experiment, an unnecessary number of participants are exposed to potentially hazardous tests, while under-populated studies expose subjects to potentially hazardous tests without advancing the research knowledge (Lenth, 2001). Finally, the study must be of adequate size, which would be relative to the goal of the study. The present study is a preliminary study, and time and cost are the main constraints. Keeping this in mind, a sample size of five subjects was considered adequate for this study.

## **4. Methodology**

In this approach of estimating the variability of the human spine motion, two methods were employed. In the first approach the subject performed flexion-extension of the spine while sitting on an unstable seat. The second set of data recorded flexion-extension motion of a human cadaveric spine that was motor controlled. Both of these methods were designed and developed by the investigators at Palmer Center for Chiropractic Research, Davenport, Iowa and made available to conduct this study.

As with most Biomechanical studies, this study involved instrumentation that accurately recorded the spine's movement. Tests were carried out on human subjects and a cadaveric spine. Each of these tests had specific goals and procedures as described below.

### **4.1 Instrumentations for Tests on Human Subjects**

A six-degree electromagnetic tracker, Liberty 24/8 (Polhemus, Vermont, USA) unit in conjunction with Motion Monitor software was used to record human lumbar movement in human subjects. 4 sensor channels were attached to the ports available on the chassis of Liberty, the other ends of which were attached to the T1, L1, L3, and S1 vertebral levels of the subject's spinous processes. The data was recorded at a maximum speed of 120 updates per second.



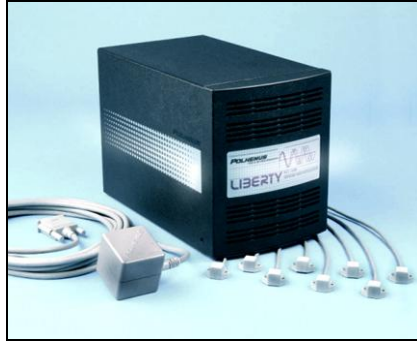


Figure 4. 1 Polhemus Unit

The Liberty unit consists mainly of the following:

a) System Electronic Unit (SEU):

System electronic units interface with the host computer via USB port and consist of the hardware and software necessary to generate and sense the magnetic field and estimate the position and orientation.

b) Source:

The source is a plastic-enclosed cube which contains electromagnetic coils that generate the magnetic field around it. It acts as the system's reference frame for sensor measurement.

c) Sensors

The sensor is a small plastic-coated cube composed of electromagnetic coils that detects the magnetic field generated by the source. It precisely measures the position and orientation as it moves. The sensor is a passive device (i.e. no active voltage is applied to it).

The Liberty unit was used with Motion Monitor software to record the human lumbar motion and export the data. The software allowed independent user-defined profiles for setting system parameters such as coordinate rotations, output format, etc.

The user can select positions in Cartesian coordinates, Euler angles, and orientations in direction cosines or quaternion's. It can be used to set tracker parameters such as sampling frequency, recording time, calibration, etc.

The general workings of the Liberty unit are described as follows:

- The source generates an electromagnetic field around it.
- This electromagnetic field is sensed by an activated sensor.
- Upon starting the recording using Motion Monitor, the motion is recorded at a sampling rate of 120 Hz and the sensors output is given as input to the host computer through the SEU.
- This data is then saved on the computer RAM for further processing and display.

#### **4.2 Experimental Set-up**

The study required subjects to perform continuously repeated trunk flexion extension-movements while sitting on an unstable seat. On its bottom, the rectangular cushioned seat (15 × 9 inches) had semi-circular wedges on either side that restricted its movement in the subject's anterior-posterior direction. The seat was kept on wooden structure, the height of which could be adjusted. A safety railing was provided on either side of the wooden structure to provide safety in situations in which subjects might lose their balance or feel discomfort during the test. The source unit was stationed on the posterior side of the seated subject at a distance of 10 inches. In order to avoid any interference with the electromagnetic field developed by the source, the whole structure was made out of wood.

During the test, subjects were asked to sit on the unstable seat with their hips and knees flexed at an angle of 90 degrees. To help shorter subjects maintain the 90-degree

knee angle, a wooden board (36 × 24 × 1 inches) was placed underneath their feet. The wooden board was placed on a rubber mat so as to avoid any slippery action.

### **4.3 Human Subjects**

5 subjects with no history of low back pain were recruited and performed repetitive trunk flexion-extension tasks. All 5 subjects were male. The criteria were as follows:

Inclusion Criteria:

- a) Men and women aged 18 to 65 years, with no history of LBP.
- b) Subjects would be examined by a professional clinician to evaluate whether they were healthy enough to perform biomedical tests.

Exclusion Criteria:

- a) Co-morbid pathology such as bone and joint pathology, extreme obesity, etc.
- b) Poor general health condition.
- c) History of spine surgery.
- d) Pregnancy.

Each eligible participant signed an institutional review board (IRB) approved informed consent form. The consent form was approved by both the Auburn University IRB and the Palmer College of Chiropractic IRB.

### **4.4 Data Acquisition**

Each of the selected participants was given a randomized unique 5-digit code and was identified with that particular code. Before performing the actual biomechanical tests each participant had to answer different written questionnaires. A brief video

demonstrating the biomechanical test was shown to each participant. A quick double-sided tape skin test was performed on each participant in order to check for any allergic reactions. Upon successfully completing the aforementioned tasks, the height and weight of each participant was measured and entered into the computer system. All the relevant information (such as height, code, and weight) for each participant was written on the biomechanics test log form. (See appendix C for details.) Upon entering the biomechanics laboratory, the lumbar repositioning (flexion-extension test) was briefly explained to each participant. Before starting the test each participant was asked whether there were any removable or non-removable metal objects on his body. If they had any non-removable metal such as a surgical plate or rod, a note was made on that particular subject's test log form. However, if participants had any removable metal on their bodies, they were asked to remove it (if possible), as metal parts may cause interference with the magnetic field generated by the source of the Liberty unit. The participant was then asked to sit straight on the unstable seat, making 90-degree angles at the knees and hips. If the participant was short a wooden board (Riser) was placed underneath the participant's feet in order to maintain the 90-degree knee angle. Two pieces of white tape were placed at the toes of each participant and tendon to center of the unstable seat distance was recorded on the test log form so that if the participants took a break in between the subtests and wished to stand, they could return to same sitting position after the break.

The test setup began with palpating the spinous processes of participants in order to identify the vertebral levels (T1, L1, L3, and S1). Meanwhile the sensors were activated. These levels were then noted on the test log form and marked with a water-soluble skin marker. An alcohol cleaning pad was used to clean these levels so that the

markers would firmly stick on the spinous processes using double-sided tape. These sensors were then covered with a piece of tape in order to prevent the double-sided tape from sticking to participant's clothes.

At this point each participant was asked to sit upright wearing the blindfold and cross his arm across the chest, resting on the shoulder (As shown in figure 4.2). This position was called neutral position. Every participant performed seven subtests. Each subtest had a different starting position, which was called the target position, and a different starting direction. The aim for the participant, starting each subtest at a different starting position (target position) and in different starting directions, was to return to the target position after rocking the pelvis forward and backward for ten complete cycles. The target position could be either neutral, between neutral and extreme forward, or between neutral and extreme backward.



Figure 4. 2 Subject in Test Position

Participants were asked to move at a comfortable speed and comfortable range and stop the test at their discretion. This represented their natural movement. This self-selected speed eliminates any potential risk to the low back due to predetermined speed. In order to avoid fatigue, every participant was given two mandatory short breaks after the second and fifth subtests. Each subtest, depending on the permutation and combination of the starting position and starting direction, was addressed with different alphabetical notations as:

Table 4. 1 Subtests

<b>Test</b>	<b>Starting Position</b>	<b>Starting Direction</b>
RA (NF)	Neutral	Forward
RB (FF)	Forward	Forward
RC (FB)	Forward	Backward
RD (BF)	Backward	Forward
RE (BB)	Backward	Backward
RF (NF)	Neutral	Forward
RG (NB)	Neutral	Backward

#### **4.5 Data Analysis**

The main aim of data analysis was to extract useful information from the recorded signal that can be processed further to understand the results. The motion monitor program was mainly used for this purpose. It provided an interface to observe the real-time data, and to record and manage the data. A preference file with certain parameters was created and saved in order to set up the test. It mainly required two parameters as input (i.e. height and weight of the subject), after which the test could be recorded. The

recorded data displayed the graphs of parameters such as flexion-extension, lateral flexion, rotation, etc. Each graph showed cursor value and the minimum and maximum of that graph in the upper right corner, which is advantageous in analyzing the real-time data. The recorded data was stored on the computer hard drive with a specific participant code. All saved data was exported by loading the same preference file which would extract particular information from that data (Figure 4.3).

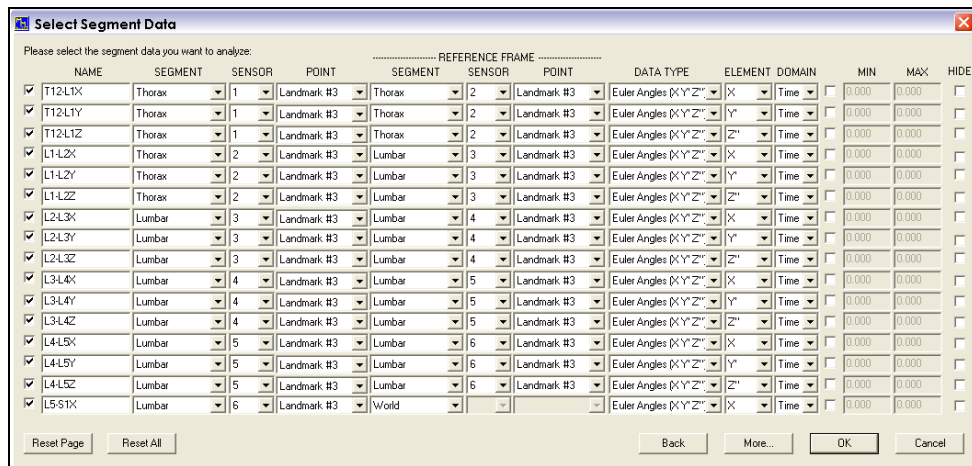


Figure 4. 3 Data Export

A time series of 10 cycles was analyzed. This allowed for the evaluation of both linear and nonlinear methods. The continuous 10 cycles allowed examination of an average of 3000 data points for each subtest. This number was considered adequate for the nonlinear analysis performed in this study (Stergiou, 2004; Pincus 1994; Harbourne, et. al 2003). It was assumed that because the same instrument was used for all subjects, the level of noise from the measurement would be consistent in all cases. Therefore, any differences would be due to the changes within the system (Kaplan et. al, 1995).

As mentioned before, to quantify the variability during lumbar movement in terms of nonlinear dynamics, the Approximate Entropy (ApEn) method was used. Entropy is a statistical concept, which was first introduced by Shanon and Weaver in 1963 as a

measure of uncertainty or variability. Similarly, ApEn is a specific method to determine complexity that can quantify the regularity or predictability of a time series (Pincus, 1994). Predictability and regularity are inversely proportional to complexity. The more predictable and regular the time series, the less would be the complexity, and vice versa. Approximate Entropy measures the logarithmic probability that a series of data points a certain distance apart will exhibit similar relative characteristics on the next incremental comparison within the state space (Pincus, 1994). Data points that exhibit greater possibilities of remaining the same distance apart upon comparison will result in lower ApEn values, while those with large differences in distance between them will result in higher ApEn values.

In order to mathematically define ApEn, we need to form a time series of data  $u$  (1),  $u$  (2) .....  $u$  ( $N$ ). These are  $N$  raw data values from measurements taken at equally spaced points in time. We then fix  $m$ , an integer, and  $r$ , a positive real number. The input parameter  $m$  is the length of compared runs, and  $r$  is the tolerance that specifies a filtering level. The first step is to form a sequence of vectors  $x(1), x(2), \dots, x(N - m + 1)$  in  $R^m$ , real  $m$ -dimensional space, defined by  $x(i) = [u(i), \dots, u(i + m - 1)]$ . The second step is to use the sequence  $x(1), x(2), \dots, x(N - m + 1)$  to construct for each  $I, 1 \leq i \leq N - m + 1$ ,  $C_i^m(r) = (\text{number of } x(j) \text{ such that } d[x(i), x(j)] \leq r) / (N - m + 1)$ . We must define  $d[x(i), x(j)]$  for vectors  $x(i)$  and  $x(j)$ . We follow the Takens modification of formula by defining  $d[x, x^*] = \max |u(a) - u^*(a)|$ , where the  $u(a)$  are the  $m$  scalar components of  $x$ .  $d$  represents the distance between the vectors  $x(i)$  and  $x(j)$ , given by the maximum difference in their respective scalar components. Next we define  $\Phi^m(r) = (N - m + 1)^{-1}$



$\sum_{i=1}^{N-m+1} \ln C_i^m(r)$ , where  $\ln$  is natural logarithm. Lastly we define Approximate Entropy as:

$$\text{ApEn}(m,r,N) = \Phi^m(r) - \Phi^{m+1}(r)$$

As seen above, calculation of ApEn requires selection of two parameters:  $m$ , the number of observation windows to be compared, and  $r$ , the tolerance factor. In order to compare the results, these parameters, along with the data length, must be kept the same for all calculations (Pincus and Goldberger, 1994).

Typically  $m = 2$  or  $3$ ;  $r$  depends greatly on the application (Pincus et. al, 1991). This choice of  $m$  is made to ensure that the conditional probabilities, defined in the equation below for fixed  $m$  and  $r$ , are reasonably estimated from the  $N$  input data points. Theoretic calculations indicate that reasonable estimates of these probabilities, for fixed  $m$  and  $r$  chosen as discussed below, are achieved with between  $10^m$  and  $30^m$  points, analogous to findings of Wolf et al. (Pincus et. al, 1991).

An important observation that we can deduce from the ApEn definition is:

$$-\text{ApEn} = \Phi^{m+1}(r) - \Phi^m(r) = \text{average over } I \text{ of } \ln [\text{conditional probability that } |u(j+m) - u(i+m)| \leq r, \text{ given that } |u(j+k) - u(i+k)| \leq r \text{ for } k = 0, 1, \dots, m-1] \dots \dots \dots (A)$$

The number of input points for ApEn computations ranges typically from 50 to 5,000 points (Stergiou, 2003; Pincus, 1994; Pincus et. al, 1991). Using fewer than 50 data points yields less meaningful results, especially for  $m = 2$  or  $3$ , while using more than 5,000 points will result in unacceptably long computational time (Pincus et. al, 1991).

For noiseless, theoretically described systems, such as Henon maps and logistic maps, it has been shown that if entropy  $(A) \leq$  entropy  $(B)$ , then  $\text{ApEn}(m, r)(A) \leq \text{ApEn}(m, r)(B)$  and vice versa. Moreover, for both theoretical and experimental systems, if

$\text{ApEn}(m_1, r_1)(A) \leq \text{ApEn}(m_1, r_1)(B)$ , then  $\text{ApEn}(m_2, r_2)(A) \leq \text{ApEn}(m_2, r_2)(B)$  and vice versa. This ability of ApEn to preserve the order is a relative property and is an important utility of ApEn (Pincus et al, 1991). Considering this, one should not conclude that for the same systems,  $\text{ApEn}(m_1, r_1)(A) \leq \text{ApEn}(m_2, r_2)(B)$ , as ApEn values differ with different  $m$  and  $r$  values. The strength of ApEn is its ability to compare systems.

As explained above there are two critical parameters ( $m$  and  $r$ ) that need to be set in order to achieve reasonable results while using ApEn. Different  $m$  and  $r$  values would result in different results.  $\text{ApEn}(2, 0.1)$  may be different from  $\text{ApEn}(3, 0.01)$  values. This leads to the question of which one should be chosen. ' $r$ ' is effectively a filter level and in order to eliminate the effect of noise in the ApEn calculation, ' $r$ ' must be chosen such that its value is above most of the noise. In order to achieve reasonable results the magnitude of noise should rarely reach ' $r$ '.

Another key factor in choosing the value of  $r$  is that it should be large enough to achieve numerically stable conditional probability estimates in equation (A) above (Pincus et. al, 1991). If the ' $r$ ' value is small, one gets unstable conditional probability estimates, while larger ' $r$ ' values results detailed system information to be lost due to filter coarseness. In the current study a value of 2 was used for  $m$  and  $r$  was 0.2 (Pincus 1990; Pincus 1994; Stergiou, 2004).

#### **4.6 Calculation of ApEn**

Consider a time series  $S_N$ , consisting of  $N$  number of sample size. To compute ApEn we must choose two input parameters,  $m$  and  $r$ . We denote a pattern of  $m$  time series, beginning at measurement  $i$  within  $S_N$ , by the vector  $p_m(i)$ . Two patterns,  $p_m(i)$  and

$p_m(j)$  , are said to be similar if the difference the difference between any pair of corresponding measurements in patterns is less than  $r$ , i.e, if

$$|N(i+k)-N(j+k)| < r, \text{ for } k=0 \text{ to } m$$

Now consider the set  $P_m$  of all patterns of length  $m$  (i.e.,  $p_m(1), p_m(2), \dots, p_m(N-m+1)$ ), within  $S_N$ . So we may define  $C_{im}(r) = n_{im}(r) / (N-m+1)$  where  $n_{im}(r)$  is the number of patterns in  $P_m$  that are similar to  $p_m(i)$  (provided similarity criterion ' $r$ '). The quantity  $C_m(r)$  is the fraction of length  $m$  that is identical to the pattern of the same length that begins at interval  $i$ . We can calculate  $C_{im}(r)$  for each pattern in  $P_m$ , and we define  $C_m(r)$  as the mean of these  $C_{im}(r)$  values. The quantity  $C_m(r)$  expresses the prevalence of repetitive patterns of length  $m$  in  $S_N$ . Finally, we define approximate entropy of  $S_N$ , for patterns of length  $m$  and similarity criterion  $r$ , as

$$\text{ApEn}(m, r) = \ln[C_m(r) / C_{m+1}(r)]$$

Thus, if we find similar patterns in a time series, ApEn estimates the logarithmic likelihood that the next intervals after each of the patterns will differ. Smaller values of ApEn imply greater likelihood that similar patterns of measurements will be followed by additional similar measurements. If the time series is highly irregular, the occurrence of similar patterns will not be predictive for the following measurements, and ApEn will be relatively large.

#### **4.7 Instrumentation for Test on Cadaver Spine**

In this approach of testing a cadaver spine, a six-degree-of-freedom motion tracking device, Optotrak 3020 (Northern Digital Inc. Ontario, Canada) along with 7 sensors were used. Each sensor was an L-shaped acrylic bracket with 3 infrared markers (Northern Digital Inc. Ontario, Canada) that emits infrared signals. 6 out of 7 sensors

were used to attach to different levels of the cadaver specimen (T12-L5). The seventh sensor was attached to a specially designed stylus which served as a digitizer (Figure 4.4). Each infrared marker was attached to a stober unit. Every stober unit could accommodate only 2 sensors at a time. Hence, a total of 4 stober units were used. Each stober unit was daisy-chained to the preceding stober unit in order to provide additional ports. Every stober unit incorporates an LED that indicates power and status information. These stober units were supplied with a stober voltage of 6.4V through the System Control Unit (SCU).



Figure 4. 4 Optotrak SCU and Stober Units with Markers on Sensors

The System Control Unit provides interference between the Optotrak 3020, the stober unit and the markers. It allows quick and easy triggering and synchronization of third-party devices. One port of the SCU was connected to the Optotrak Data Acquisition Unit II (ODAU II); it is used for true-synchronous capture of data from third-party hardware devices such as force plates, pressure transducers, etc. Another port was connected to the Optotrak 3020 unit that detects the perturbation of infrared markers on triggering. A computer is connected to the SCU through the PCI card. The PCI card provides the port in order to connect the SCU to the computer.

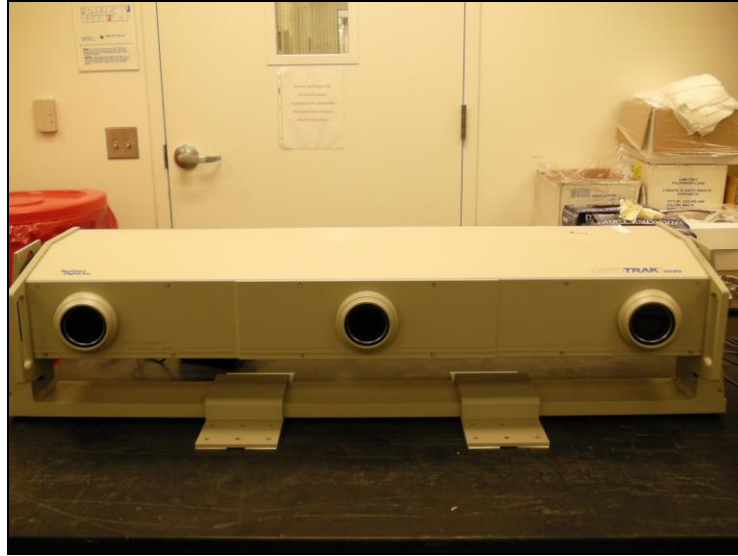


Figure 4. 5 Optotrak 3020 Unit

In our effort to understand the inter-vertebral variability due only to injuries made in the cadaver spine, we wanted to keep other parameters such as motion control, distance of movement, etc. fixed. If we had controlled the cadaver motion by hand, there would have been variability due to injuries as well as due to hand movement. Hence, we used a servo motor (CMC Cleveland, OH, USA) to control the flexion-extension movement of the cadaver spine. This servo motor was triggered by another computer using the Labview program (National Instrument, Austin Texas). The Labview program provided an interface to write the program in order to control the motion of servo motor. The servo motor had a plunger that could move forward and backward by the displacement and time/cycle given as input to the Labview program. A specially designed U-joint yoke was attached to the tip of a plunger. The U-joint yoke provided a flexible connection between the cadaver specimen and the motor plunger. A steel cup of a 6-inch diameter was firmly fixed to the leveled table through a force transducer, which could measure the forces and moments with respect to global axes. This cup could accommodate the PVC cup that was fixed to the sacrum of the cadaver spine that provided the stability and support to the

cadaver spine. Eight Philips-head screws were used to restrict the motion between the PVC cup and the steel cup.

On triggering the servo motor using the computer, the servo motor plunger pushed and pulled the specimen with a defined distance for a complete 10 cycles. Simultaneously a pulse was sent out to the SCU, which then triggered the Optotrak 3020 unit. On activating, the Optotrak 3020 system precisely detected the markers' movement and sent those signals to the computer, which then saved them on the computer RAM. Motion monitor (Innovative Sports Training, Inc. IL) software was used to display, record, play back and manage the data.

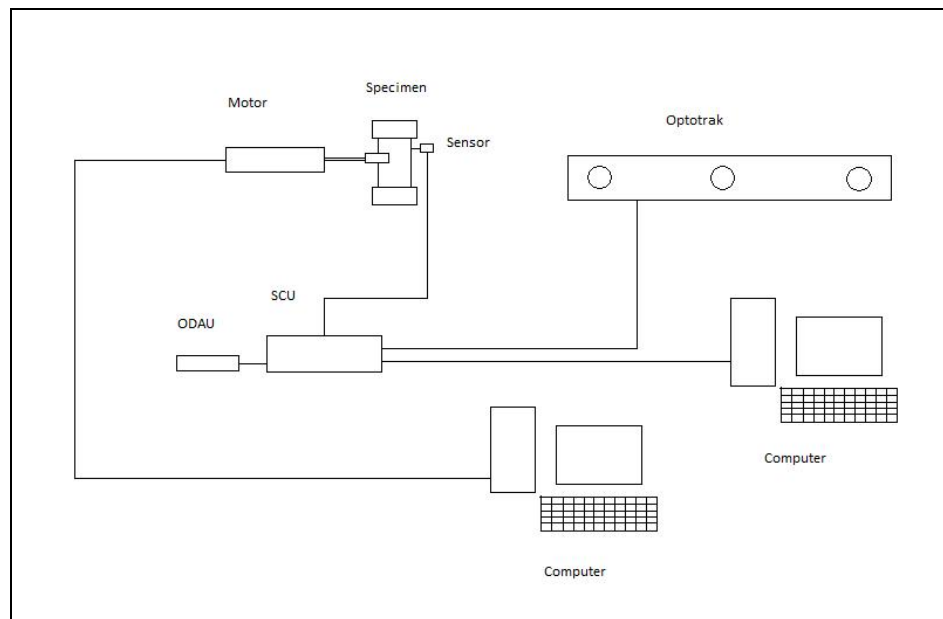


Figure 4. 6 Schematic Diagram of the Set-up

#### 4.8 Potting the Specimen

In order to carry out a test on cadaver specimen, it needs to be prepared so that the specimen can accommodate the steel cup firmly fixed at the sacrum level. Two different-sized PVC cups of diameters 5 inches and 4 inches were fixed using (8d) screws at the T12 and S1 levels, respectively. In order to get permanent fixed joint, additional filling material (Bondo body filler) was used to fill the cup. On solidification, the screws and the filling material provided a firm joint between the cups and the cadaver spine.

#### 4.9 Digitization

As mentioned before, there are several vertebral levels in the lumbar spine. Each of these vertebrae is interconnected to each other through a facet joint that provides flexibility between these vertebrae. As a result each vertebra moves differently with respect to the others and the global coordinate system. In order to estimate the motion of different vertebrae, we need to align each intervertebral local coordinate axis with the global coordinate axis. This is achieved through the process of digitization.

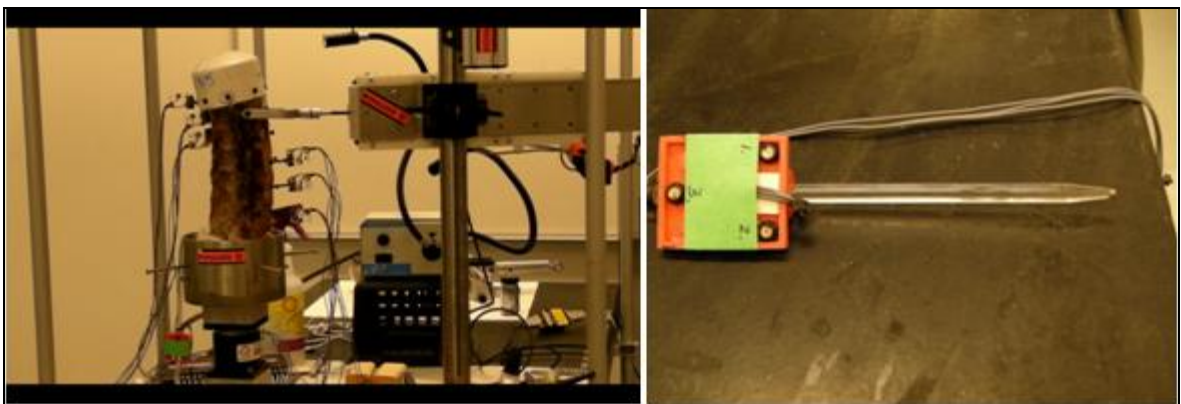


Figure 4. 7 Cadaver Test Set-up and Stylus with Markers

For digitization 3 small Philips headed screws (2d) were drilled at the anterior and 2 sides, making 90 degree angles with each other at each vertebral level of the cadaver spine (T12-L5). These screws were placed anteriorly, right laterally, and left laterally to determine the local coordinate axes for that particular vertebral level. The specimen was fixed to the steel cup so that it was vertical. A stylus with a copper ball (diameter = 3mm) was used as digitizer. It was used to record the position of each of those small screws during the initial set-up for the Motion Monitor software. Each position data was recorded for a period of 2 seconds. A total of 18 data samples were collected for each small screw.

Alongside the small screws on the anterior/posterior sides of the specimen another screw (6d) was drilled at each vertebral level on the specimen. These screws facilitated the attachment of each sensor at different vertebral levels. In order to fix the yoke to the spine, these screws were drilled on the posterior side for the upper vertebral levels (T12-L2). For the lower levels (L3-L5), these screws were fixed on the anterior side of the cadaver spine.

#### **4.10 Data Acquisition**

The cadaver specimen with two PVC cups attached at each end was mounted vertically on the steel cup using four 20d-sized screws. A yoke extending from the servo motor plunger was attached at the L1 level of the cadaver, so that it could restrict its motion in the anterior-posterior direction. A sensor with 3 markers each was fixed to each screw at different vertebral levels on the cadaveric spine.

The cadaveric specimen was tested for the effects of speed and injuries to the intervertebral segments. Upon running the Labview program, which also triggered the



Optotrak unit, the servo motor reciprocated the plunger in the anterior-posterior direction for 10 complete cycles. This resulted in intervertebral movements in the specimen which was then recorded by the Optotrak unit. The same procedure was repeated at a higher plunger speed and was recorded. On completion of this test, the specimen was then cut about an inch deep on the right side of the disc at the L4-L5 level using an incision blade. The complete aforementioned procedure was then repeated twice at 2 different speeds. The test progressed with making another inch-deep cut at the L4-L5 level on the right hand capsule of the cadaveric specimen. Triggering the servo motor resulted in intervertebral movement in the cadaveric spine which was recorded simultaneously by the Optotrak 3020 unit.

#### **4.11 Data Analysis**

Motion Monitor software was used for recording and extracting important information from the data. The software provided a platform to set up the experiment, a global coordinate system, and markers, as well as selecting the frame rate. It allowed a real-time visual feedback. It provided an option to trigger with an external pulse from ODAU to record the signal without actually hitting the record button.

The experiment was first set up using the digitizing process, by recording the signal for two seconds at each vertebral level. Following digitization, the data was recorded for a period of 20 seconds at a frequency of 100 Hz, which was triggered externally. A preference file with certain parameters was created and saved. After loading the preference file, the recorded data displayed the graphs of flexion-extension. The data was then saved to the hard drive of the computer in .exp format. This saved data, when exported loading the same preference file, extracted only the intended information

described by the preference file, such as the flexion- extension data. This file was in ASCII format which was then converted to the Excel file and loaded in the MATLAB R2008 to process it further for linear and nonlinear methods.

## **5. Results**

Linear tools such as mean, standard deviation, and coefficient of variation, and nonlinear techniques such as approximate entropy were calculated to estimate the neuromuscular control of stability during repeated trunk flexion-extension movements in human subjects and the cadaveric spine. Phase plane plots for flexion-extension time series data were also calculated.

### **5.1 Human Volunteer Study**

Subjects included 5 males with no history of lower back pain and with average mean age = 31.5 years, SD = 12.32 years; mean weight = 64.47 kg, SD = 7.184 kg; and mean height = 67 inches, SD = 2.371 inches. All subjects were physically examined by a professional clinician before entering the study. Each participant performed seven subtests with different starting positions and directions. The phase plane plots for each subtest are shown below.

# Phase Plane Plots for Subject #1

RA

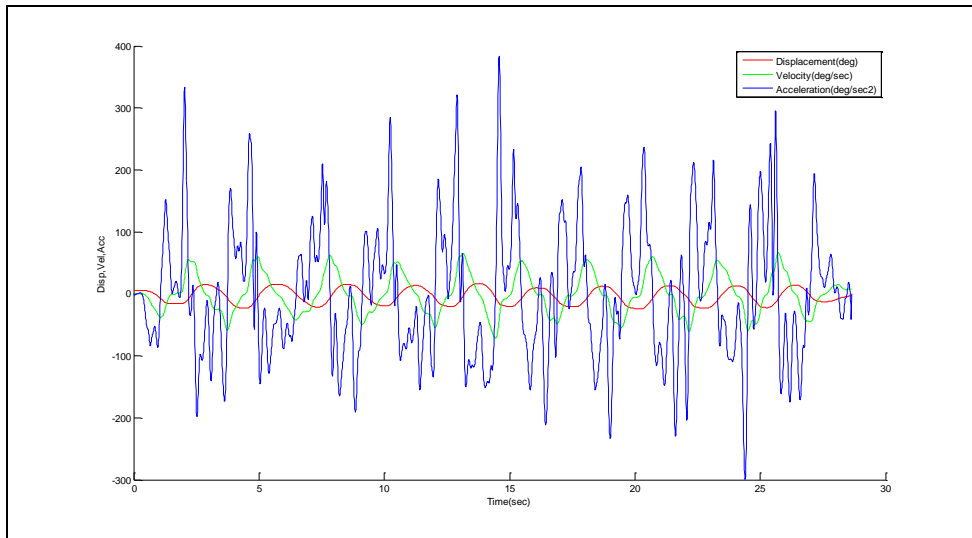


Figure 5. 1 Displacement Time Series with Velocity and Acceleration

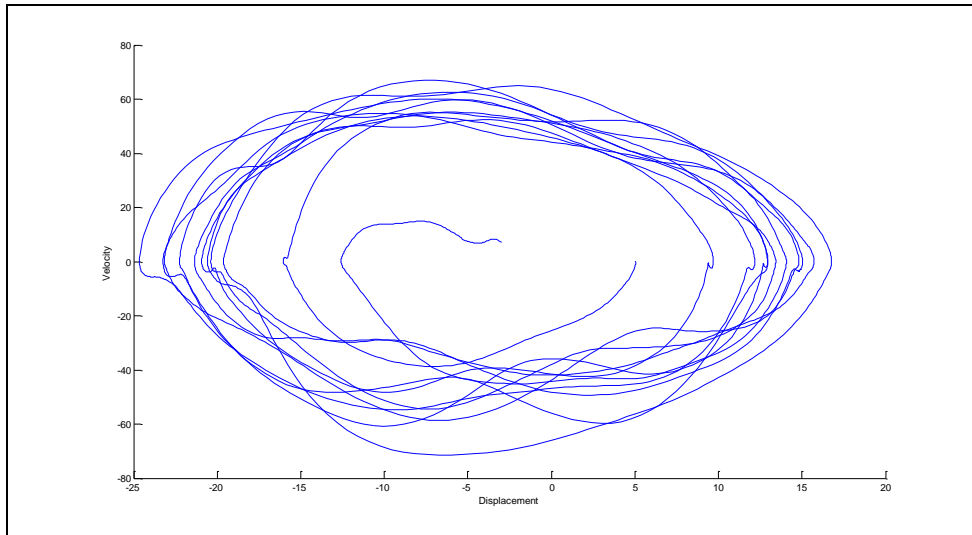


Figure 5. 2 Phase Plane Plot

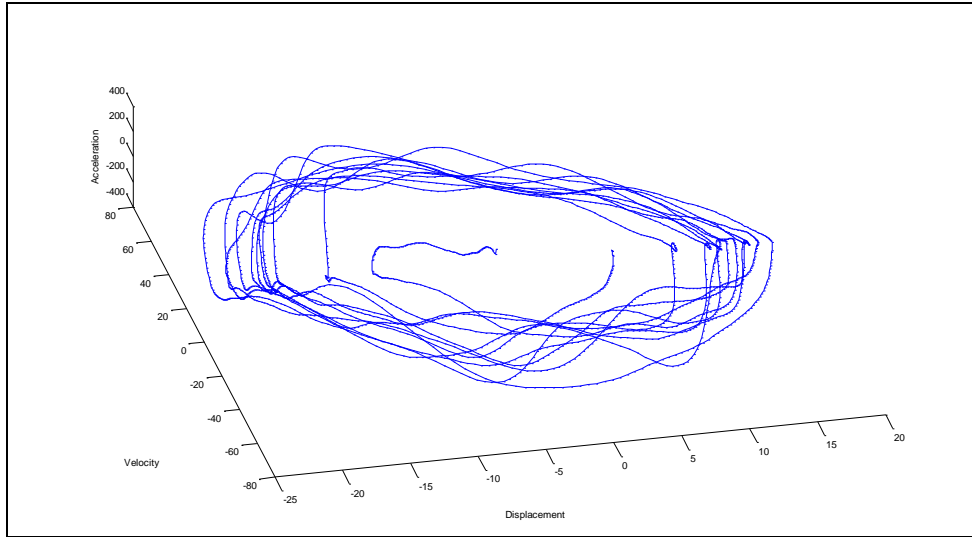


Figure 5. 3 3-D Phase Plane Plot

Figure 5.1 shows the displacement time series with velocity and acceleration for the lumbar flexion-extension movement, with neutral as starting position and forward as starting movement. As seen from figure 5.2 and 5.3, the phase plane plots show some elegant patterns with some divergence in the trajectories. Hence, the structure can be thought of having less variability.

**RB**

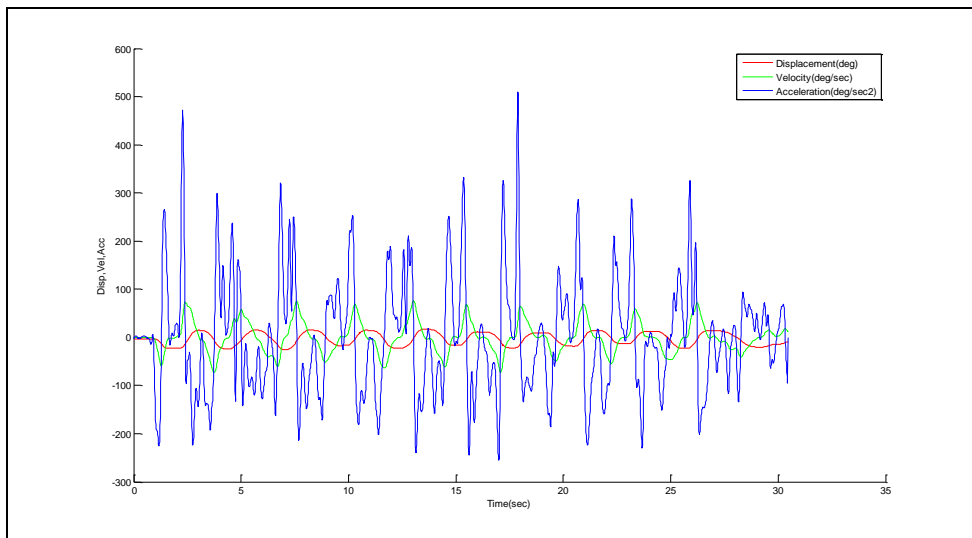


Figure 5. 4 Displacement Time Series with Velocity and Acceleration

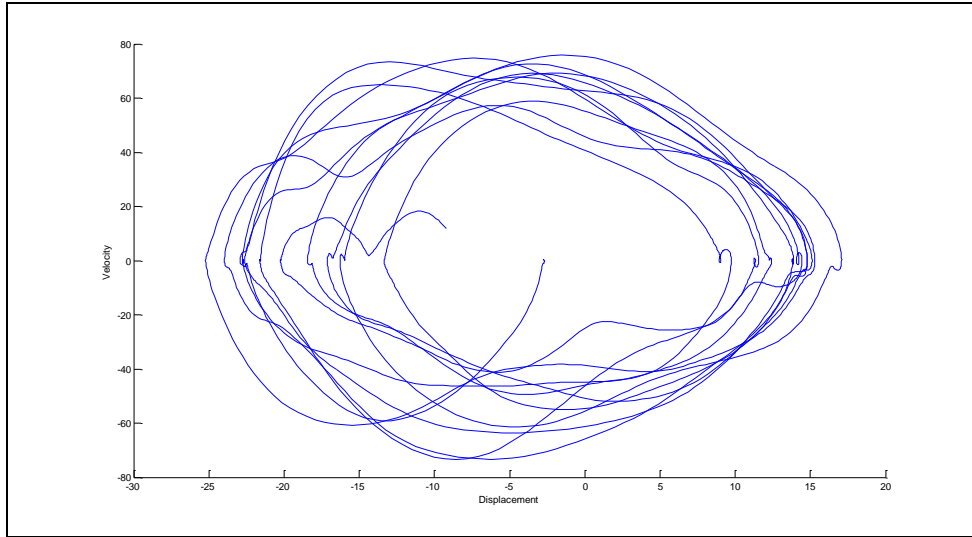


Figure 5. 5 Phase Plane Plot

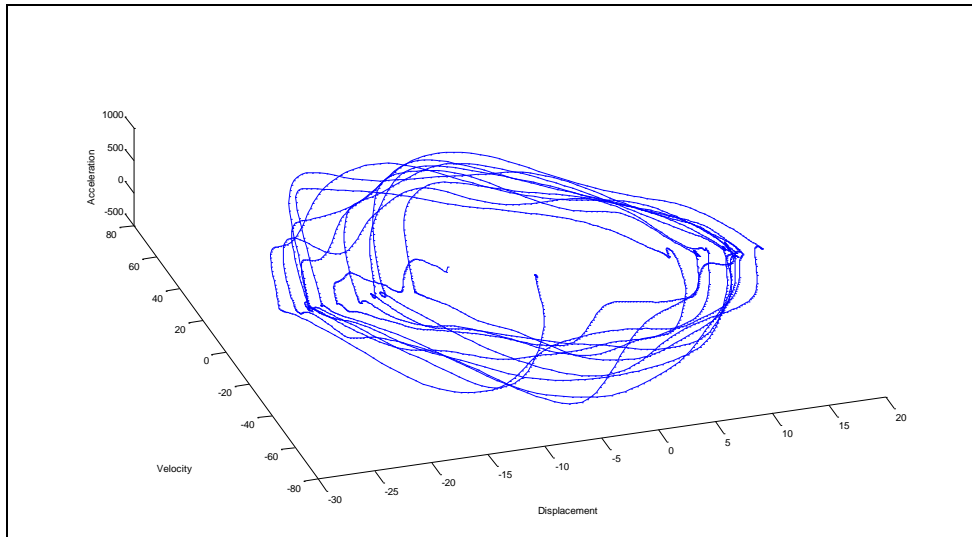


Figure 5. 6 3-D Phase Plane Plot

Figure 5.4 shows a time series with forward as starting position and direction of first motion. Compared to phase plots of RA (Neutral-Forward) movement, these phase plane plots show more divergence in their trajectories. It can be concluded that this may be due to more variability.

RC

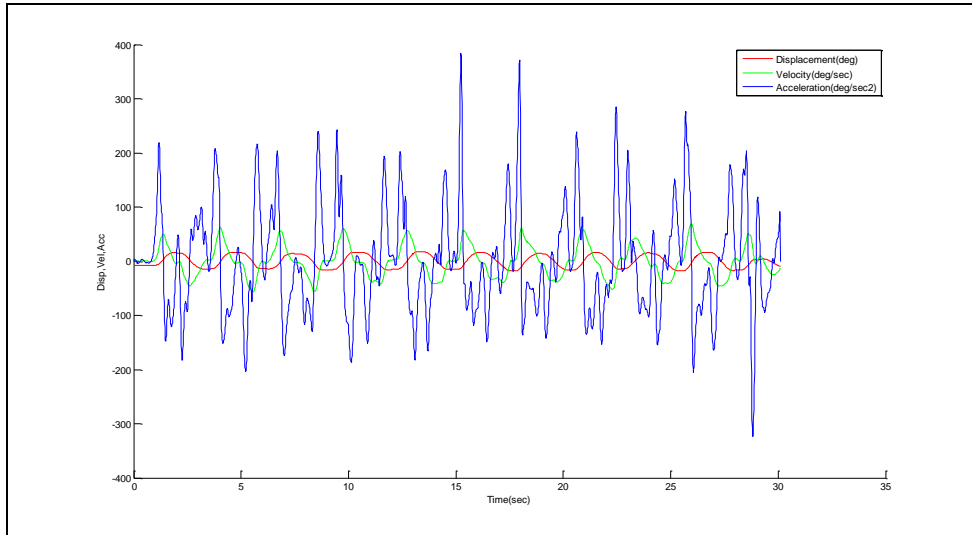


Figure 5. 7 Displacement Time Series with Velocity and Acceleration

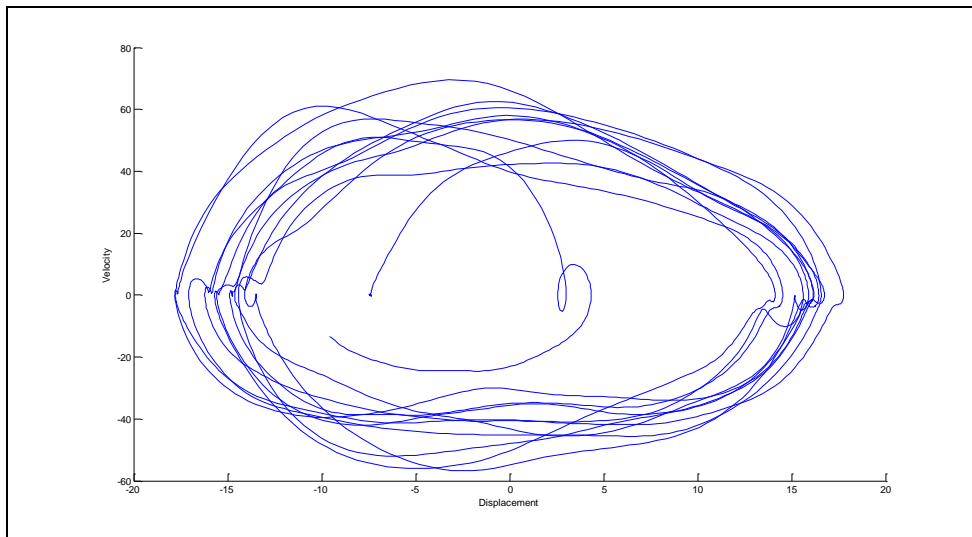


Figure 5. 8 Phase Plane Plot

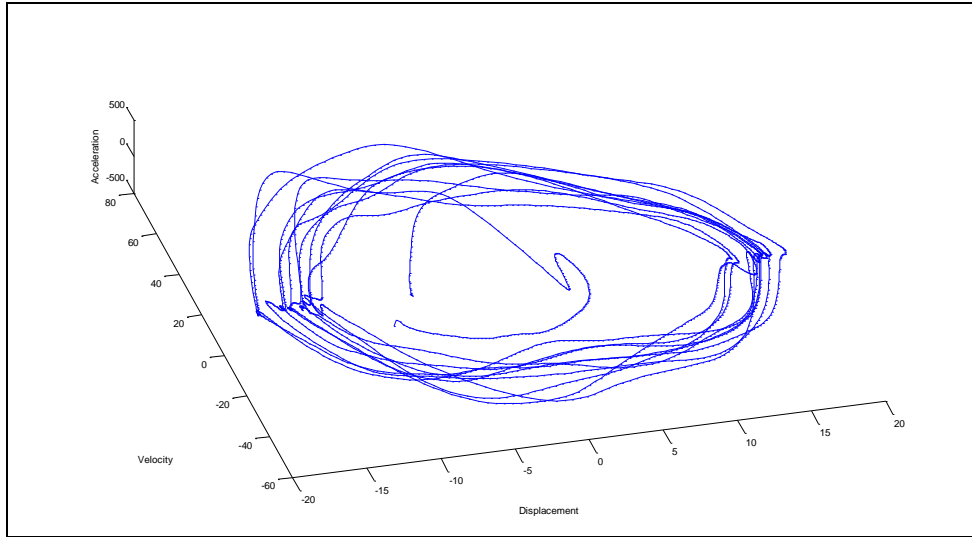


Figure 5. 9 3-D Phase Plane Plot

The time series for forward target position and backward starting movement is shown in figure 5.7. The phase plane plots for the RC subtest has more periodic pattern and less divergence in the trajectories. It can be said that its variability is near to the variability of the RA subtest.

**RD**

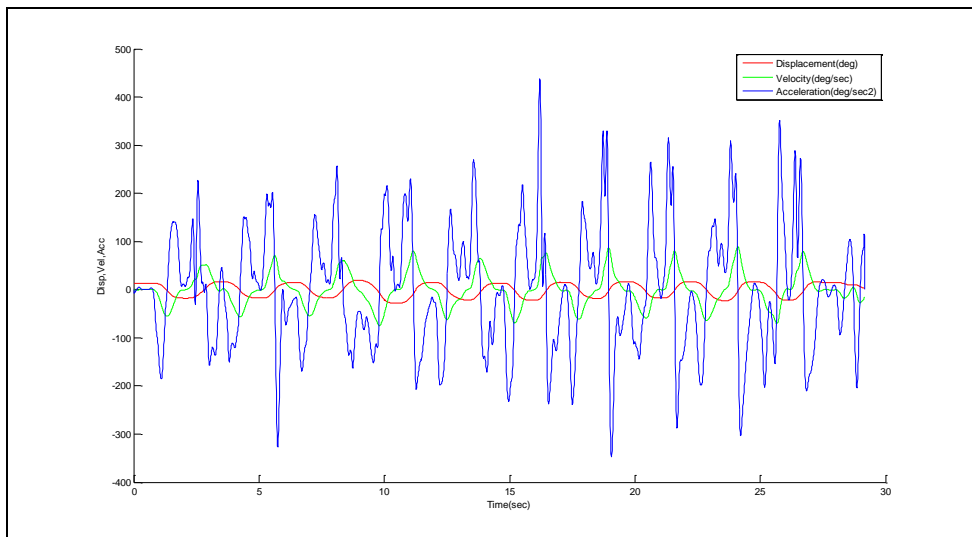


Figure 5. 10 Displacement Time Series with Velocity and Acceleration



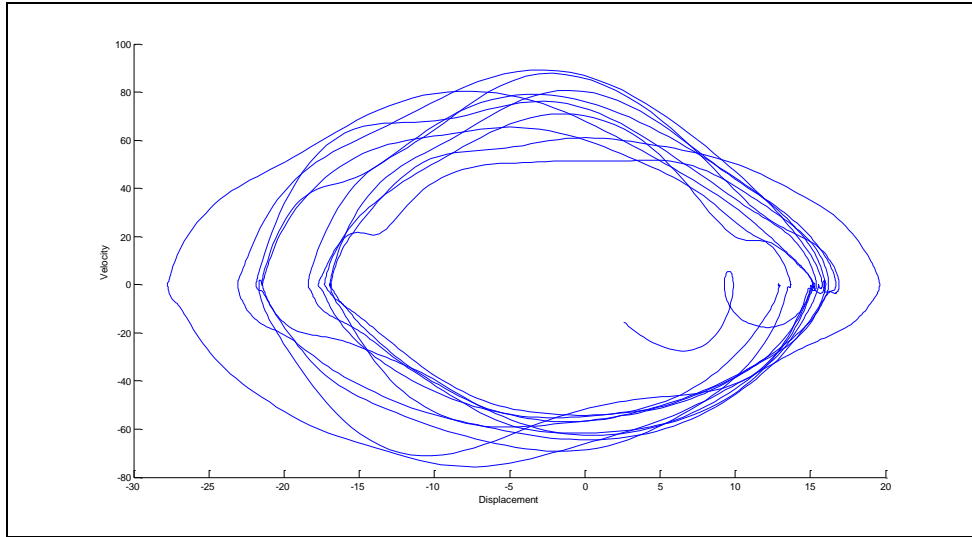


Figure 5. 11 Phase Plane Plot

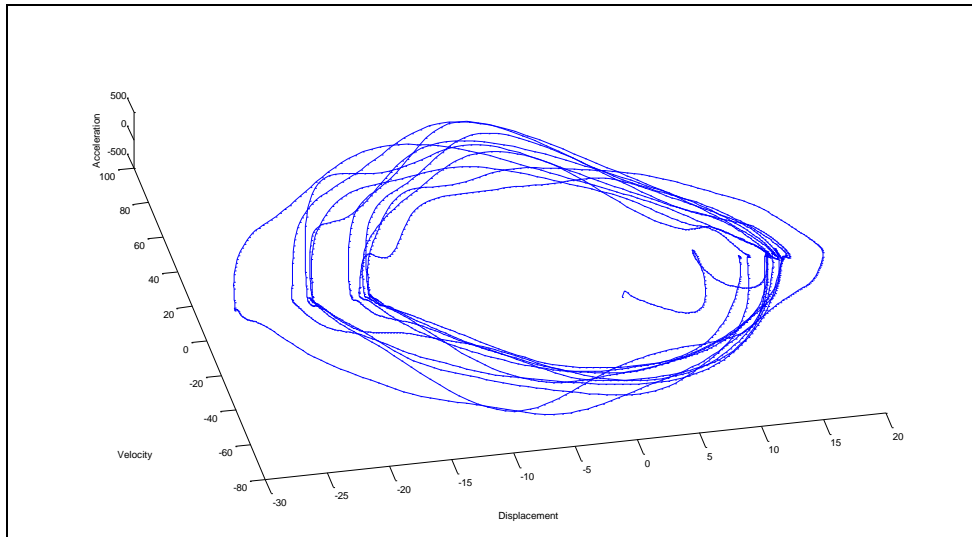


Figure 5. 12 3-D Phase Plane Plot

The divergence in the trajectories is evidence of variability in the structure of the time series. It can be seen that the trajectories separate out with greater distance on the left side of the phase plane plot (Figure 5.8). These phase plane plots are plotted for backward target position and first motion as forward.

RE

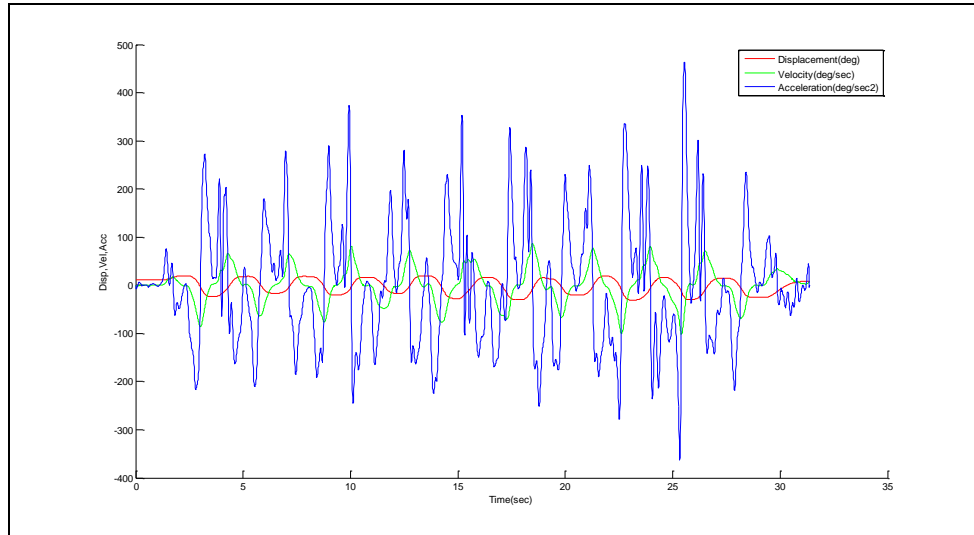


Figure 5. 13 Displacement Time Series with Velocity and Acceleration

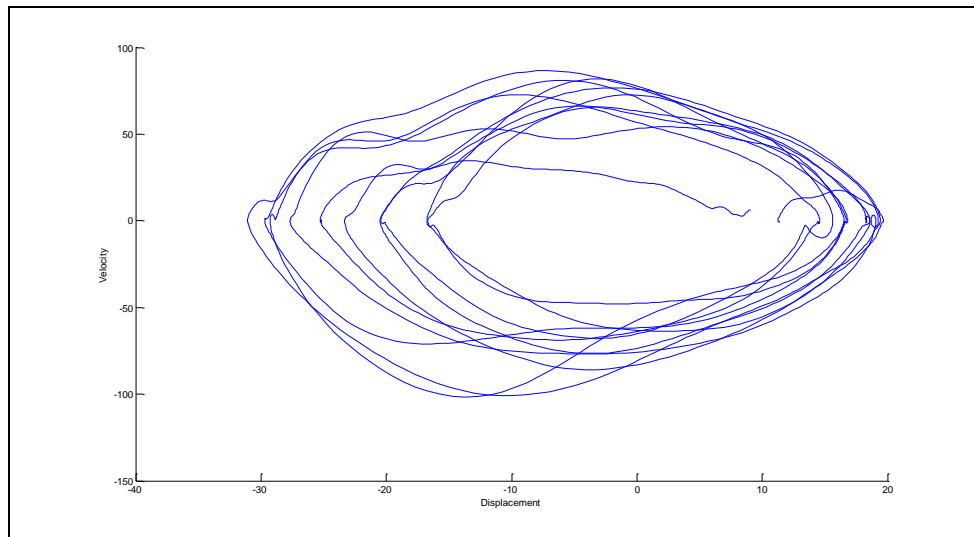


Figure 5. 14 Phase Plane Plot

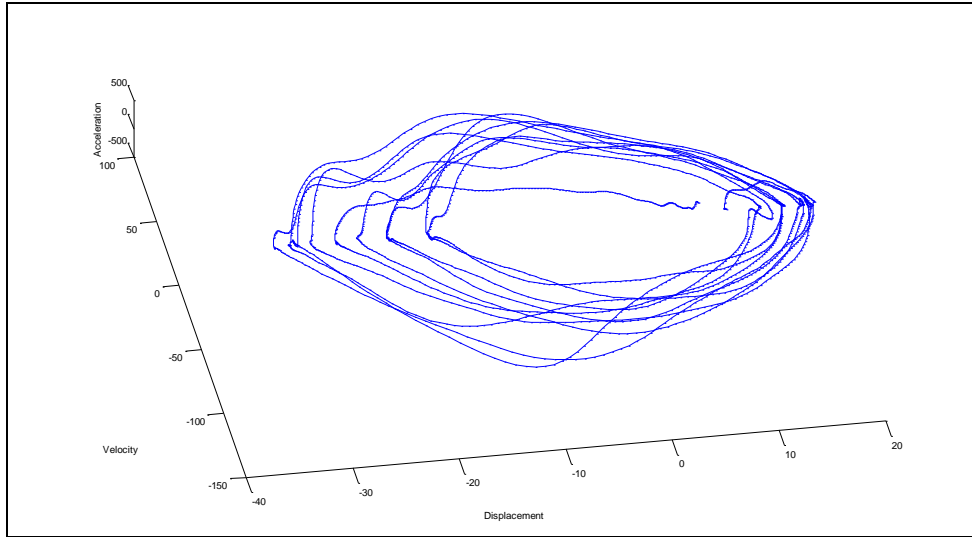


Figure 5. 15 3-D Phase Plane Plot

Figure 5.10 shows the time series for backward target position with first motion as backward. As seen in the phase plots for RD, RE phase plots show similar patterns, and it could be said that the variability of the two is similar.

**RF**

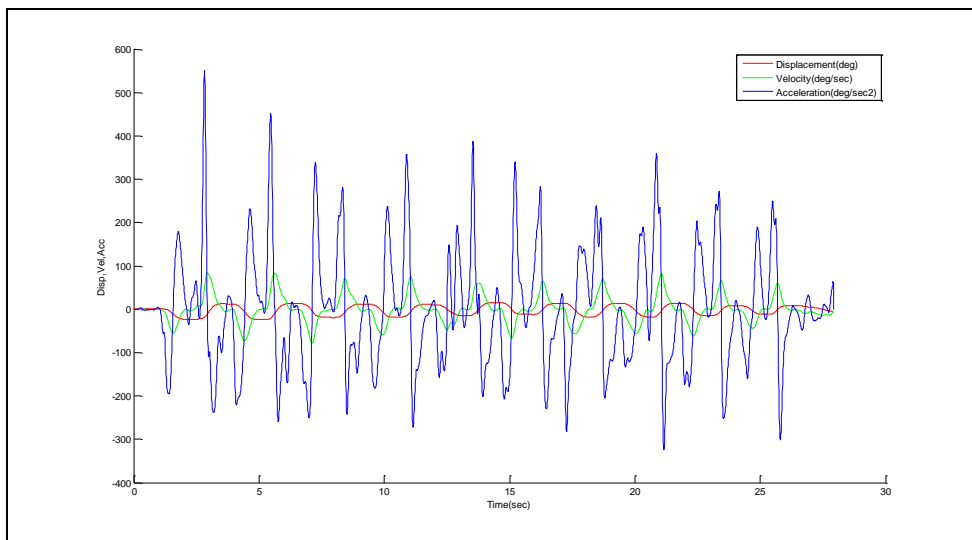


Figure 5. 16 Displacement Time Series with Velocity and Acceleration

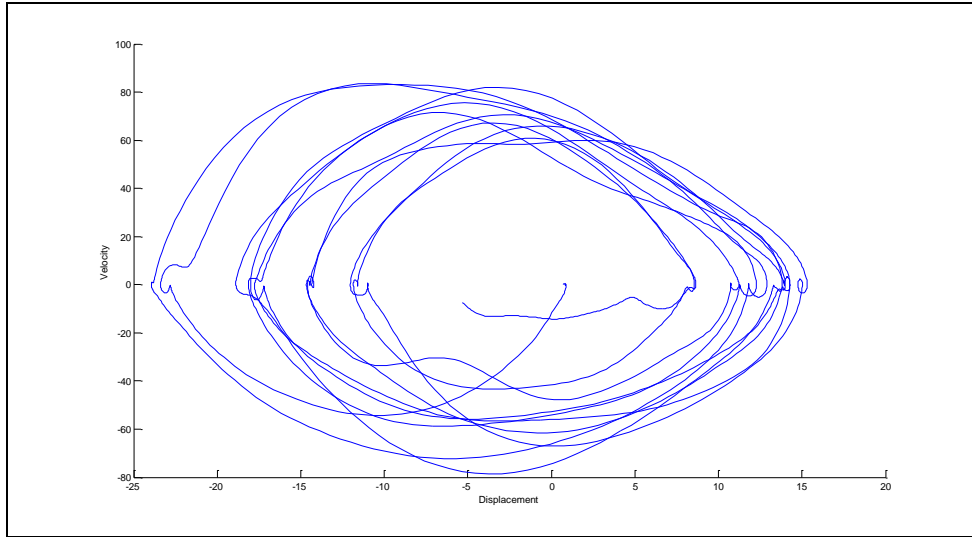


Figure 5. 17 Phase Plane Plot

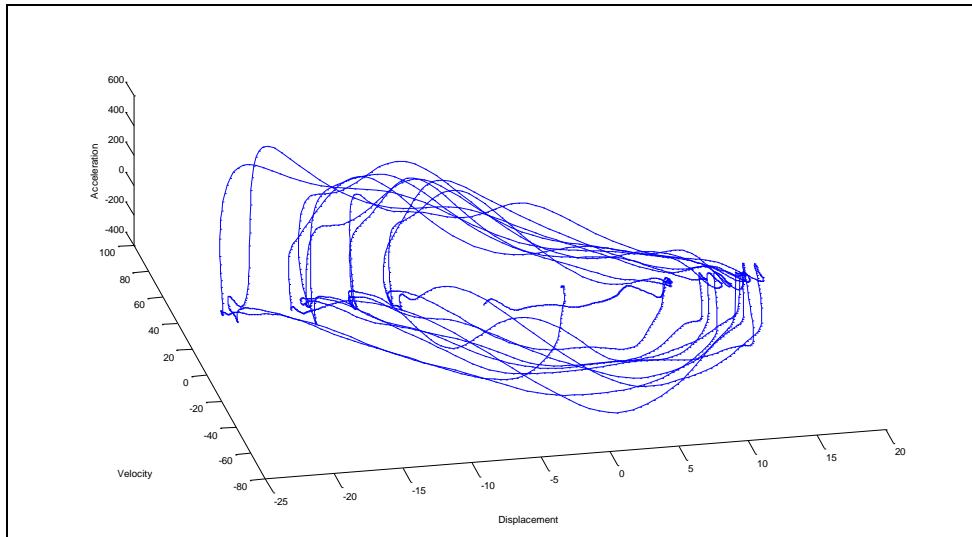


Figure 5. 18 3-D Phase Plane Plot

Figure 5.17 and 5.18 show phase plane plots for a time series with neutral as target position and forward motion as first motion. These plots show a maximum separation of the trajectories, and it can be claimed that this time series has maximum variability.

RG

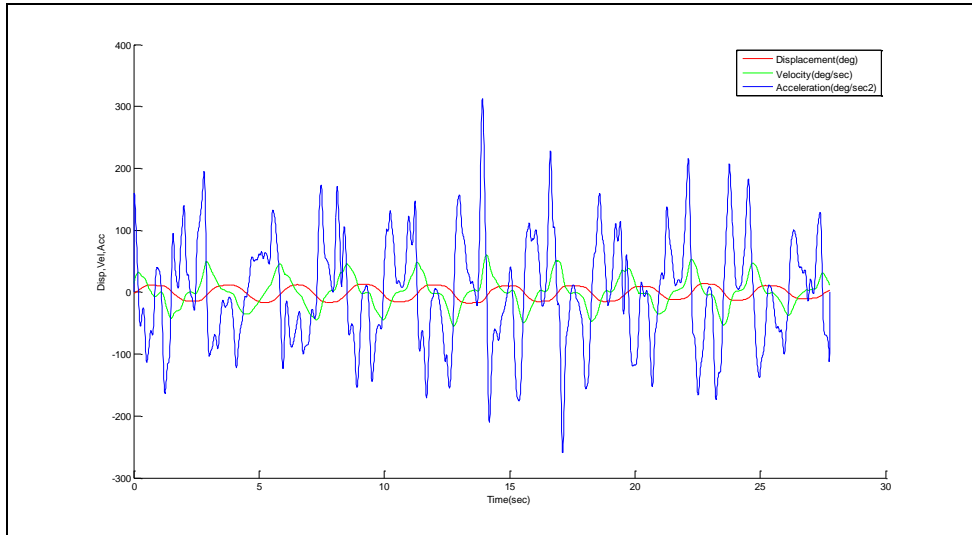


Figure 5. 19 Displacement Time Series with Velocity and Acceleration

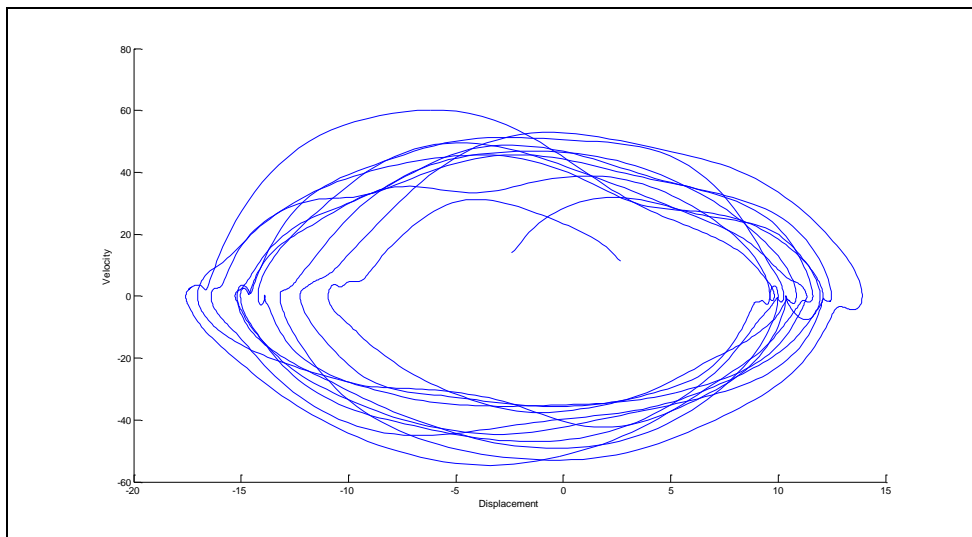


Figure 5. 20 Phase Plane Plot

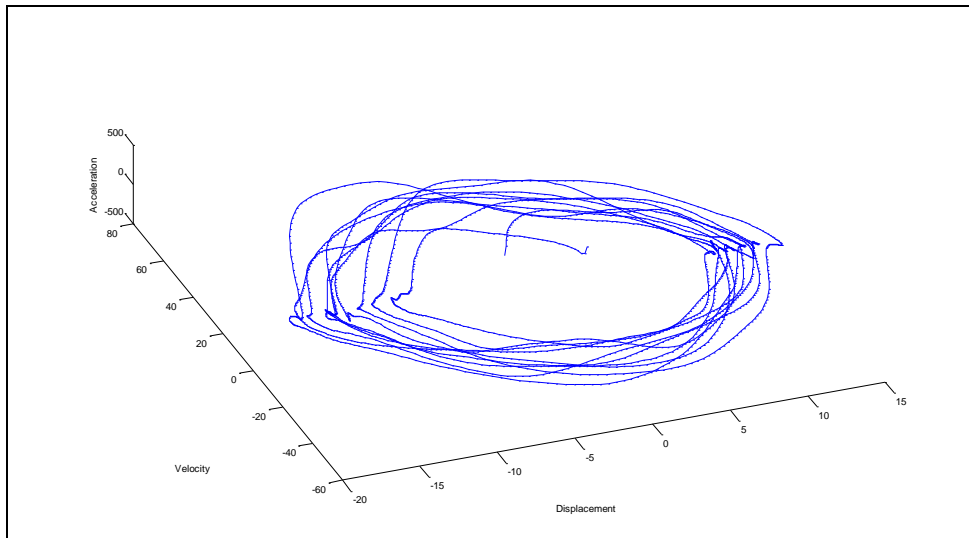


Figure 5. 21 3-D Phase Plane Plot

Figure 5.19 shows a time series for neutral target position with initial backward movement. The phase plane plots show uniform separation of the trajectories, and it can be said that there is a moderate amount of variability in this time series.

Although interpretations are made by observing the phase plane plots, they are very subjective. Therefore, there is always an element of doubt when coming to conclusions based on these observations. As said earlier, phase plane plots are just representations of the state space and should be used as a guideline and not as a method to distinguish the time series.

In order to get more assured results, linear and nonlinear techniques were used. Mean, standard deviation, coefficient of variation, and approximate entropy were computed using MATLAB R2008a for each of the time series data (See Appendix B for programs).

Variation in velocity during flexion–extension tasks in human subjects and cadaveric specimens may help us to understand the effect of LBP on lumbar spine movements and help us to distinguish between healthy subjects and LBP subjects. Hence,

change in velocity over directional movement of lumbar spine for complete flexion-extension task was estimated in this study. Each cycle was divided into four sections depending on lumbar spine movement with respect to neutral position. Mean, SD, and CV was then estimated for complete ten cycles.

Table 5.1 below shows the values for each of the subtests performed on a subject.

Table 5. 1 Linear and Nonlinear Measures

**Subject # 1**

<b>Test Condition</b>		<b>Mean</b>	<b>SD</b>	<b>CV (%)</b>	<b>ApEn</b>
RA (NF)	Total ROM	25.16346	2.938947	11.67942	0.32
	Angular Velocity Forward (V1)	-33.9267	6.729789	-19.8362	
	Angular Velocity Backward (V2)	48.71503	6.514936	13.37357	
	Angular Velocity Backward (V3)	24.15682	4.532175	18.76147	
	Angular Velocity Forward (V4)	-20.9836	5.04977	-24.0654	
RB (FF)	Total ROM	28.80245	5.18246	17.99312	0.2463
	Angular Velocity Forward (V1)	-30.3168	6.789041	-22.3937	
	Angular Velocity Backward (V2)	39.69756	9.539105	24.02945	
	Angular Velocity Backward	35.19676	10.7602	30.57157	

	(V3)				
	Angular Velocity Forward (V4)	-26.6625	5.309553	-19.9139	
RC (FB)	Total ROM	16.91608	1.606685	9.497971	0.2441
	Angular Velocity Backward (V1)	40.28309	4.4422	11.02746	
	Angular Velocity Forward (V2)	-29.5164	3.606675	-12.2192	
	Velocity Forward (V3)	-23.352	7.452419	-31.9134	
	Angular Velocity Backward (V4)	19.57475	6.829137	34.88749	
RD (BF)	Total ROM	10.76923	3.038641	28.21595	0.2222
	Angular Velocity Forward (V1)	-38.9616	6.185729	-15.8765	
	Angular Velocity Backward (V2)	51.20373	8.025324	15.67332	
	Angular Velocity Backward (V3)	11.37887	6.493213	57.06378	
	Angular Velocity Forward (V4)	-8.43334	4.009456	-47.5429	
RE (BB)	Total ROM	19.11888	5.711879	29.87559	0.1945
	Angular Velocity Backward (V1)	16.24144	5.849587	36.01644	
	Angular Velocity Forward	-15.6025	5.188226	-33.2525	



	(V2)				
	Angular Velocity Forward (V3)	-50.5192	14.54363	-28.7883	
	Angular Velocity Backward (V4)	46.69309	11.17078	23.92385	
RF (NF)	Total ROM	28.01136	5.323007	19.00303	0.1917
	Angular Velocity Forward (V1)	-31.0571	7.949072	-25.595	
	Angular Velocity Backward (V2)	40.10805	10.43883	26.02678	
	Angular Velocity Backward (V3)	26.76865	7.03382	26.27634	
	Angular Velocity Forward (V4)	-20.4708	7.899119	-38.5872	
RG (NB)	Total ROM	22.16171	2.642313	11.92287	0.3065
	Angular Velocity Backward (V1)	28.66511	7.5263	26.25596	
	Angular Velocity Forward (V2)	-20.5705	4.063352	-19.7533	
	Angular Velocity Forward (V3)	-26.257	5.744034	-21.8762	
	Angular Velocity Backward (V4)	22.17435	5.369799	24.21626	

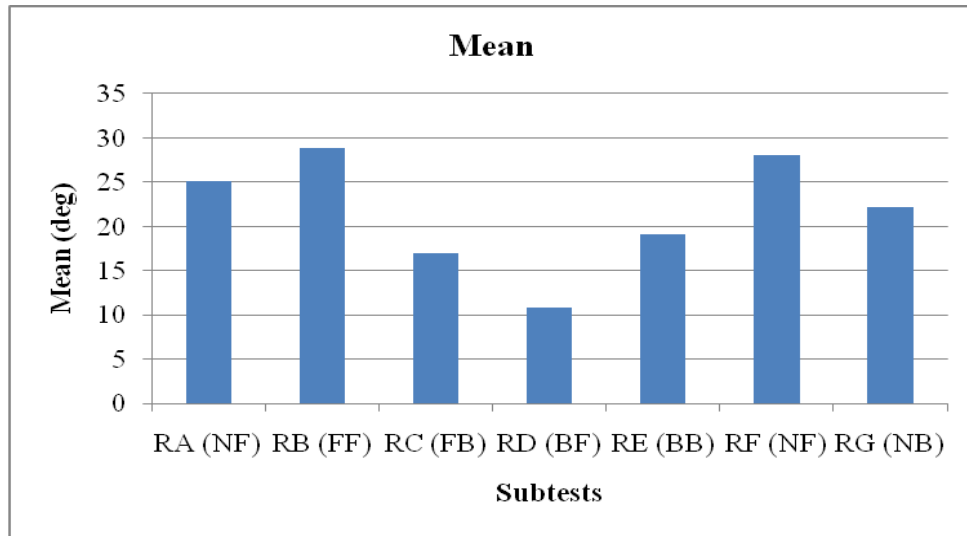


Figure 5. 22 Mean Values for Subtests

As seen in figure 5.22, the mean values for total range of motion increased for the first two subtests and then reduced to the minimum value for the RD subtest. The mean again rose for the RF subtest and eventually decreased, revealing an M-shaped function of variability.

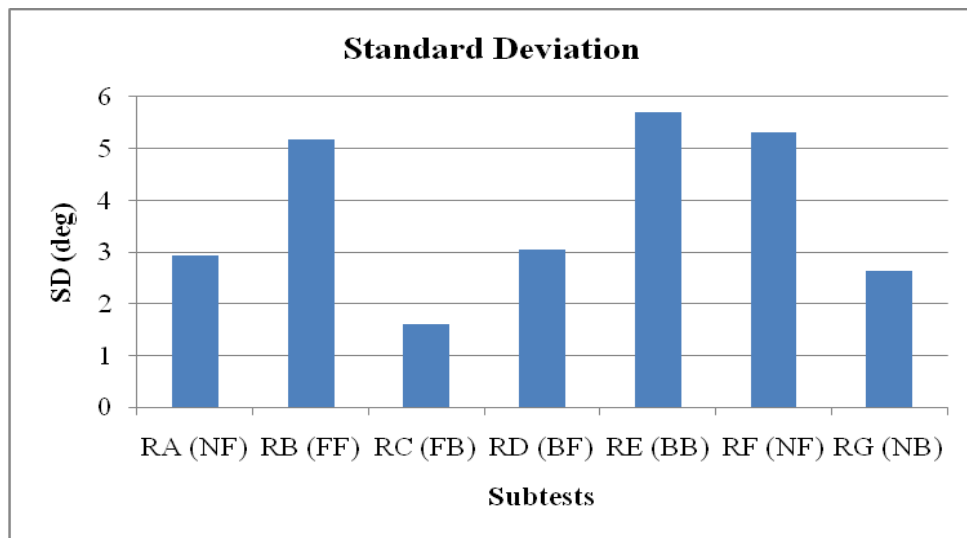


Figure 5. 23 Standard Deviation for Subtests

In the case of standard deviation, the graph shows a rise and decline to the minimum for the RC subtest, followed by another rise and decline in values. The shape was similar to the graph of mean values, but the variability was lowest for RC.

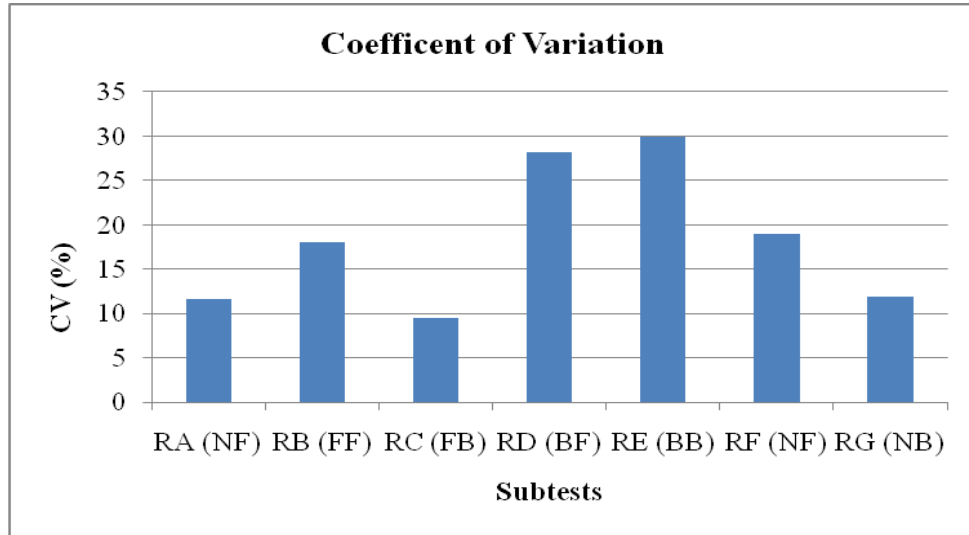


Figure 5. 24 Coefficient of Variation for Subtests

The coefficient of variation also shows a similar pattern, with the RC subtest having minimum variability.

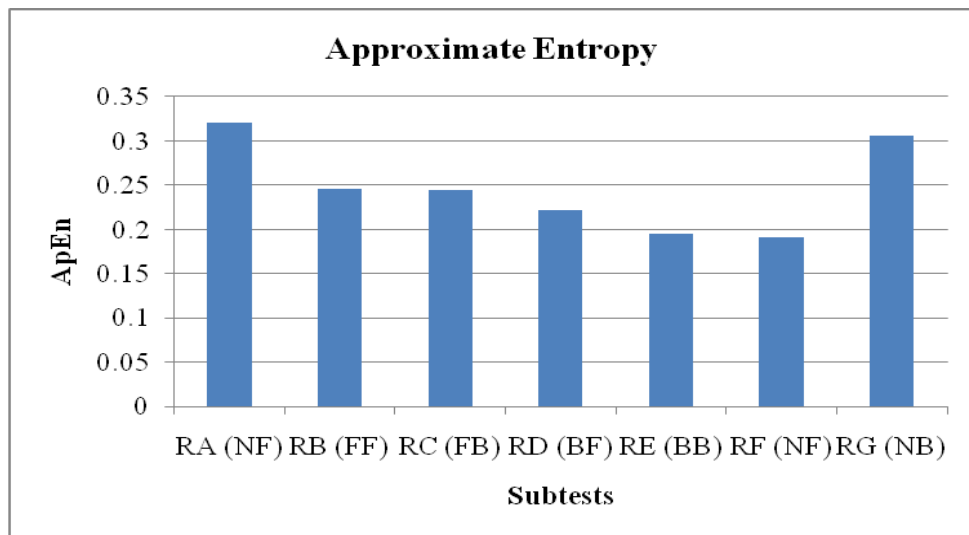


Figure 5. 25 Approximate Entropy for Subtests

On the other hand, ApEn measurements show a completely different pattern. The values show a gradual decline before a rise for final subtest, showing that complexity decreased as the test progressed.

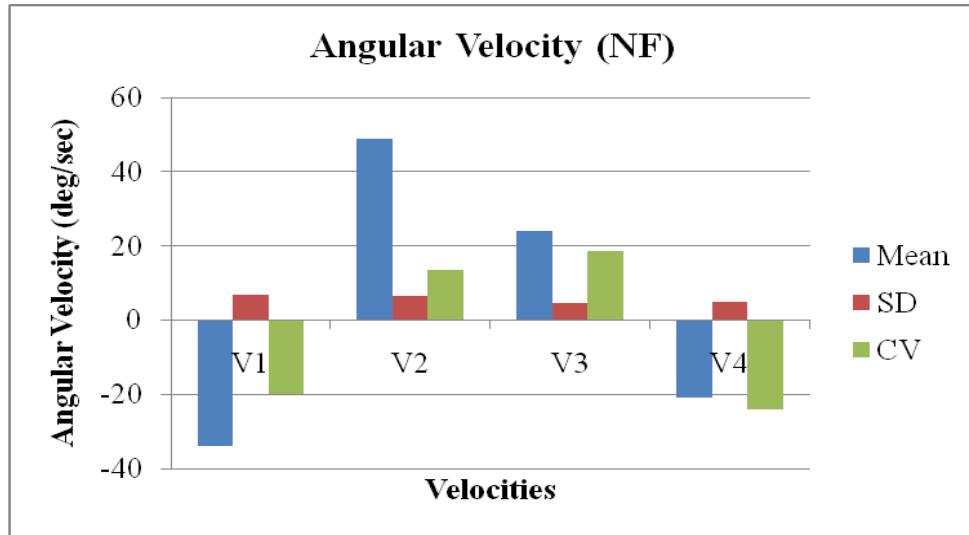


Figure 5. 26 Variations in Angular Velocity

Figure 5.26 shows variation in angular velocity of lumbar spine movement. The mean values show that the subject moved quickly while moving from neutral to backward, while CV values show angular velocity while moving from backward to neutral. SD values were almost uniform for all cases.

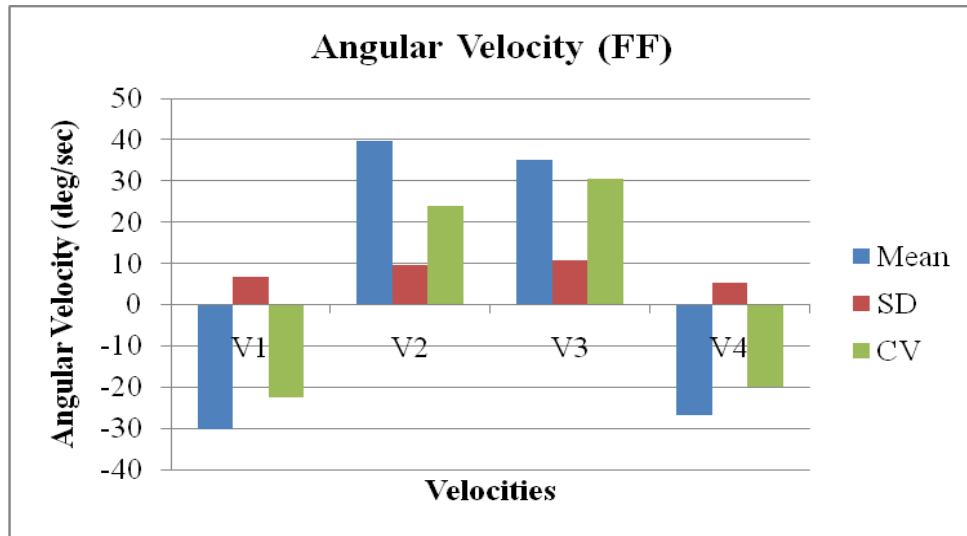


Figure 5. 27 Variations in Angular Velocity

As before, the mean of angular velocity is maximum for backward movement from front position to neutral position, while CV shows more angular velocity for neutral-to-backward movement.

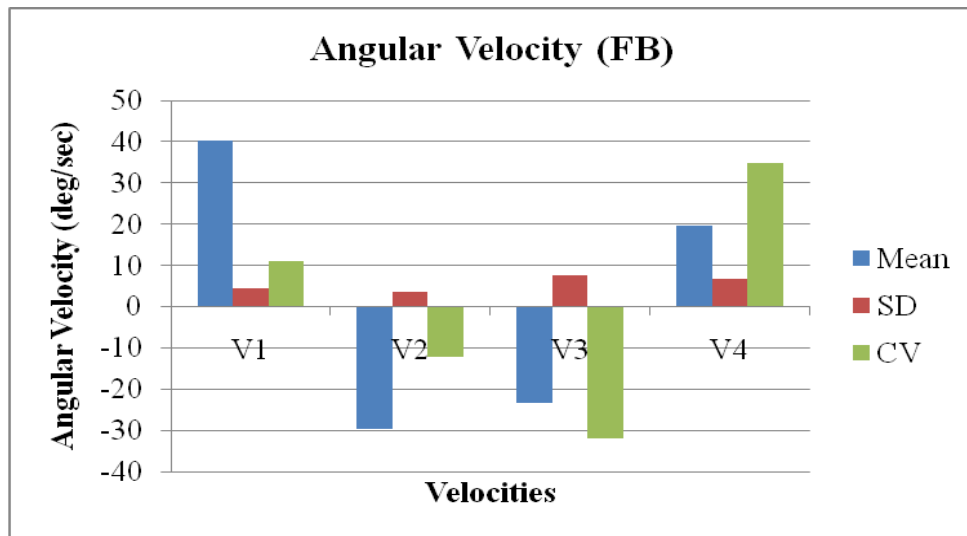


Figure 5. 28 Variations in Angular Velocity

Figure 5.28 show the angular velocity was greater for neutral-to-backward movement, while CV was greater for front position to neutral position, with SD remaining more or less uniform.

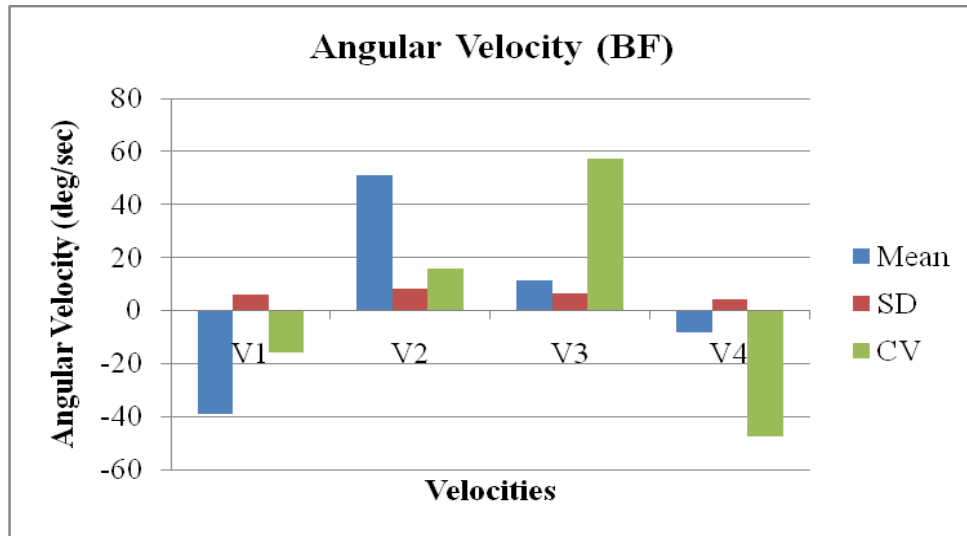


Figure 5. 29 Variations in Angular Velocity

In figure 5.29, the mean value of angular velocity was maximum for front position to backward position, while CV was greater for neutral to backward position. SD was higher for forward to backward movement.

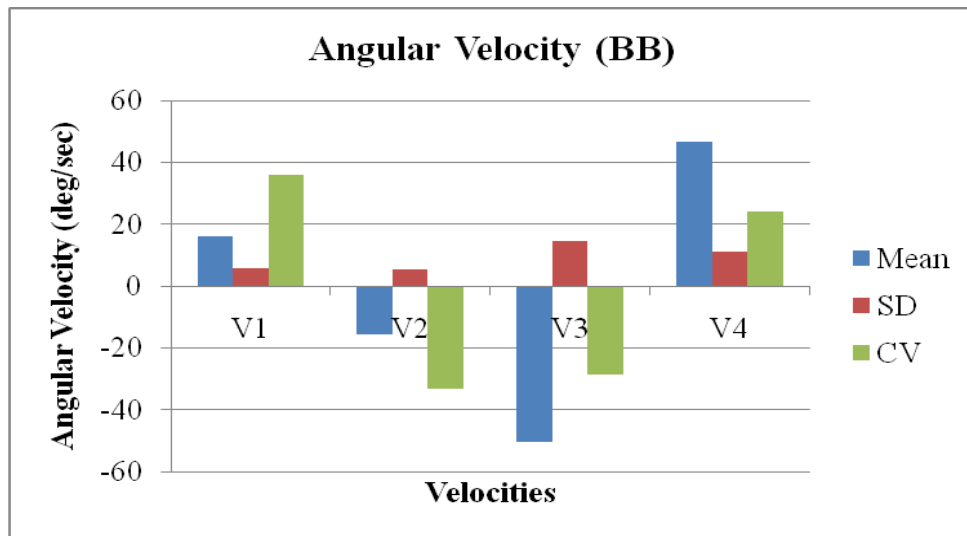


Figure 5. 30 Variations in Angular velocity

The mean value for this subtest shows a higher value of angular velocity while moving from neutral to forward position, while CV and SD are highest for neutral-to-backward movement and neutral-to-forward movement respectively.

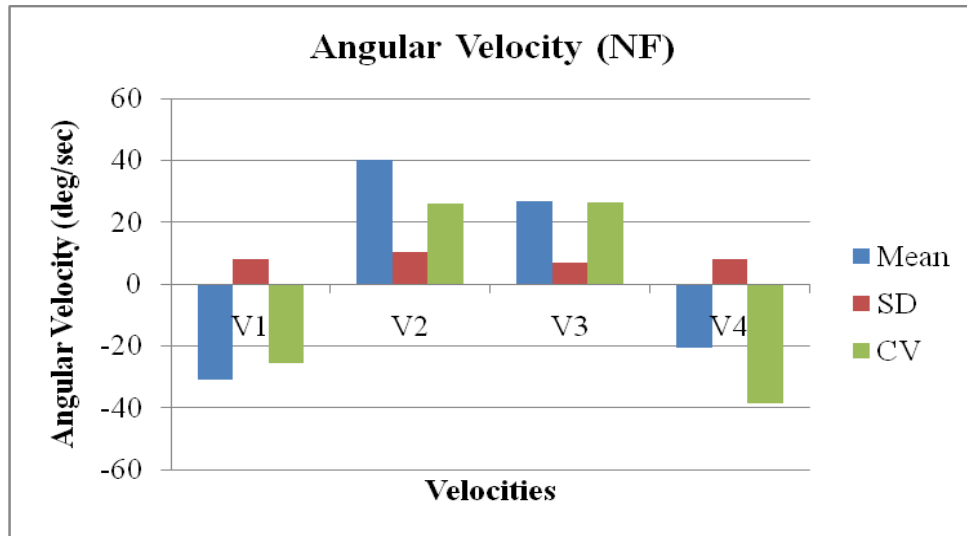


Figure 5. 31 Variations in Angular Velocity

Figure 5.31 shows higher value of mean of angular velocity while moving from forward to neutral position, with CV at its maximum for backward to neutral position. SD values remained uniform.

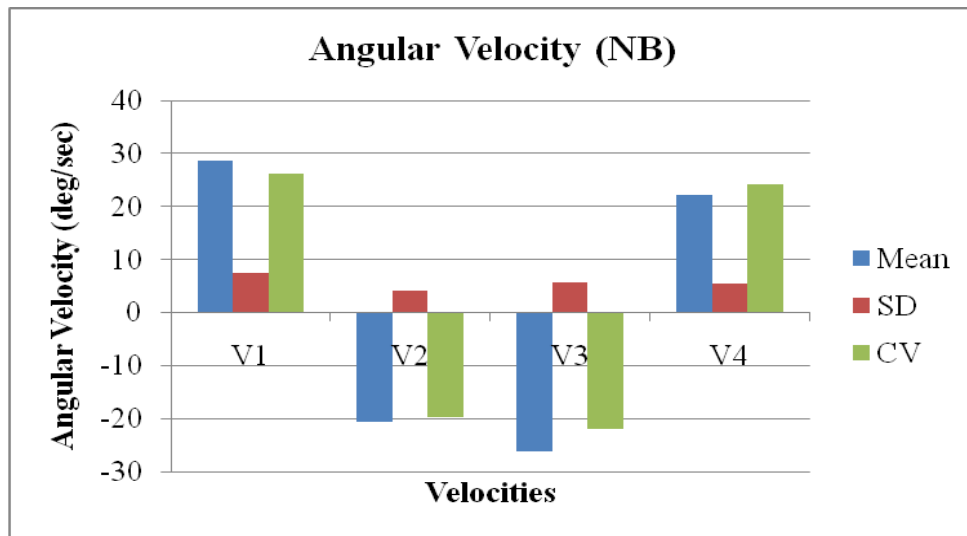


Figure 5. 32 Variations in Angular Velocity

Mean, SD, and CV for this subtest correlate well and show similar results, with angular velocity being at its maximum for neutral-to-backward movement.

Table 5. 2 Linear and Nonlinear Measures

**Subject # 2**

Similar measures were computed for remaining subjects.

<b>Test Condition</b>		<b>Mean</b>	<b>SD</b>	<b>CV (%)</b>	<b>ApEn</b>
<b>RA (NF)</b>	Total ROM	12.41608	1.227959	9.89007	0.3247
	Angular Velocity Forward (V1)	-11.9891	2.426826	-20.242	
	Angular Velocity Backward (V2)	10.40492	2.123236	20.40609	
	Angular Velocity Backward (V3)	11.39617	4.007765	35.16764	
	Angular Velocity Forward (V4)	-11.3373	4.197697	-37.0255	
<b>RB (FF)</b>	Total ROM	15.23287	1.667311	10.94548	0.2834
	Angular Velocity Forward (V1)	-18.4673	2.835653	-15.355	
	Angular Velocity Backward (V2)	15.06725	2.066963	13.71825	
	Angular Velocity Backward (V3)	16.61443	2.739847	16.49077	
	Angular Velocity Forward (V4)	-15.2235	1.680097	-11.0362	
<b>RC (FB)</b>	Total ROM	12.19406	2.106081	17.27137	0.3517



	Angular Velocity Backward (V1)	13.54575	3.753753	27.71166	
	Angular Velocity Forward (V2)	-14.8997	4.951029	-33.2291	
	Angular Velocity Forward (V3)	-12.2544	2.962727	-24.1769	
	Angular Velocity Backward (V4)	11.12784	2.537487	22.80304	
RD (BF)	Total ROM	8.15035	2.757983	33.83883	0.2487
	Angular Velocity Forward (V1)	-10.7115	5.781007	-53.9701	
	Angular Velocity Backward (V2)	9.599615	3.189955	33.23003	
	Angular Velocity Backward (V3)	14.89396	2.437355	16.36472	
	Angular Velocity Forward (V4)	-10.5298	3.052364	-28.988	
RE (BB)	Total ROM	11.14685	2.094973	18.7943	0.3273
	Angular Velocity Backward (V1)	18.80549	6.628579	35.24809	
	Angular Velocity Forward (V2)	-16.6217	3.477871	-20.9237	
	Angular Velocity	-13.5795	5.260933	-38.7417	

	Forward (V3)				
	Angular Velocity Backward (V4)	9.607045	2.551823	26.56199	
RF (NF)	Total ROM	8.933566	2.349299	26.29744	0.275
	Angular Velocity Forward (V1)	-8.87902	3.418681	-38.5029	
	Angular Velocity Backward (V2)	7.304628	3.012098	41.23547	
	Angular Velocity Backward (V3)	18.10217	4.15362	22.94542	
	Angular Velocity Forward (V4)	-14.273	2.823111	-19.7794	
RG (NB)	Total ROM	11.49755	0.928005	8.07133	0.2634
	Angular Velocity Backward (V1)	19.35916	2.527288	13.05474	
	Angular Velocity Forward (V2)	-19.9396	1.871287	-9.38476	
	Angular Velocity Forward (V3)	-8.97626	3.015788	-33.5974	
	Angular Velocity Backward (V4)	6.650135	2.724628	40.97101	

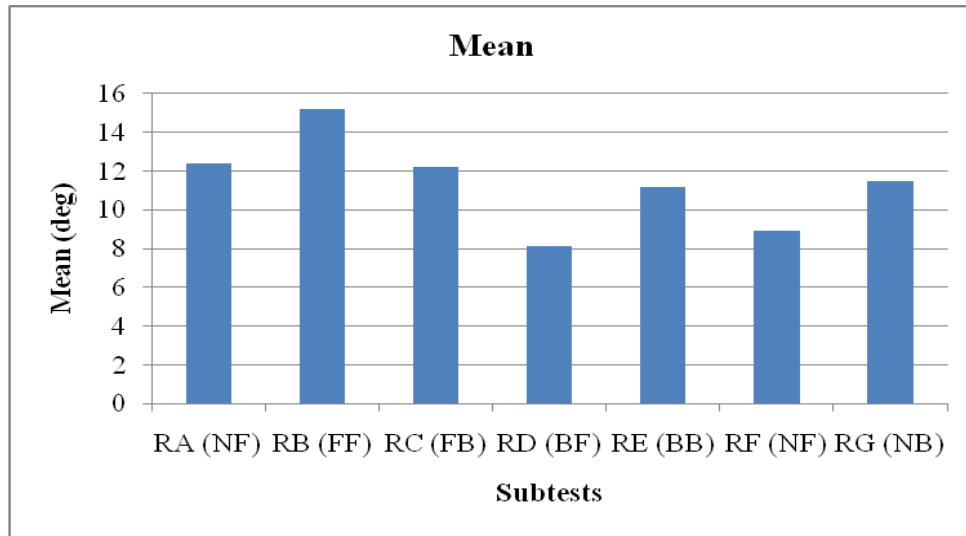


Figure 5. 33 Mean Values for Subtests

The mean value shows a rise and then reaches its minimum value at RD. The mean values rise again for RE and remain almost uniform. A similar pattern was observed for the previous participant.

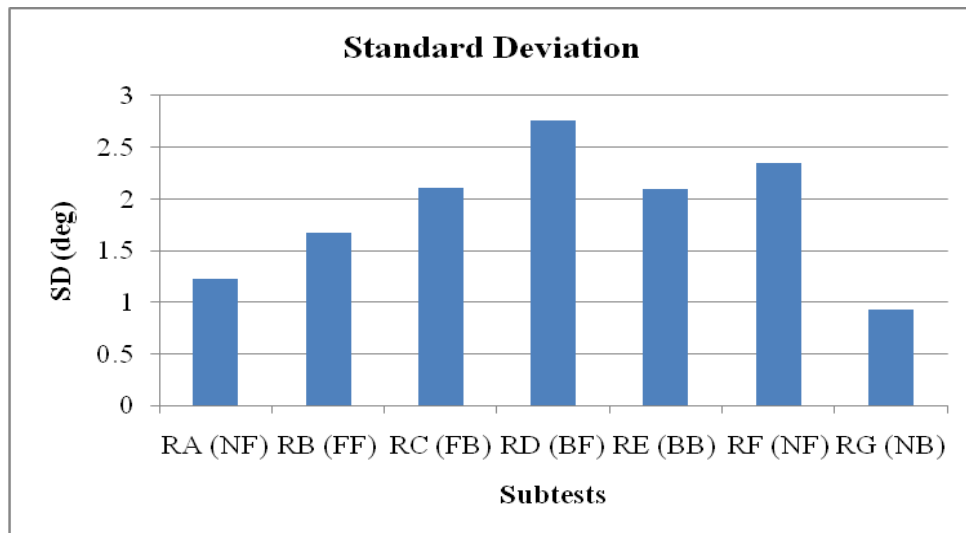


Figure 5. 34 Standard Deviation for Subtests

The standard deviation graph shows a gradual increase in values with the maximum for the RD subtest, which shows an increase in variability followed by a decline with the minimum at final subtest RG.

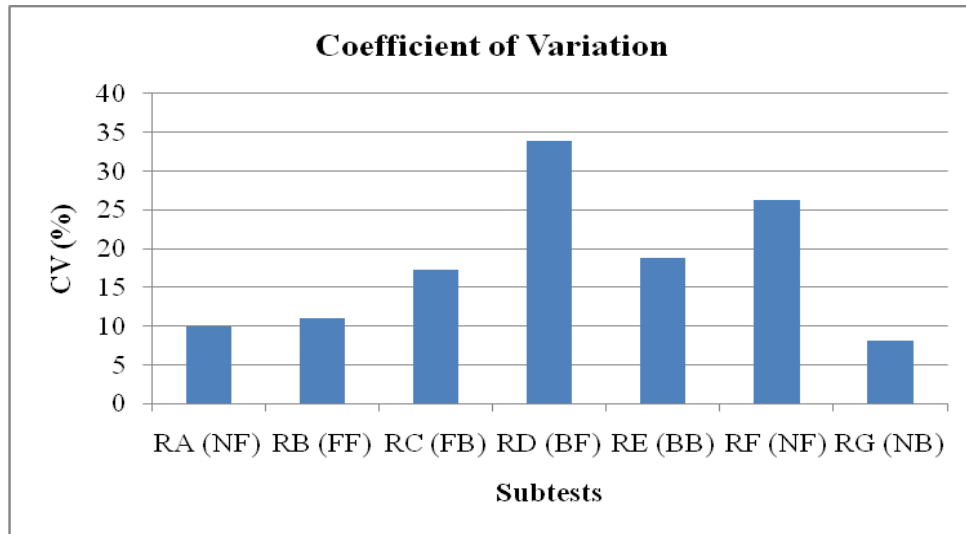


Figure 5. 35 Coefficient of Variation for Subtests

The coefficient of variance values show a similar pattern of variability as that of standard deviation.

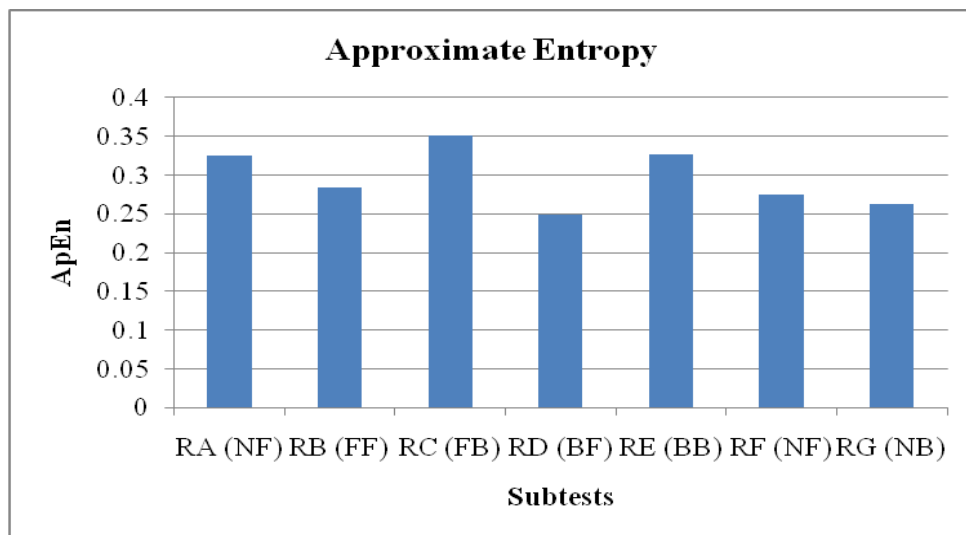


Figure 5. 36 Approximate Entropy for Subtests

The values show complexity, rising and falling alternatively. The result can be correlated with the previous ApEn graph.

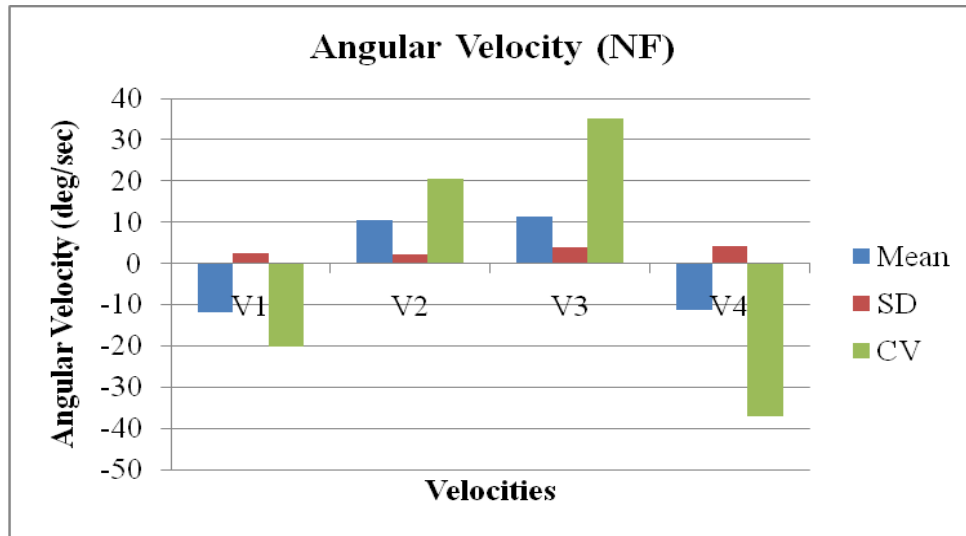


Figure 5. 37 Variations in Angular Velocity

The mean and SD of angular velocity is more or less uniform for all cases in this subtest, with CV for angular velocity being at its maximum for backward to neutral position.

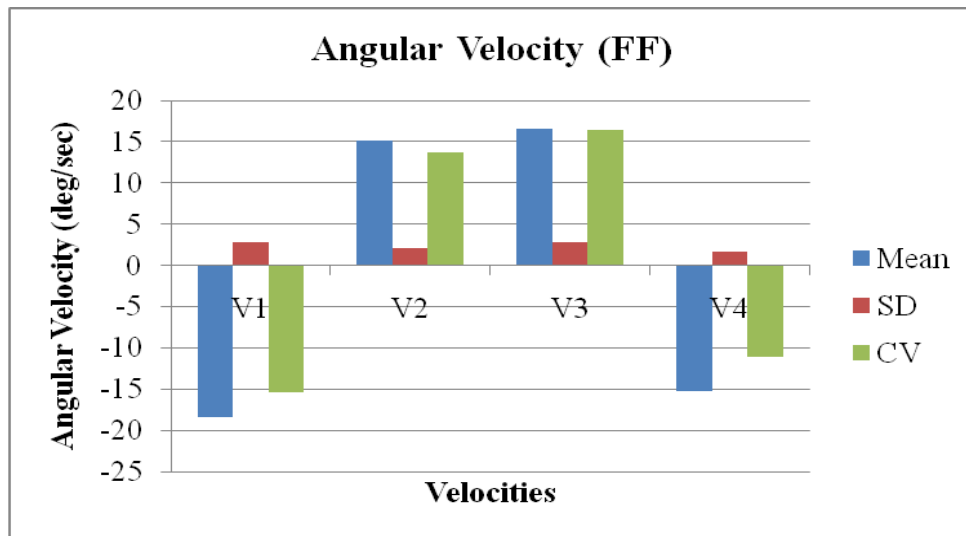


Figure 5. 38 Variations in Angular Velocity

The mean, SD, and CV of angular velocity for this subtest is more or less similar throughout and shows a strong correlation with each other. Mean was maximum for

neutral to forward movement, while SD and CV remained high for neutral to backward motion.

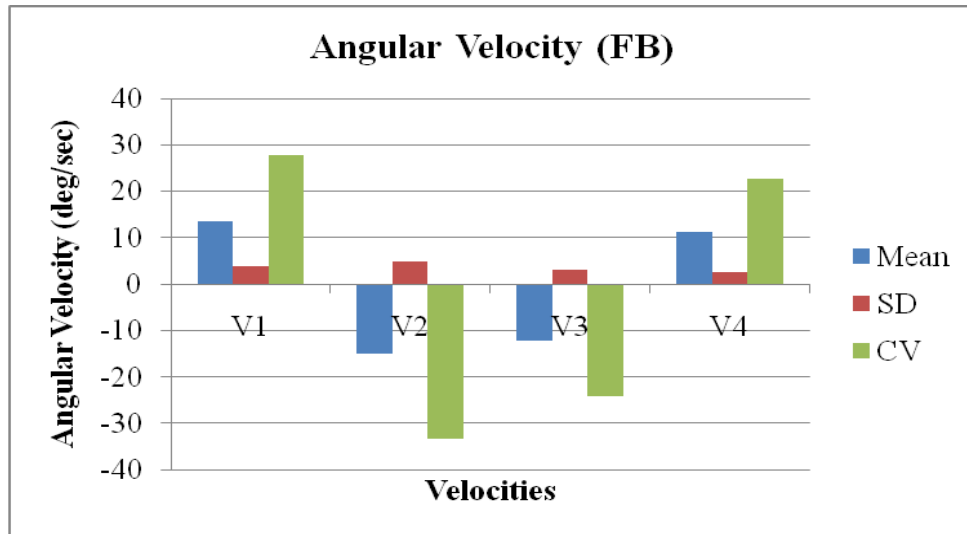


Figure 5. 39 Variations in Angular Velocity

In figure 5.39, the mean and CV of angular velocity is higher for backward-to-neutral movement, while the SD values remain constant throughout.

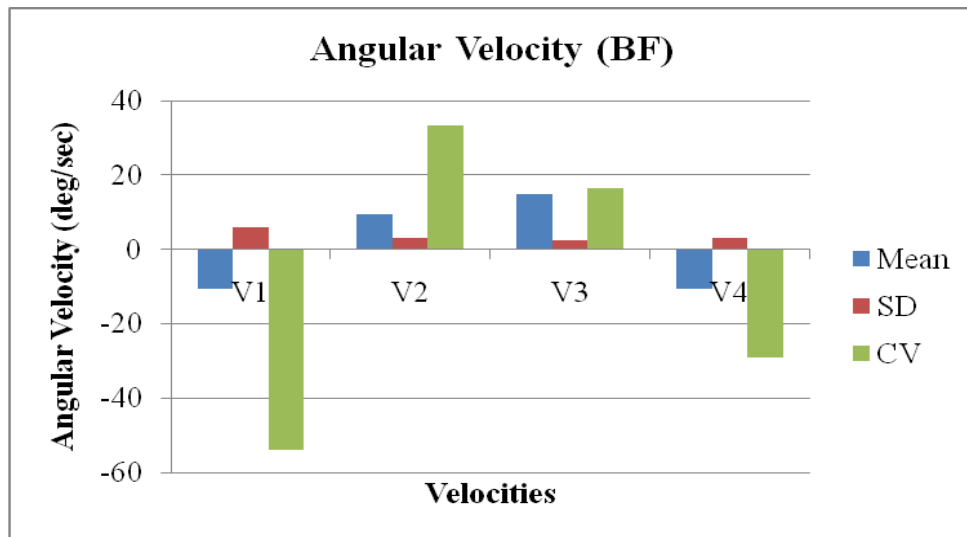


Figure 5. 40 Variations in Angular Velocity

The mean and SD of angular velocity for this subtest is almost uniform while CV shows its maximum value for neutral-to-forward movement.

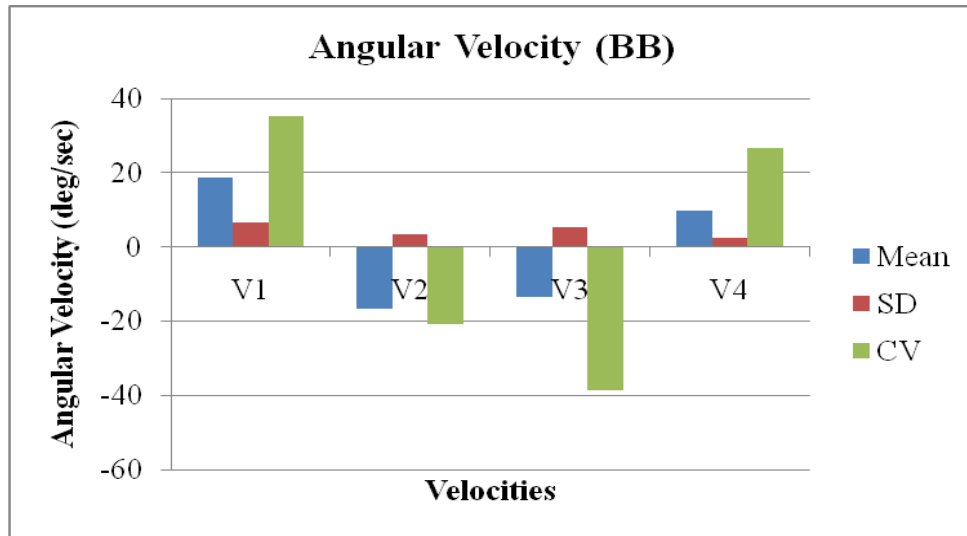


Figure 5. 41 Variations in Angular Velocity

Figure 5.41 shows a maximum value of mean and SD of angular velocity for neutral-to-backward movement of lumbar spine, while CV was highest for neutral-to-forward motion.

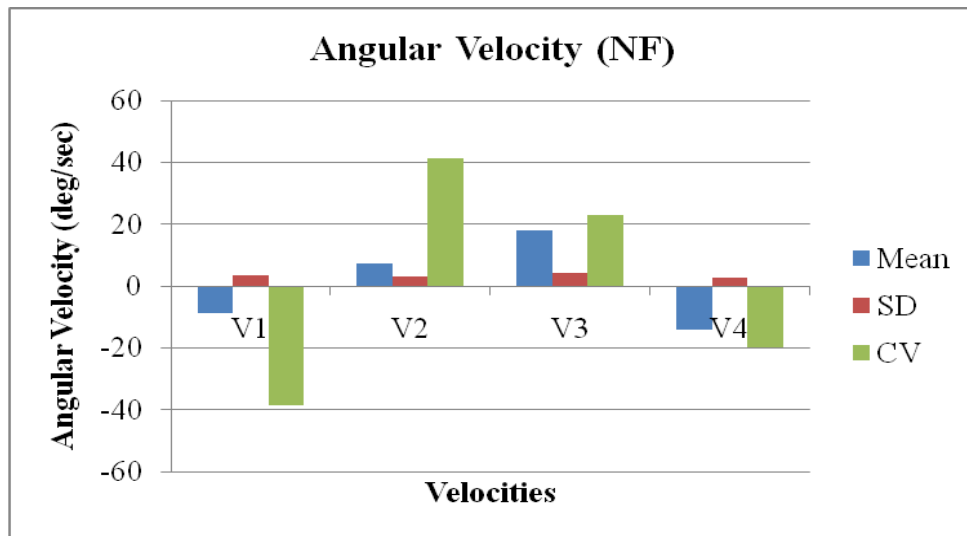


Figure 5. 42 Variations in Angular Velocity

In this case, the mean of angular velocity was highest for neutral-to-backward movement while CV showed higher values for forward-to-neutral movement.

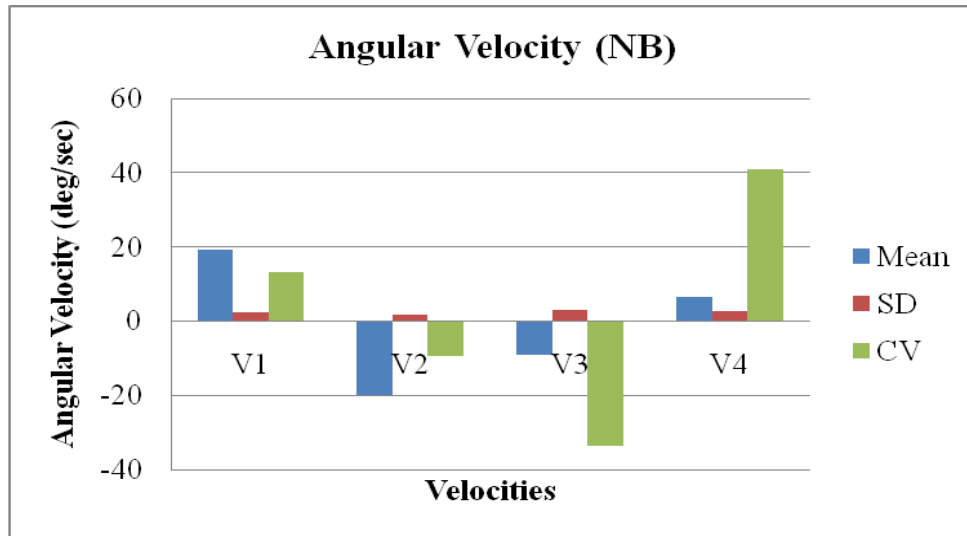


Figure 5. 43 Variations in Angular Velocity

Figure 5.43 showed higher values of mean for backward-to-neutral movement, while CV was higher for forward-to-neutral movement.

Table 5. 3 Linear and Nonlinear Measures

**Subject # 3**

Test Condition		Mean	SD	CV (%)	ApEn
RA (NF)	Total ROM	36.73951	3.056539	8.319488	0.2378
	Angular Velocity Forward (V1)	-29.0413	5.056237	-17.4105	
	Angular Velocity Backward (V2)	48.12021	10.75091	22.34178	
	Angular Velocity Backward (V3)	52.99896	28.6905	54.13409	
	Angular Velocity Forward	-50.9074	28.60734	-56.1949	



	(V4)				
RB (FF)	Total ROM	28.51049	3.063703	10.74588	0.3383
	Angular Velocity Forward (V1)	-34.9918	12.57378	-35.9335	
	Angular Velocity Backward (V2)	43.68193	8.517696	19.49936	
	Angular Velocity Backward (V3)	71.21064	10.73873	15.08024	
	Angular Velocity Forward (V4)	-63.4849	8.360227	-13.1688	
RC (FB)	Total ROM	34.42308	3.107815	9.028289	0.2714
	Angular Velocity Backward (V1)	56.40662	13.6145	24.13636	
	Angular Velocity Forward (V2)	-59.9368	10.26253	-17.1222	
	Angular Velocity Forward (V3)	-32.4561	10.47805	-32.2837	
	Angular Velocity Backward (V4)	41.95977	8.2506	19.66312	
RD (BF)	Total ROM	14.45804	2.228288	15.4121	0.236
	Angular Velocity Forward (V1)	-49.8195	10.30889	-20.6925	
	Angular Velocity Backward	68.94928	7.31262	10.6058	

	(V2)				
	Angular Velocity Backward (V3)	37.75827	5.450713	14.43581	
	Angular Velocity Forward (V4)	-45.4241	6.416788	-14.1264	
RE (BB)	Total ROM	12.70629	2.736122	21.53359	0.2031
	Angular Velocity Backward (V1)	34.86804	11.47596	32.91256	
	Angular Velocity Forward (V2)	-41.7084	10.18281	-24.4143	
	Angular Velocity Forward (V3)	-46.3261	4.326236	-9.33866	
	Angular Velocity Backward (V4)	64.24768	6.847152	10.65743	
RF (NF)	Total ROM	37.49126	1.898663	5.064281	0.2017
	Angular Velocity Forward (V1)	-32.046	5.813095	-18.1399	
	Angular Velocity Backward (V2)	50.79108	6.88803	13.5615	
	Angular Velocity Backward (V3)	57.08177	8.580514	15.03197	
	Angular Velocity Forward (V4)	-61.5926	5.16197	-8.38083	

RG (NB)	Total ROM	35.8951	4.15122	11.56486	0.1993
	Angular Velocity Backward (V1)	59.91014	18.08741	30.19089	
	Angular Velocity Forward (V2)	-60.4231	9.658142	-15.9842	
	Angular Velocity Forward (V3)	-39.6265	8.803663	-22.2166	
	Angular Velocity Backward (V4)	57.10554	9.258534	16.21302	

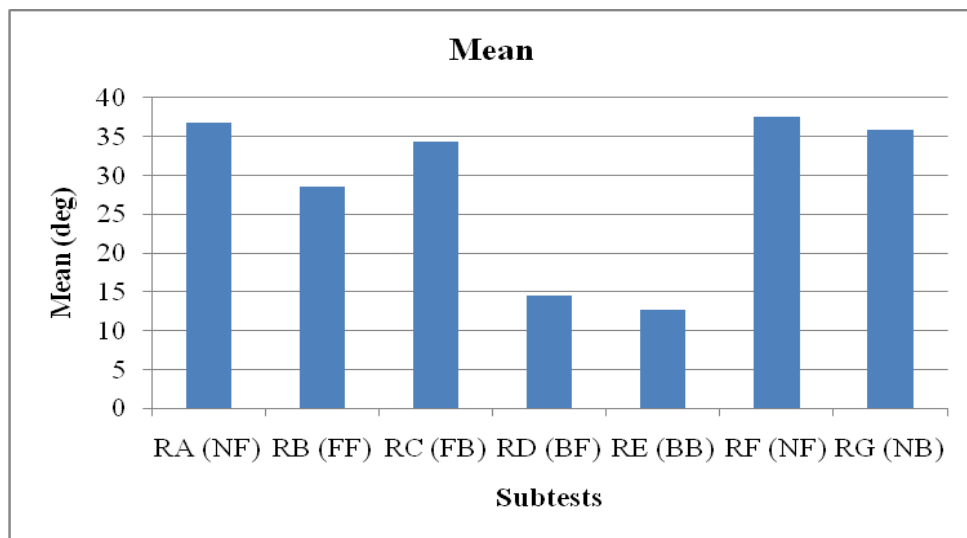


Figure 5. 44 Mean Values for Subtests

The mean values remained almost uniform for the first three subtests and decrease sharply at RD, followed by sharp rise, showing that variability in motion was maximum for initial and final subtests.

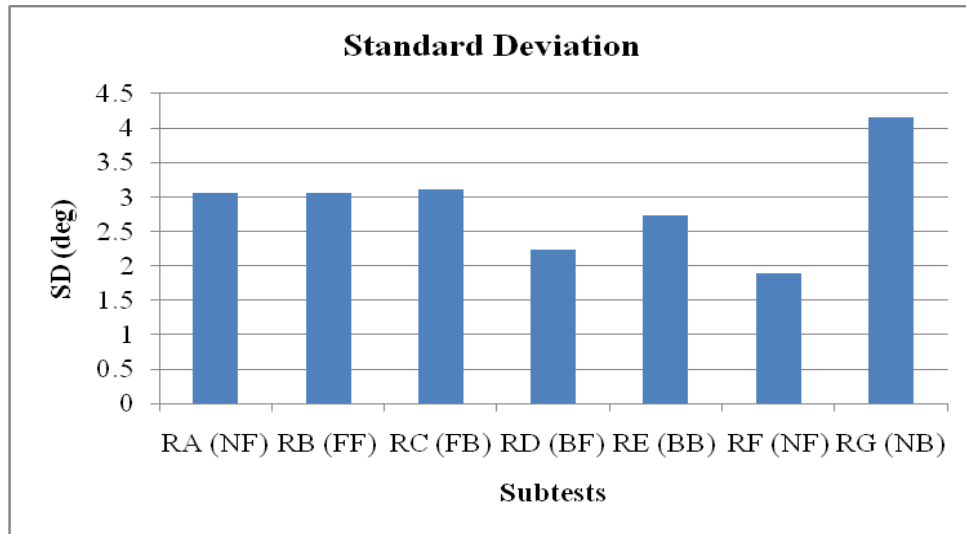


Figure 5. 45 Standard Deviation for Subtests

The standard deviation graph shows uniform values for most of the subtests, with a sharp rise for the final subtest.

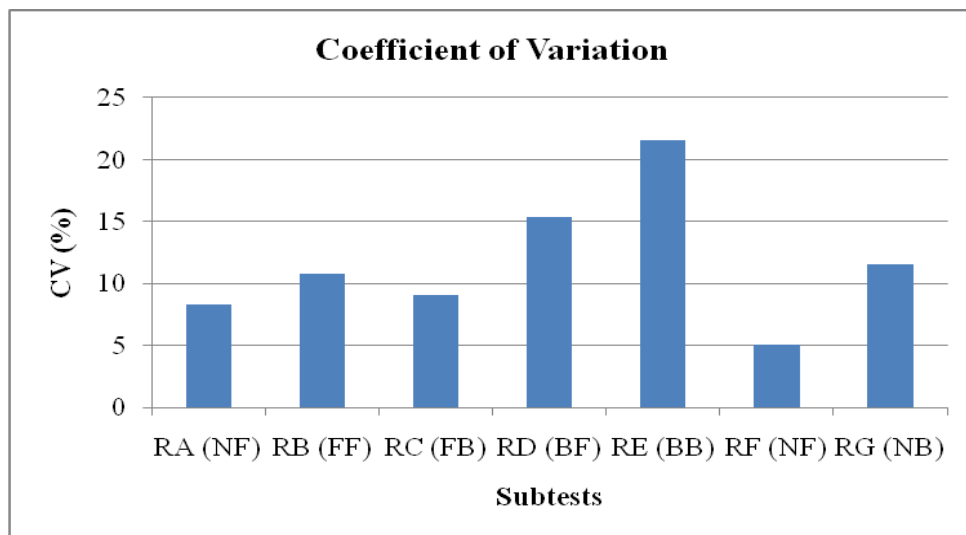


Figure 5. 46 Coefficient of Variation for Subtests

This time, the values of the coefficient of variation do not correlate with standard deviation values and show a gradual rise followed by a sharp decline for the final subtests, describing a decrease in variability for initial and final subtests.

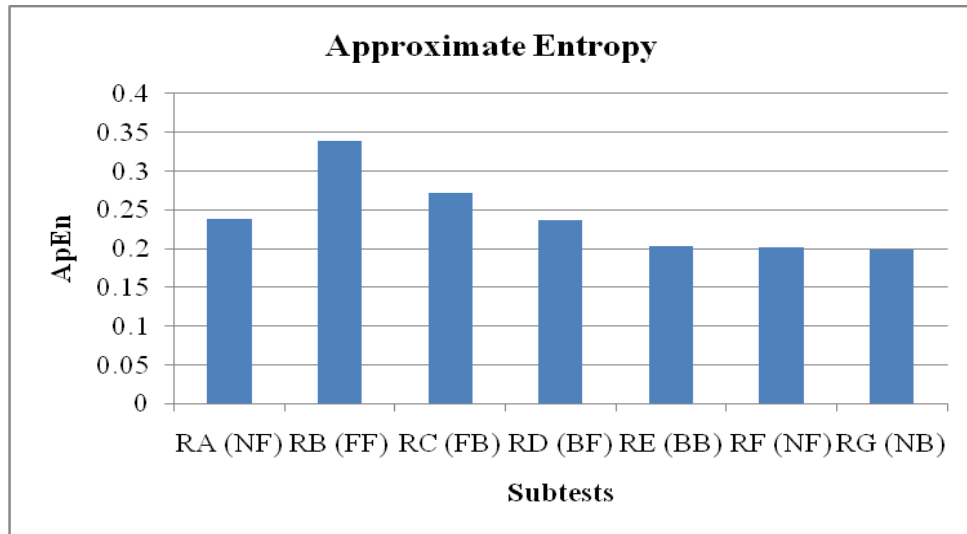


Figure 5. 47 Approximate Entropy for Subtests

The approximate entropy continues to show a similar pattern, with a gradual decrease in complexity with the subtests.

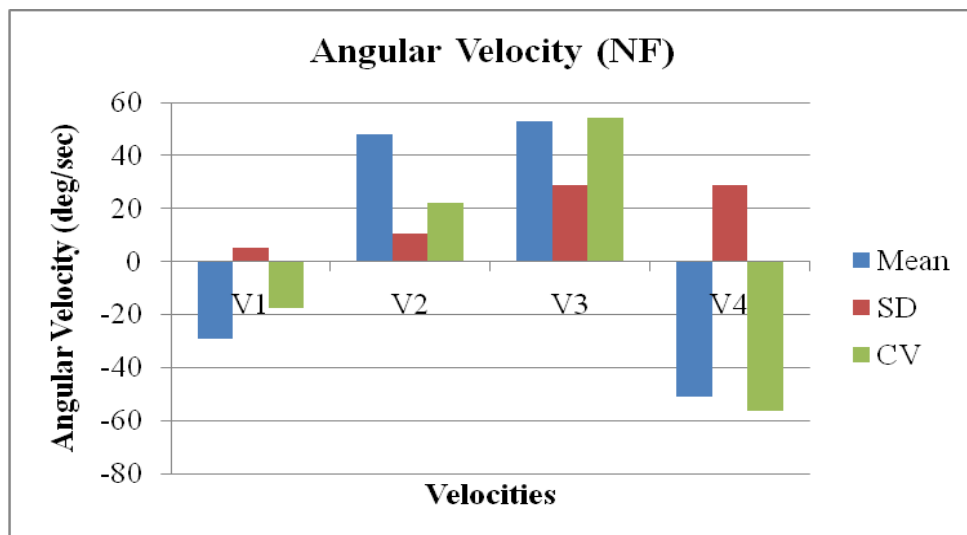


Figure 5. 48 Variations in Angular Velocity

In this subtest the mean, SD, and CV are higher for backward-to-neutral movement.

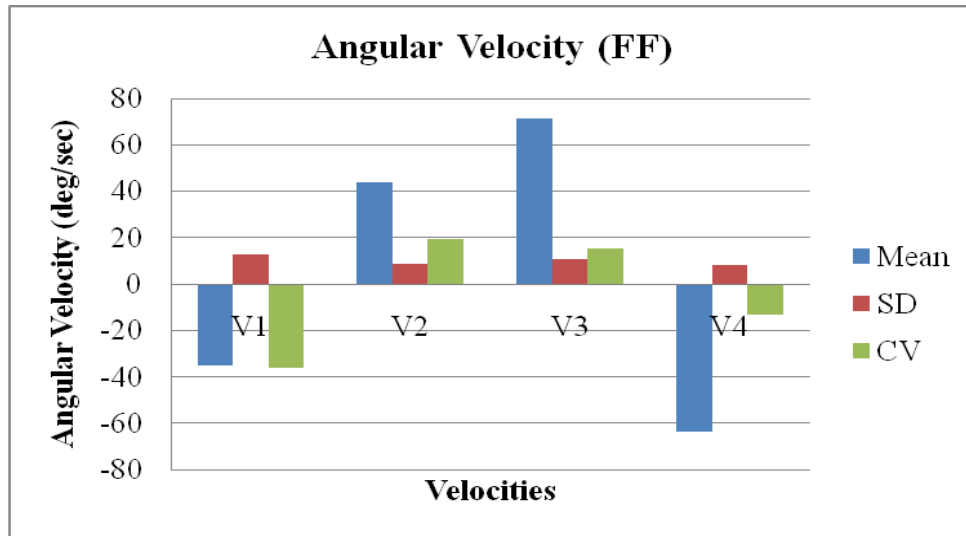


Figure 5. 49 Variations in Angular Velocity

In figure 5.49 the mean of angular velocity depicts higher values for neutral-to-backward movement, while CV is maximum for neutral-to-forward motion. SD of angular velocity remains uniform.

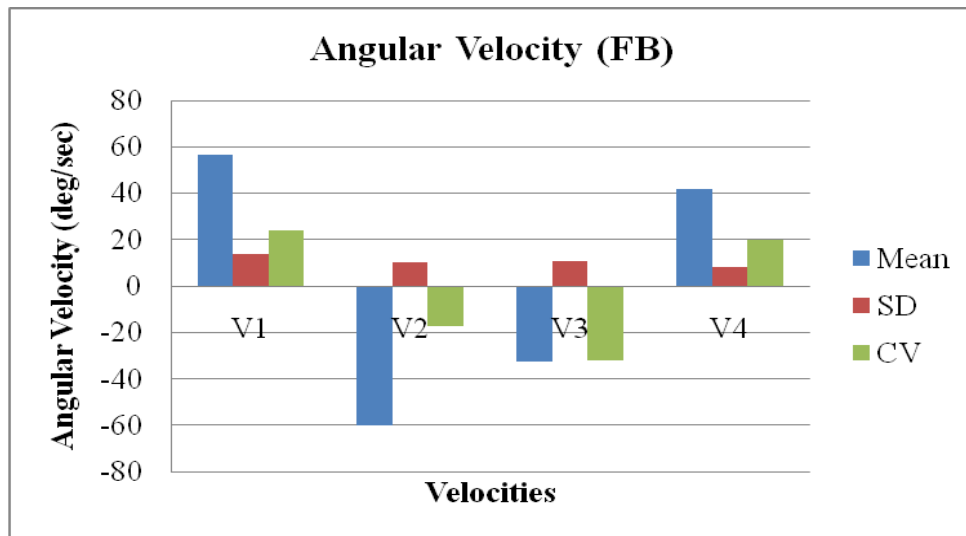


Figure 5. 50 Variations in Angular Velocity

The mean values of angular velocity for the FB subtest show higher angular velocity for backward-to-neutral movement, while CV was maximum for neutral-to-forward direction.

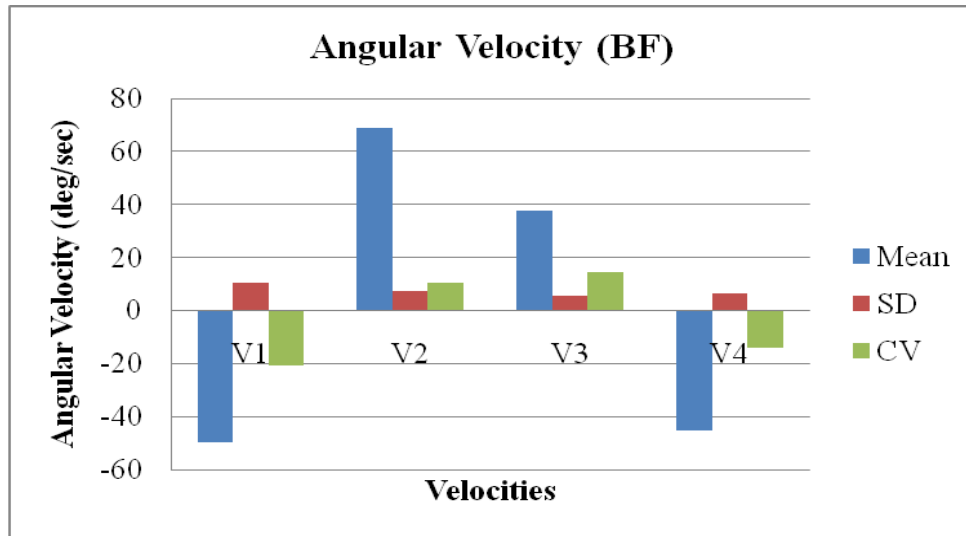


Figure 5. 51 Variations in Angular Velocity

Figure 5.51 shows higher values of mean of angular velocity for forward-to-neutral lumbar spine movement, while SD and CV of velocity are higher for neutral-to-forward movement.

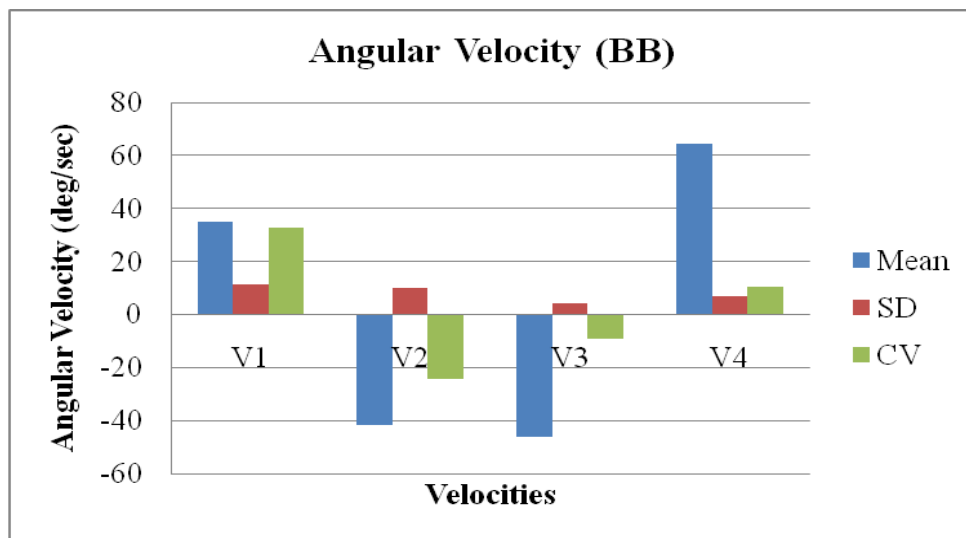


Figure 5. 52 Variations in Angular Velocity

Figure 5.52 shows mean value of angular velocity at maximum for forward-to-neutral movement, while SD and CV show higher values for neutral-to-backward movement.

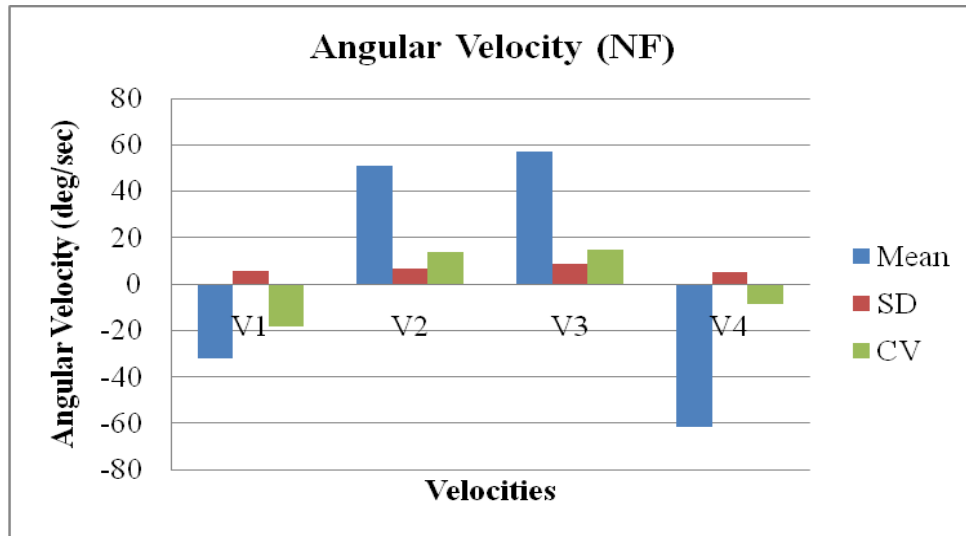


Figure 5. 53 Variations in Angular Velocity

For the NF subtest, the mean of angular velocity was maximum for backward-to-neutral position, while CV shows higher values for neutral-to-forward movement.

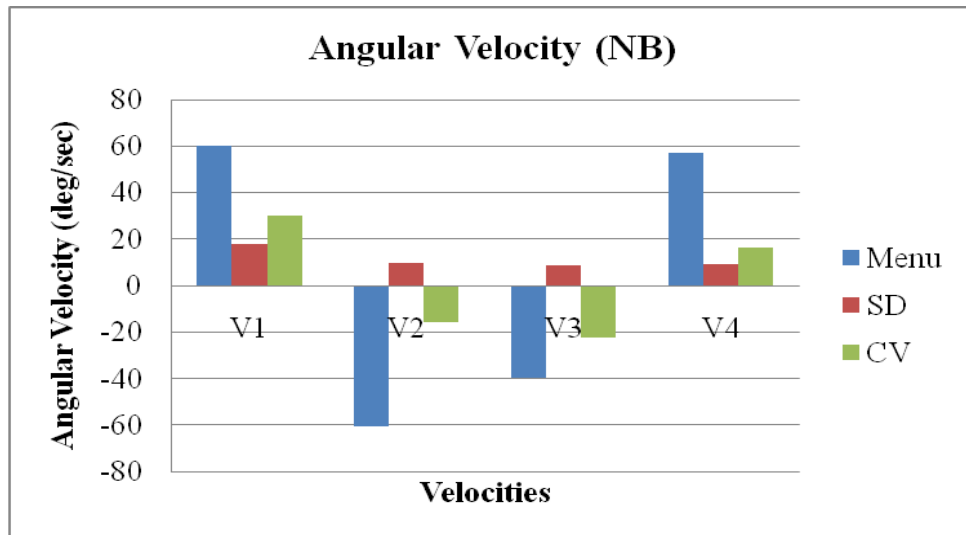


Figure 5. 54 Variations in Angular Velocity

The mean values for this subtest are higher for neutral-to-backward as well as backward-to-neutral movements. SD and CV of angular velocity had higher values for neutral-to-backward movement.



Table 5. 4 Linear and Nonlinear Measures

**Subject # 4**

<b>Test Condition</b>		<b>Mean</b>	<b>SD</b>	<b>CV (%)</b>	<b>ApEn</b>
<b>RA (NF)</b>	Total ROM	33.77797	2.284872	6.764385	<b>0.153</b>
	Angular Velocity Forward (V1)	-14.2121	2.774334	-19.5209	
	Angular Velocity Backward (V2)	16.93159	3.2964	19.46894	
	Angular Velocity Backward (V3)	34.69094	7.296463	21.03277	
	Angular Velocity Forward (V4)	-22.6464	2.868871	-12.6681	
<b>RB (FF)</b>	Total ROM	16.28671	2.457953	15.09177	<b>0.2392</b>
	Angular Velocity Forward (V1)	-15.0804	7.142536	-47.3629	
	Angular Velocity Backward (V2)	16.03047	3.765113	23.48722	
	Angular Velocity Backward (V3)	23.12471	2.786331	12.04915	
	Angular Velocity Forward (V4)	-20.8657	4.401871	-21.0962	
<b>RC (FB)</b>	Total ROM	39.02972	3.831347	9.816486	<b>0.2334</b>

	Angular Velocity Backward (V1)	42.80203	7.865588	18.37667	
	Angular Velocity Forward (V2)	-45.5397	7.544675	-16.5672	
	Angular Velocity Forward (V3)	-14.8892	9.539037	-64.0668	
	Angular Velocity Backward (V4)	15.36966	5.489797	35.7184	
RD (BF)	Total ROM	19.38199	2.771309	14.29837	0.2073
	Angular Velocity Forward (V1)	-19.5606	4.270326	-21.8313	
	Angular Velocity Backward (V2)	19.69281	4.273012	21.69833	
	Angular Velocity Backward (V3)	23.82195	4.271951	17.93283	
	Angular Velocity Forward (V4)	-23.1147	5.567579	-24.0867	
RE (BB)	Total ROM	25.45804	2.998514	11.77826	0.2065
	Angular Velocity Backward (V1)	18.51214	7.067774	38.17912	
	Angular Velocity Forward (V2)	-26.0891	7.496292	-28.7335	
	Velocity Forward	-27.9967	6.604632	-23.5908	

	(V3)				
	Angular Velocity Backward (V4)	29.43636	8.561432	29.08455	
RF (NF)	Total ROM	30.36189	4.518289	14.88145	0.1873
	Angular Velocity Forward (V1)	-17.9121	8.960335	-50.0238	
	Angular Velocity Backward (V2)	13.66101	6.092742	44.59949	
	Angular Velocity Backward (V3)	42.74039	7.127892	16.67718	
	Angular Velocity Forward (V4)	-31.3397	4.781819	-15.258	
RG (NB)	Total ROM	35.74301	2.16374	6.053603	0.1909
	Angular Velocity Backward (V1)	51.36497	12.12502	23.60562	
	Angular Velocity Forward (V2)	-34.3373	3.970481	-11.5632	
	Angular Velocity Forward (V3)	-22.5267	5.884504	-26.1223	
	Angular Velocity Backward (V4)	18.51593	5.072447	27.39504	

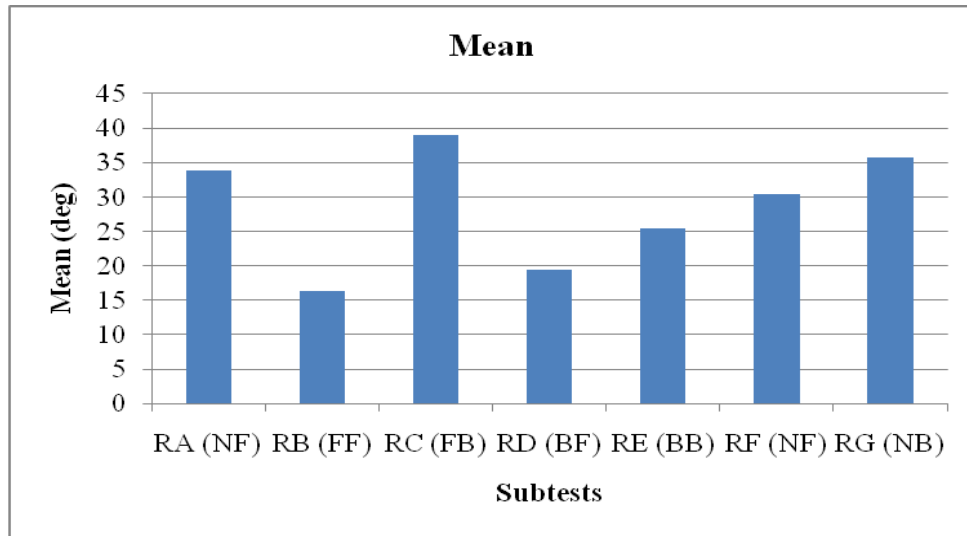


Figure 5. 55 Mean Values for Subtests

The mean values show a gradual increase, with increase in variability at first and second subtests.

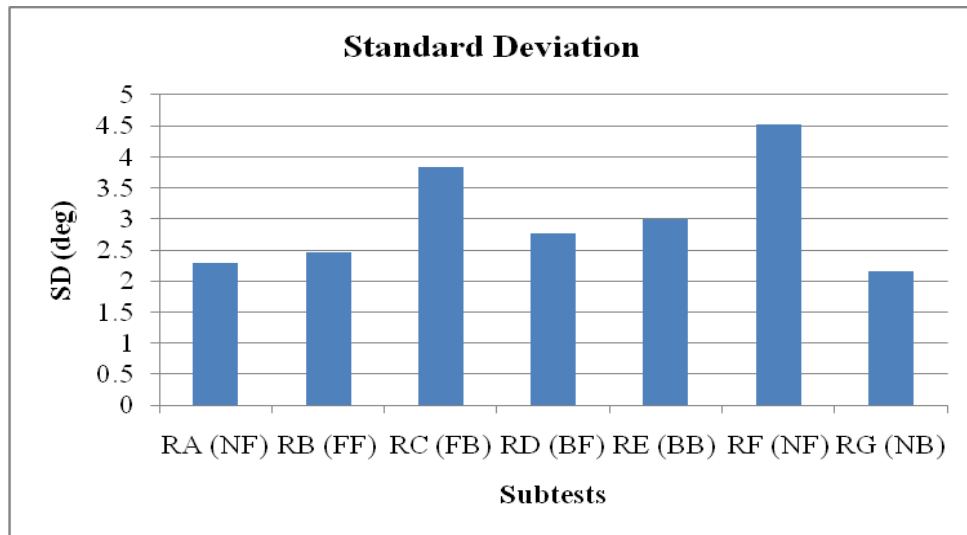


Figure 5. 56 Standard Deviation for Subtests

This standard deviation graph shows consistent variability, with a sudden rise for couple of tests, eventually depicting the M-shaped pattern also seen for first two subjects.

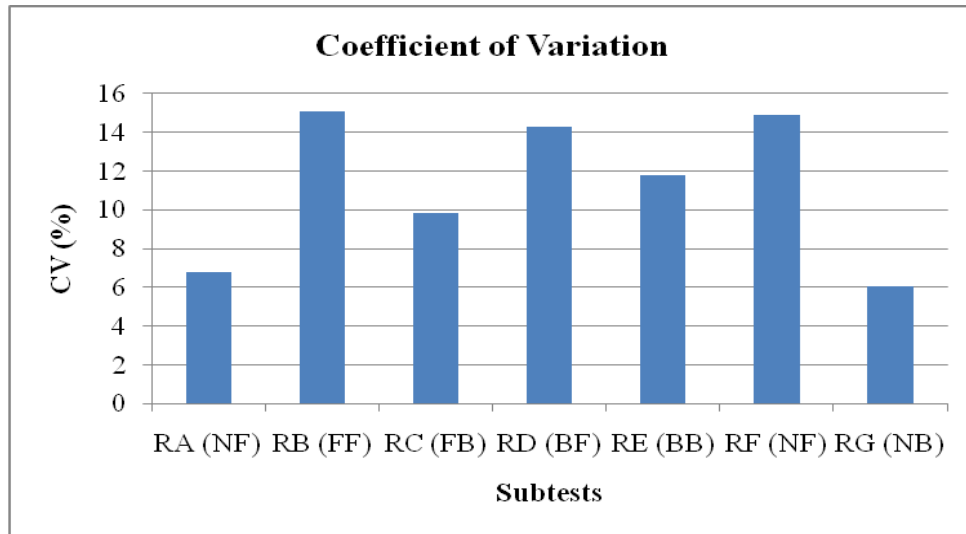


Figure 5. 57 Coefficient of Variation for Subtests

The variability shown by the coefficient of variation graph was higher for alternate subtests.

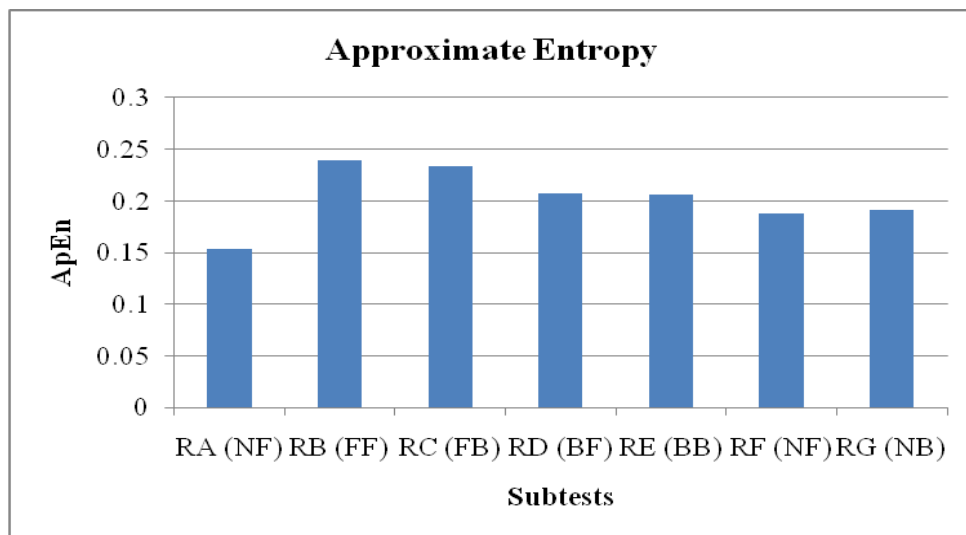


Figure 5. 58 Approximate Entropy for Subtests

As seen before, ApEn values decreased gradually after a low complexity for first subtest.

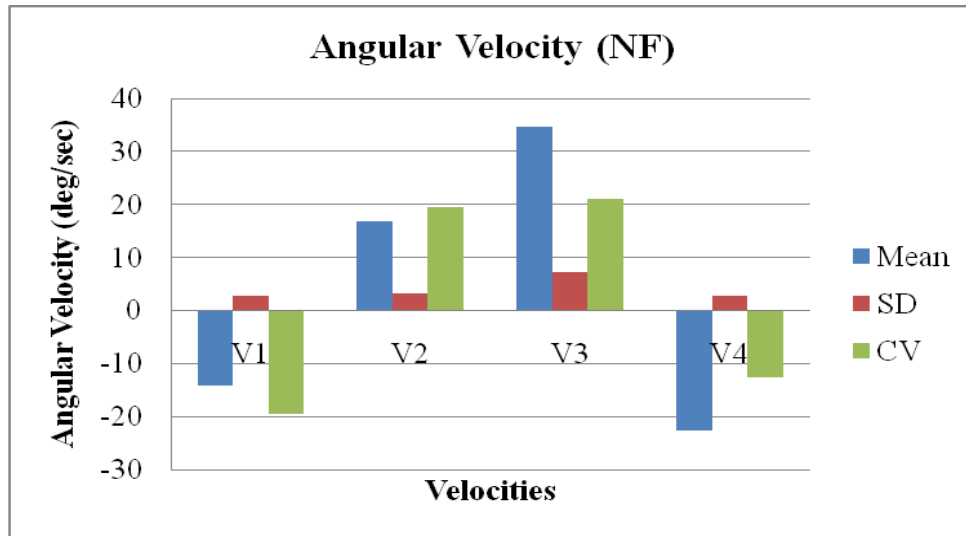


Figure 5. 59 Variations in Angular Velocity

The mean, SD, and CV values of angular velocity were maximum for neutral-to-backward movement.

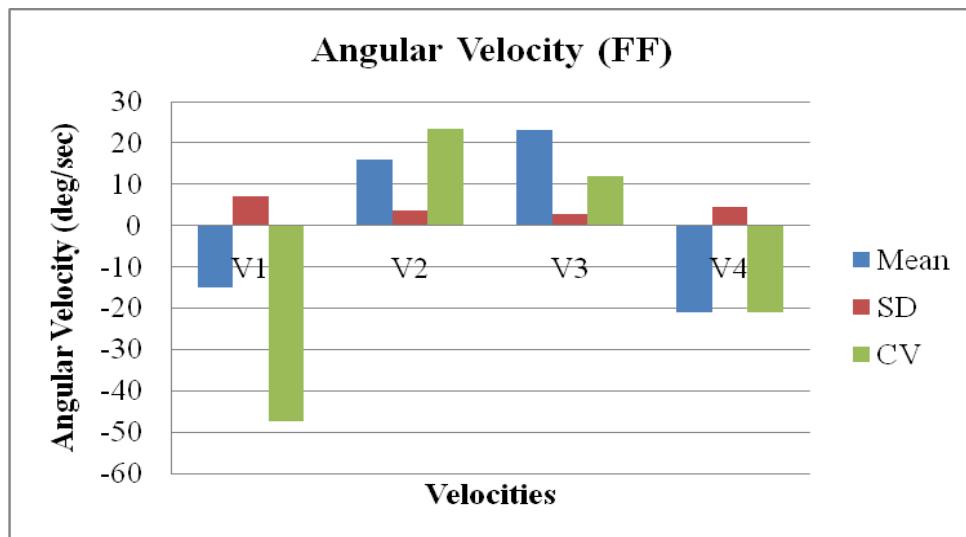


Figure 5. 60 Variations in Angular Velocity

This subtest shows higher values for CV and SD of angular velocity for neutral-to-forward direction, while the mean was maximum for neutral-to-backward direction.

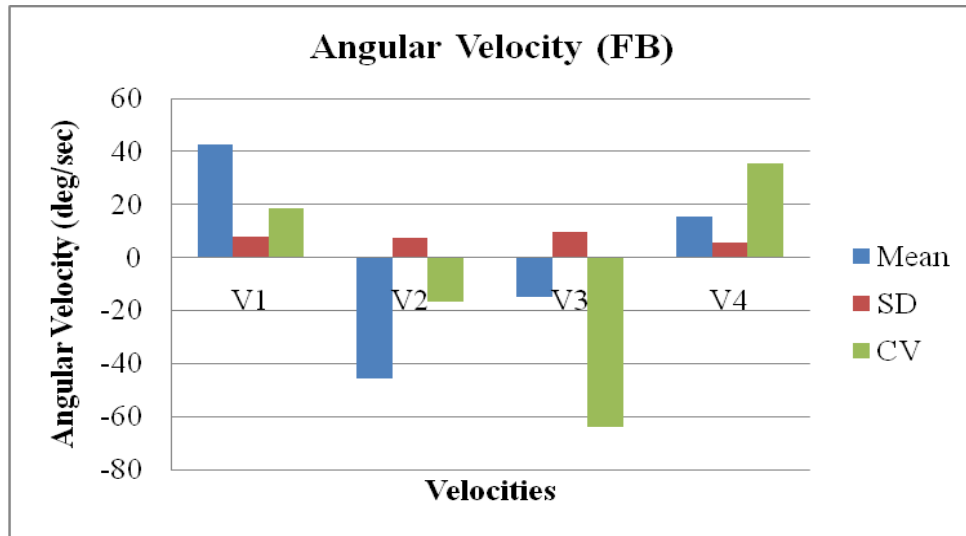


Figure 5. 61 Variations in Angular Velocity

The mean of angular velocity in figure 5.61 shows a higher value for neutral-to-backward and backward-to-neutral movements. The CV values are maximum for neutral-to-forward direction, with SD being uniform.

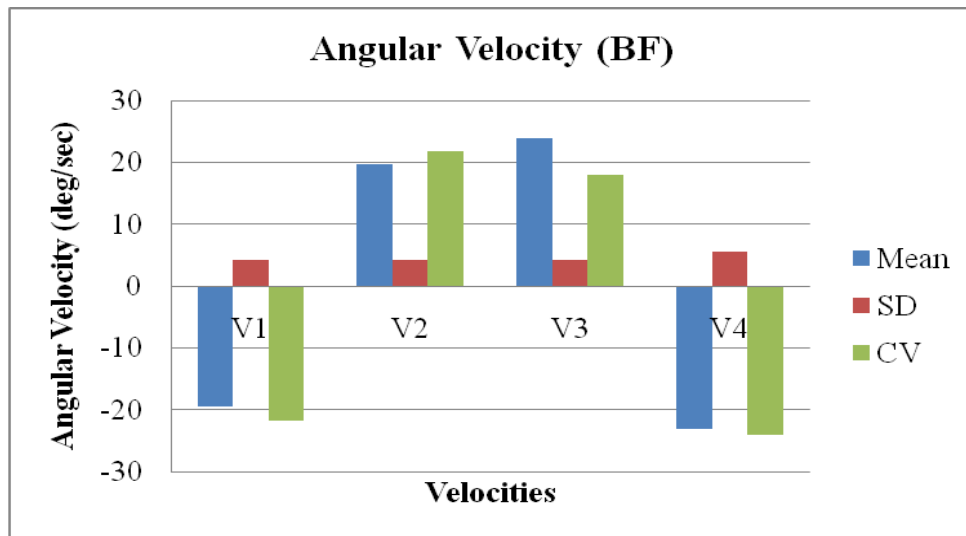


Figure 5. 62 Variations in Angular Velocity

Figure 5.62 shows mean, SD, and CV values of angular velocity are more or less uniform for all four sections of the cycle, with mean being maximum for neutral-to-backward movement and CV higher for backward-to-neutral movement.

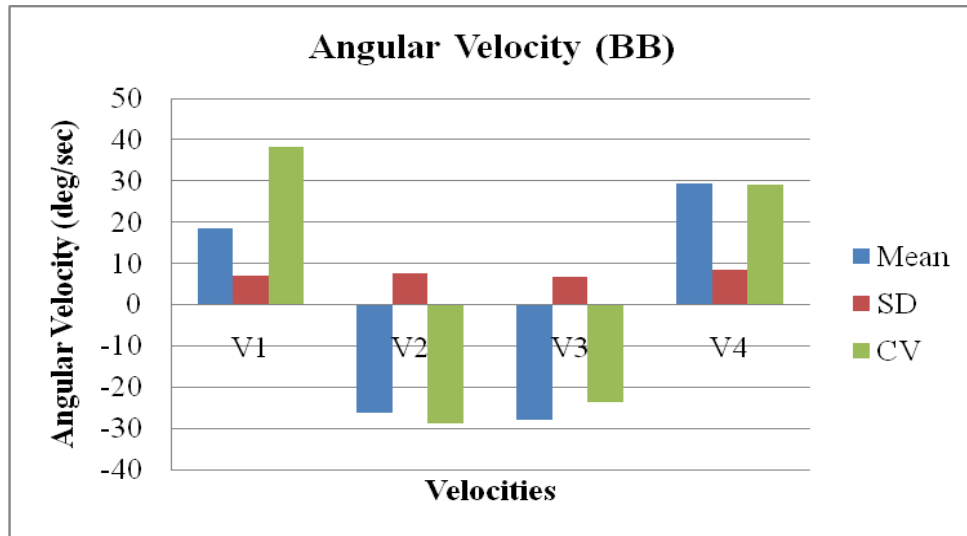


Figure 5. 63 Variations in Angular Velocity

For the BB subtest, mean of angular velocity has maximum value for forward-to-neutral movement, while CV is higher for neutral-to-backward movement.

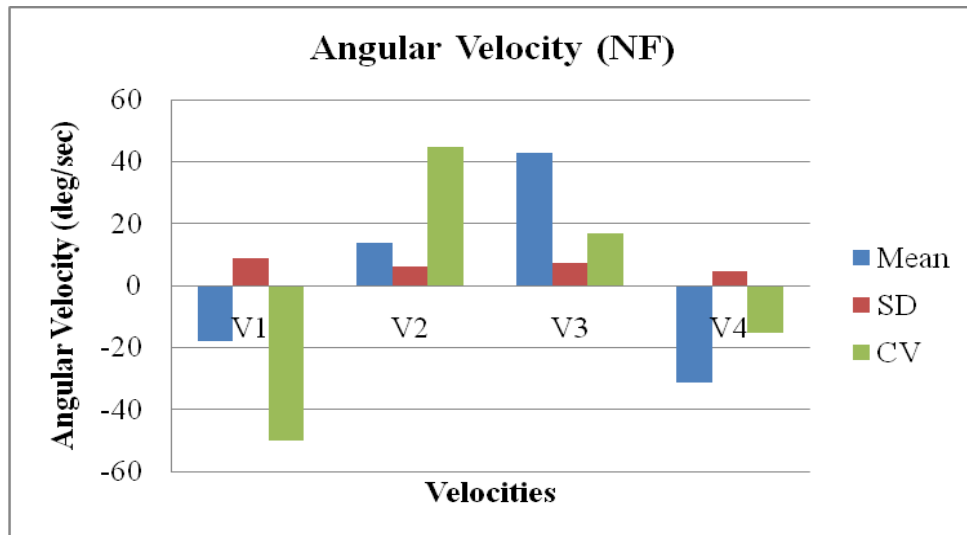


Figure 5. 64 Variations in Angular Velocity

Figure 5.64 shows higher mean values for neutral-to-backward movement, while CV is maximum for neutral-to-forward movement.



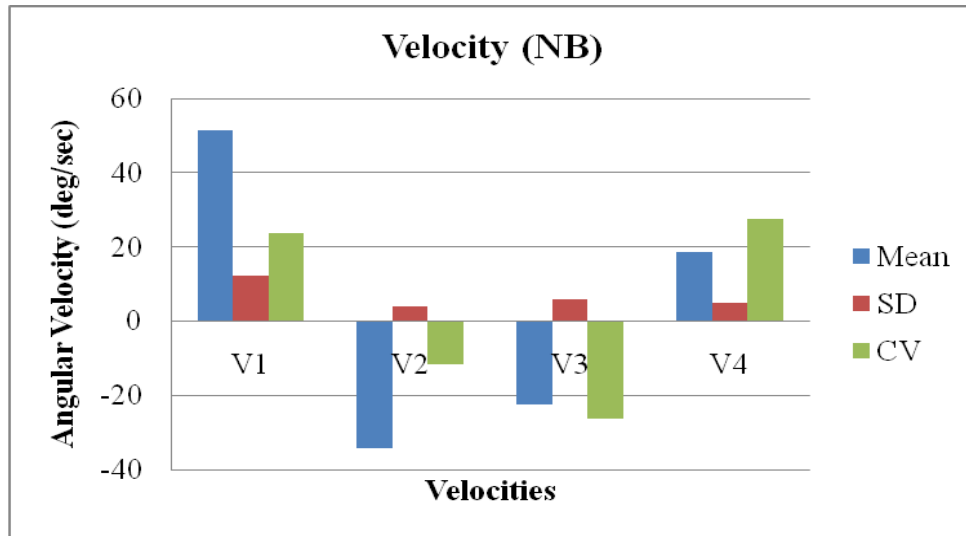


Figure 5. 65 Variations in Angular Velocity

The mean of the angular velocity shows higher values while moving backward from neutral position, while CV is maximum while moving from forward-to-neutral direction.

Table 5. 5 Linear and Nonlinear Measures

**Subject # 5**

Test Condition		Mean	SD	CV (%)	ApEn
RA (NF)	Total ROM	5.83479	1.606169	27.52745	0.1493
	Angular Velocity Forward (V1)	-5.42485	2.209598	-40.731	
	Angular Velocity Backward (V2)	6.615675	1.904245	28.78384	
	Angular Velocity Backward (V3)	6.08009	3.136002	51.57821	
	Angular Velocity Forward	-5.24073	2.785412	-53.1494	

	(V4)				
RB (FF)	Total ROM	5.512587	1.054312	19.12554	0.2044
	Angular Velocity Forward (V1)	-6.68542	2.715881	-40.624	
	Angular Velocity Backward (V2)	9.493815	3.447403	36.31209	
	Angular Velocity Backward (V3)	8.985679	3.201779	35.63202	
	Angular Velocity Forward (V4)	-8.01148	3.324271	-41.4938	
RC (FB)	Total ROM	7.188811	1.195438	16.62915	0.2036
	Velocity Backward (V1)	9.869443	1.546233	15.66687	
	Angular Velocity Forward (V2)	-8.25132	1.583974	-19.1966	
	Angular Velocity Forward (V3)	-6.35202	1.81681	-28.6021	
	Angular Velocity Backward (V4)	10.37606	4.416373	42.56312	
RD (BF)	Total ROM	4.867832	1.589348	32.65001	0.1958
	Angular Velocity Forward (V1)	-7.41343	1.088973	-14.6892	
	Angular Velocity Backward (V2)	9.248163	1.925909	20.82478	

	Angular Velocity Backward (V3)	8.447628	3.017001	35.71418	
	Angular Velocity Forward (V4)	-7.79239	2.896464	-37.1704	
RE (BB)	Total ROM	7.31049	1.404553	19.21284	0.225
	Angular Velocity Backward (V1)	8.004571	2.694866	33.66659	
	Angular Velocity Forward (V2)	-8.95576	2.372645	-26.4929	
	Angular Velocity Forward (V3)	-7.82318	1.506173	-19.2527	
	Angular Velocity Backward (V4)	8.243921	2.697588	32.72215	
RF (NF)	Total ROM	7.907692	0.825406	10.43801	0.2072
	Angular Velocity Forward (V1)	-7.92154	1.936026	-24.44	
	Angular Velocity Backward (V2)	10.00056	1.840471	18.40367	
	Angular Velocity Backward (V3)	8.662963	1.654945	19.10368	
	Angular Velocity Forward (V4)	-7.15391	1.371799	-19.1755	
RG (NB)	Total ROM	9.94965	0.756835	7.606651	0.2026

	Angular Velocity Backward (V1)	10.96658	1.490266	13.58916	
	Angular Velocity Forward (V2)	-9.68718	1.520841	-15.6995	
	Angular Velocity Forward (V3)	-8.42253	2.65833	-31.5621	
	Angular Velocity Backward (V4)	8.325599	1.89399	22.74899	

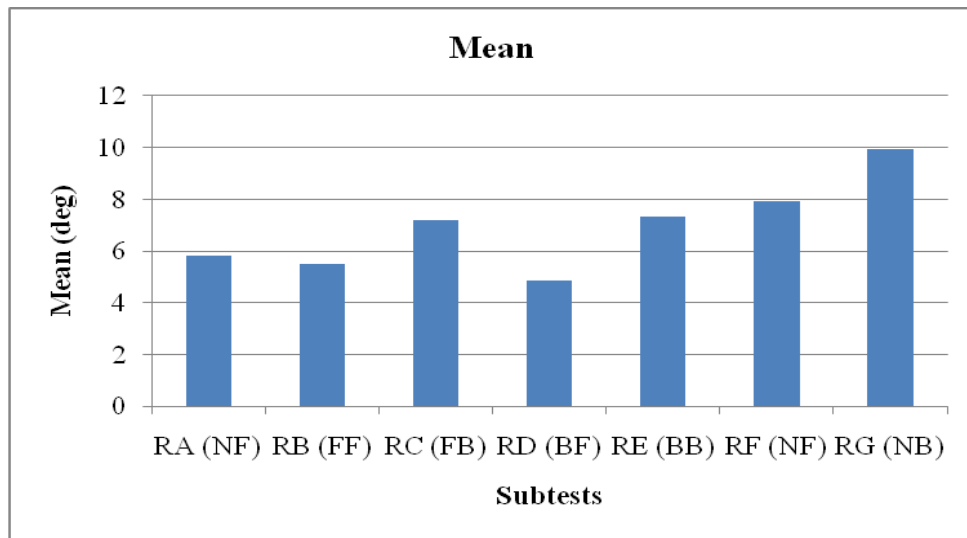


Figure 5.66 Mean Values for Subtests

The graph shows a gradual increase in variability as the tests progress, with maximum variability at the final subtest.

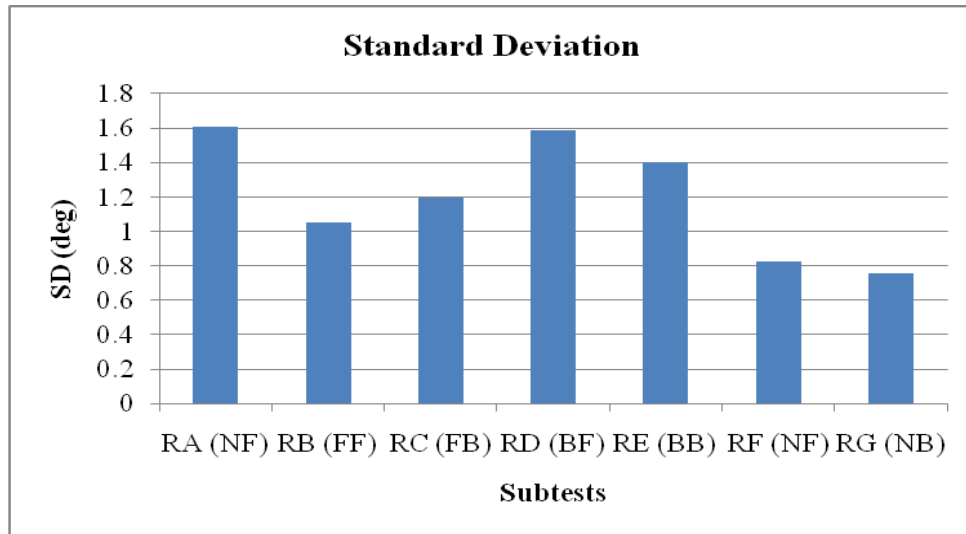


Figure 5. 67 Standard Deviation for Subtests

The standard deviation graph shows decline in variability after high variability for the first test. The variability increases for RD, followed by a gradual decline before reaching minimum at the last subtest.

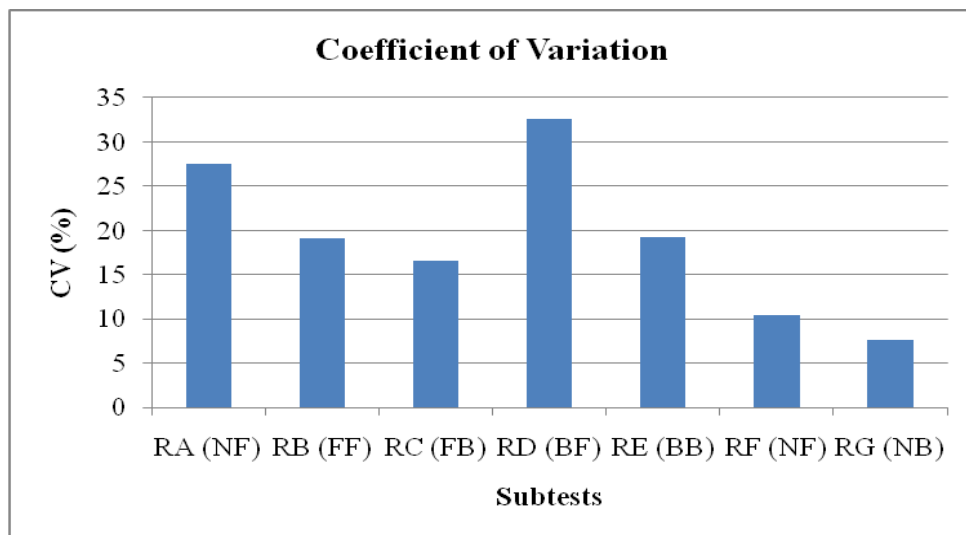


Figure 5. 68 Coefficient of Variation for Subtests

The coefficient of variation graph shows a gradual decrease in variation for first half of the subtests, followed by a sudden rise at RD. After that, there is decline in variability.

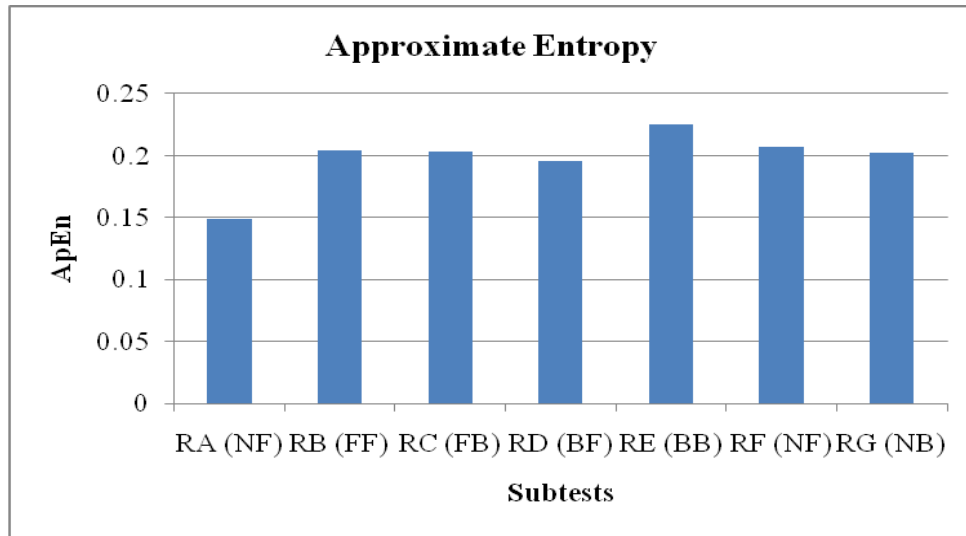


Figure 5. 69 Approximate Entropy for Subtests

This graph depicts an initial increase in ApEn values, after which the values are fairly uniform throughout.

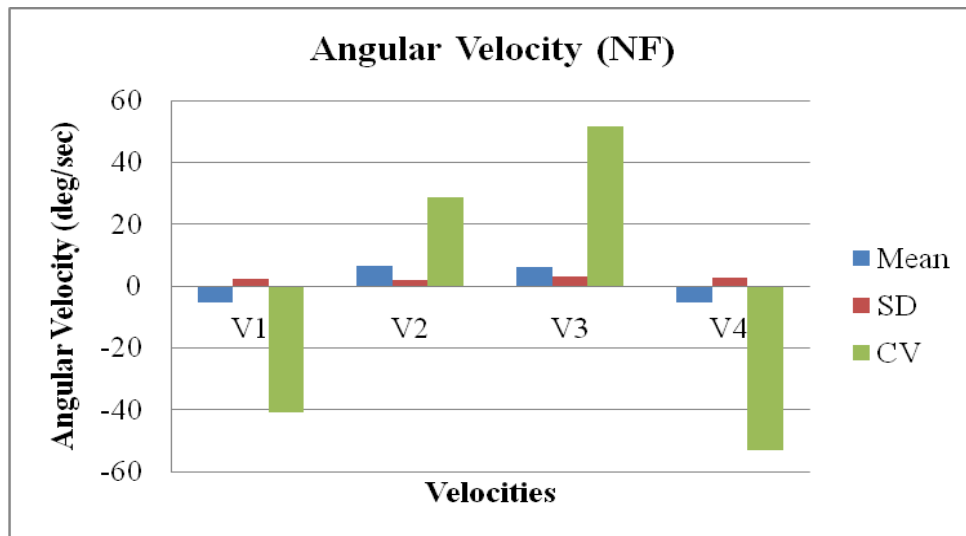


Figure 5. 70 Variations in Angular Velocity

The mean and SD for angular velocity for the NF subtest shows uniform values throughout, while CV is higher for neutral-to-backward and backward-to-neutral movements.

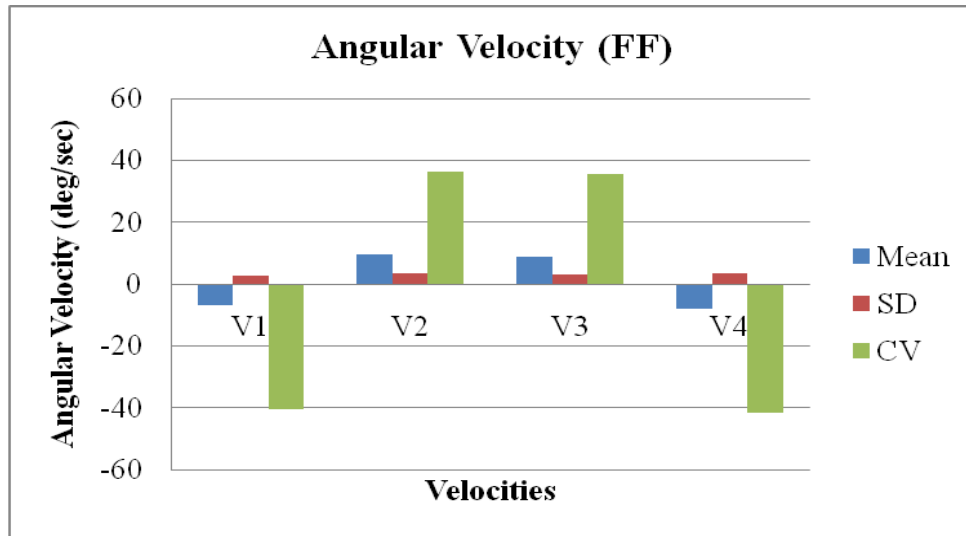


Figure 5. 71 Variations in Angular Velocity

For subtest FF, the mean, SD, and CV are uniform for all four sections of the cycle and show correlation among them.

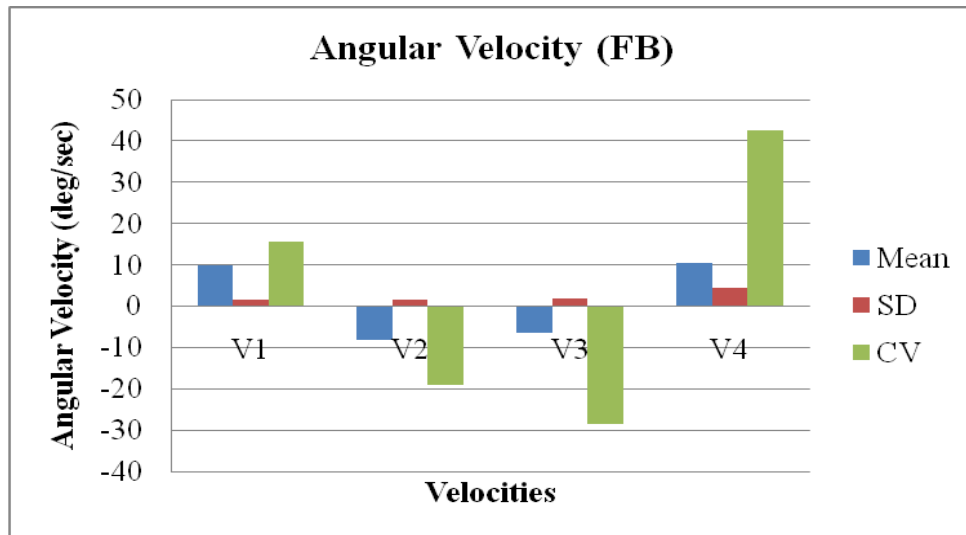


Figure 5. 72 Variations in Angular Velocity

Figure 5.72 shows higher mean values of angular velocity for movement in neutral-to-backward and forward-to-neutral directions, while CV is maximum for forward-to-neutral movement.

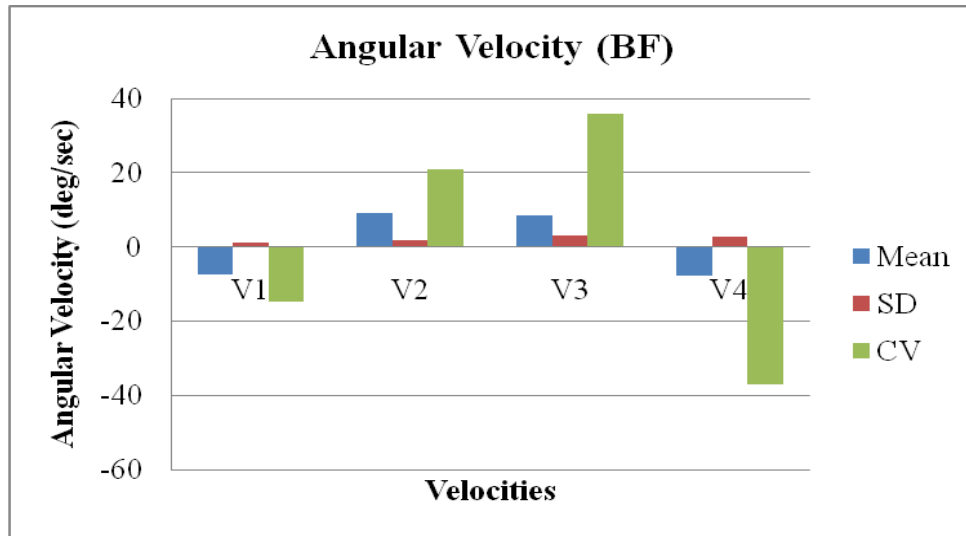


Figure 5. 73 Variations in Angular Velocity

Figure 5.73 shows higher mean of angular velocity values for backward movement, but the CV of angular velocity shows higher values for neutral-to-backward and backward-to-neutral directions.

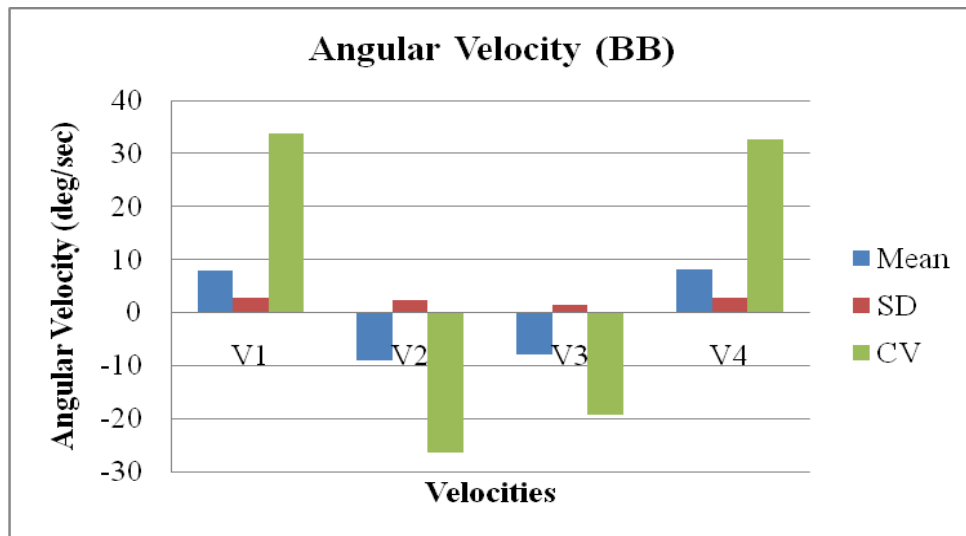


Figure 5. 74 Variations in Angular Velocity

For the BB subtest, the mean and SD of angular velocity is uniform, while the CV is higher for neutral-to-backward and forward-to-backward movements.



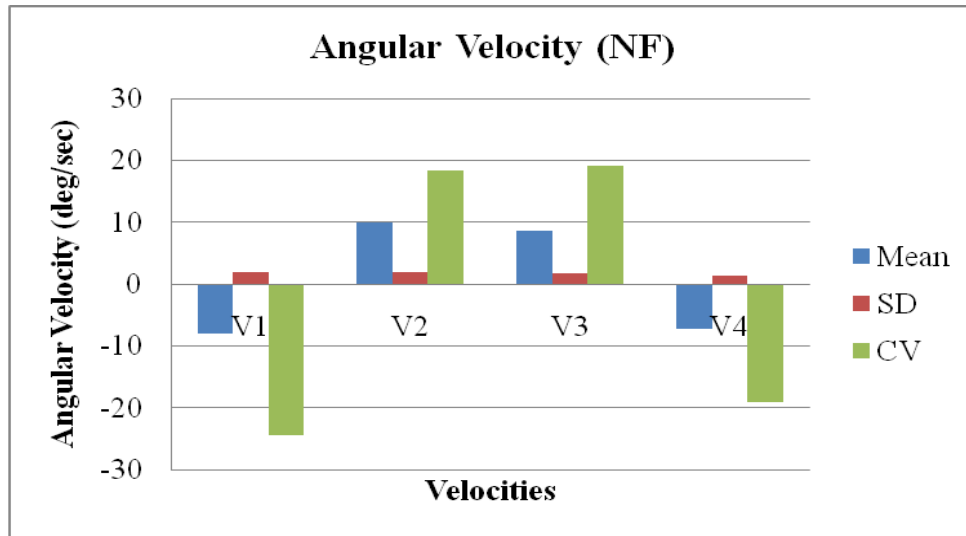


Figure 5. 75 Variations in Angular Velocity

Figure 5.75 depicts uniform values for mean, SD, and CV of angular velocity.

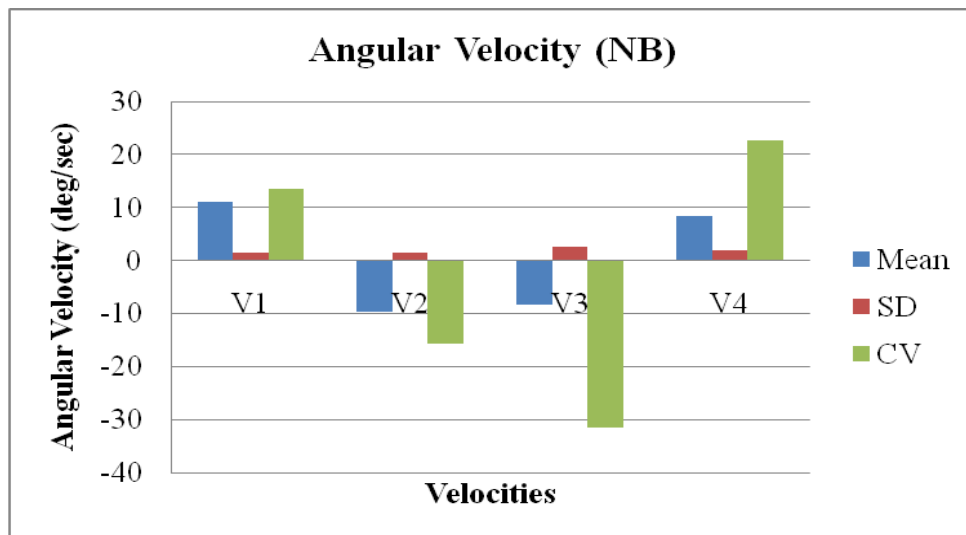


Figure 5. 76 Variations in Angular Velocity

Figure 5.76 shows higher mean of angular velocity values for neutral-to-backward movement, while CV is higher for neutral-to-forward direction.

As seen from the above results, the linear techniques do not show any particular pattern and it is difficult to conclude anything from these results. However, ApEn have

similar pattern in all the subtests for all participants and mostly shows decreases in complexity as the tests progressed.

Variations in angular velocity graphs do not show any peculiar trends as well. Although they show variation in angular velocity from subtest to subtest, they fail to show any particular pattern in healthy subjects that can be attributed to them.

## **5.2 Cadaver Study**

Variability in a cadaveric specimen was also analyzed. The effect of speed and injury was analyzed for intervertebral segments. A second-order Butterworth filter with a cut-off frequency of 10 Hz (Sample rate = 100; Nyquist frequency = sample rate/2 = 50 Hz;  $W_n = \text{cut off freq}/\text{Nyquist freq} = 10/50 = 0.2 \text{ Hz}$ ), similar to the one used for the subject test, was used. But the velocity and acceleration graph showed noise.

To reduce the effect of noise, the velocity and acceleration data was filtered, but the results did not show any improvement. Hence, in order to nullify this error, a filter with a cut-off frequency of 1Hz was used to estimate velocity and acceleration data.

The phase plane plot for each cadaveric test is shown below.

### Cadaver without Cut at Slower Speed:

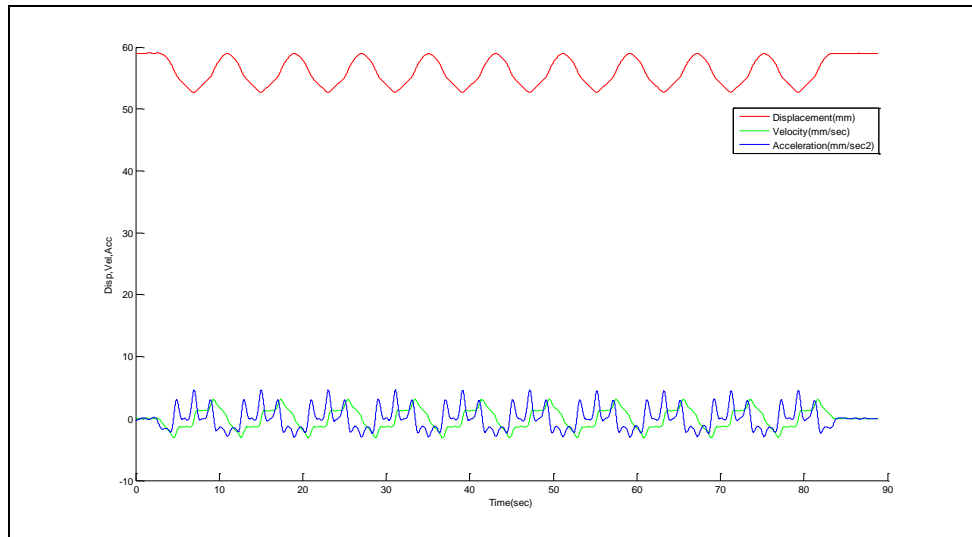


Figure 5. 77 Displacement Time Series with Velocity and Acceleration

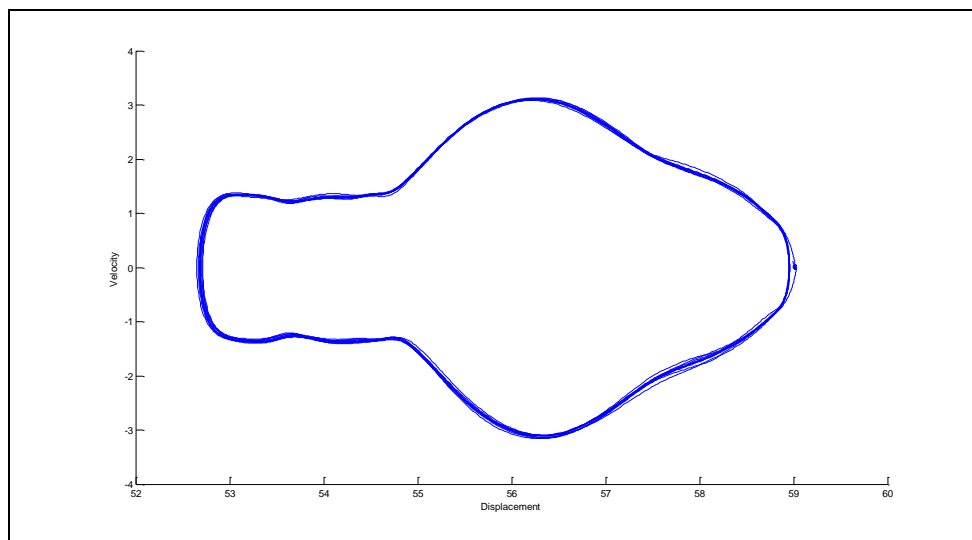


Figure 5. 78 Phase Plane Plot

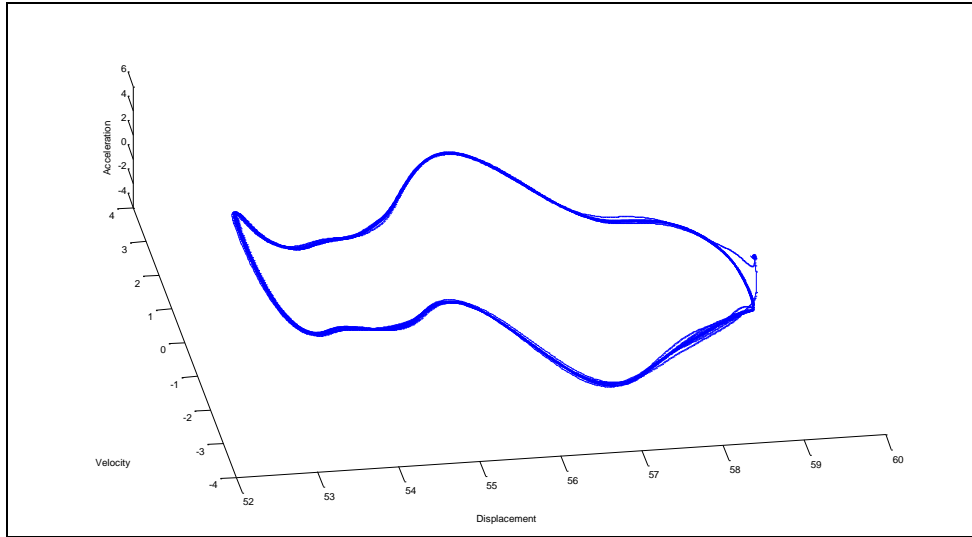


Figure 5. 79 3-D Phase Plane Plot

As seen from figures 5.43 and 5.44, the plot shows an elegant pattern with minimal separation in the trajectories. Hence, it can be concluded that this is a highly periodic system.

**Cadaver without Cut at Higher Speed:**

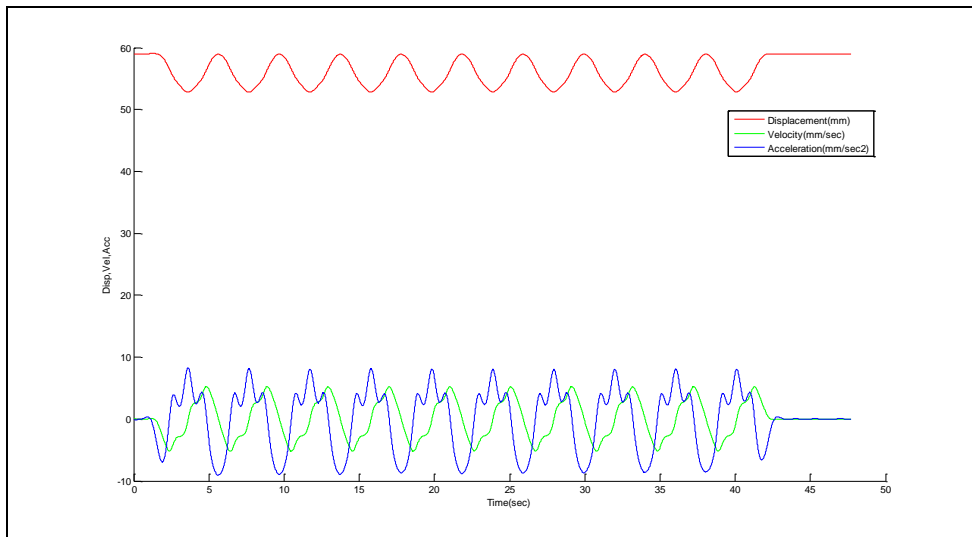


Figure 5. 80 Displacement Time Series with Velocity and Acceleration

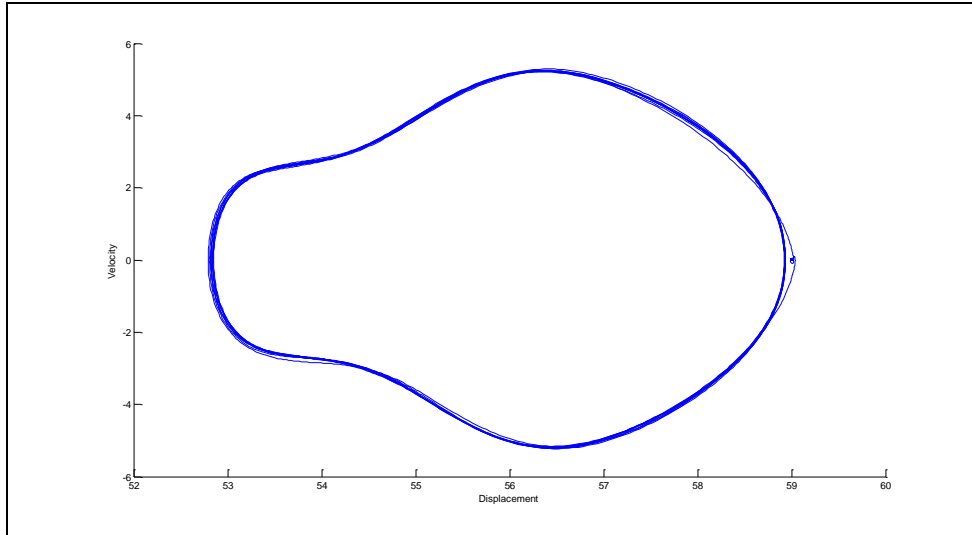


Figure 5. 81 Phase Plane Plot

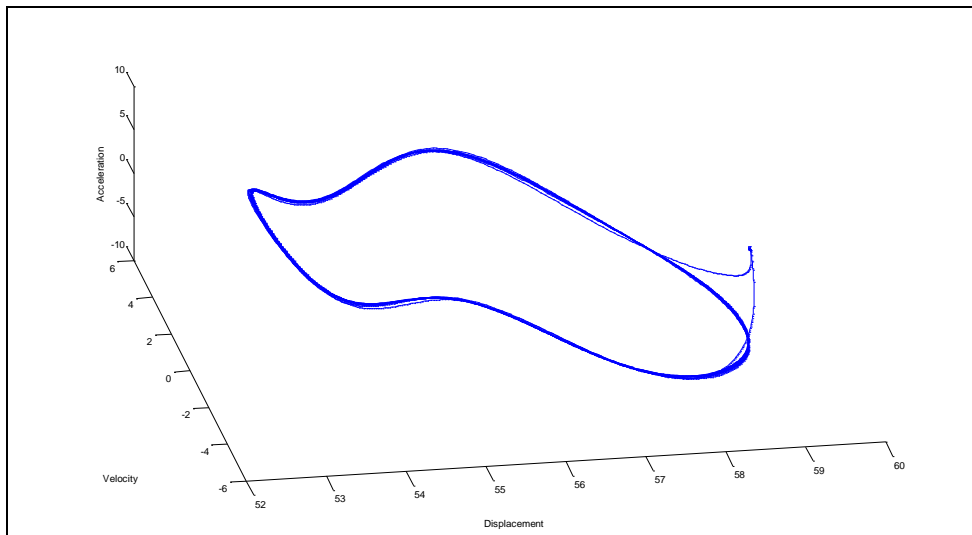


Figure 5. 82 3-D Phase Plane Plot

As seen from phase plots in figures 5.46 and 5.47, the trajectories do not separate out much and are similar to those in the first case.

## Cadaver Disc Cut at Slower Speed:

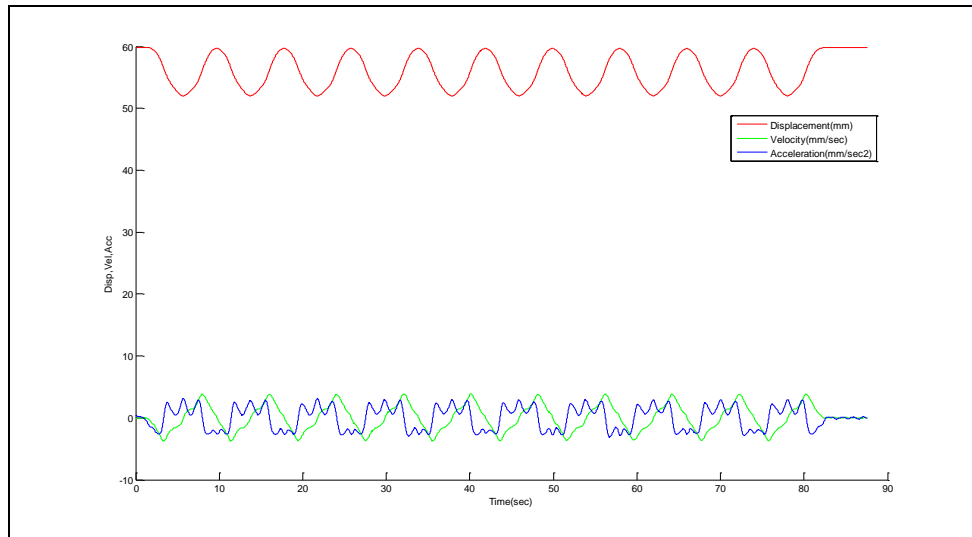


Figure 5. 83 Displacement Time Series with Velocity and Acceleration

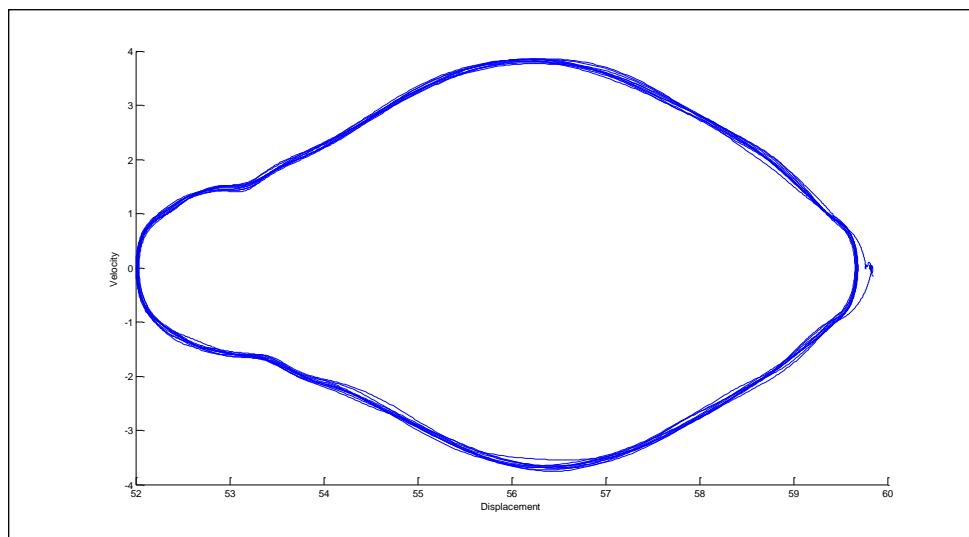


Figure 5. 84 Phase Plane Plot

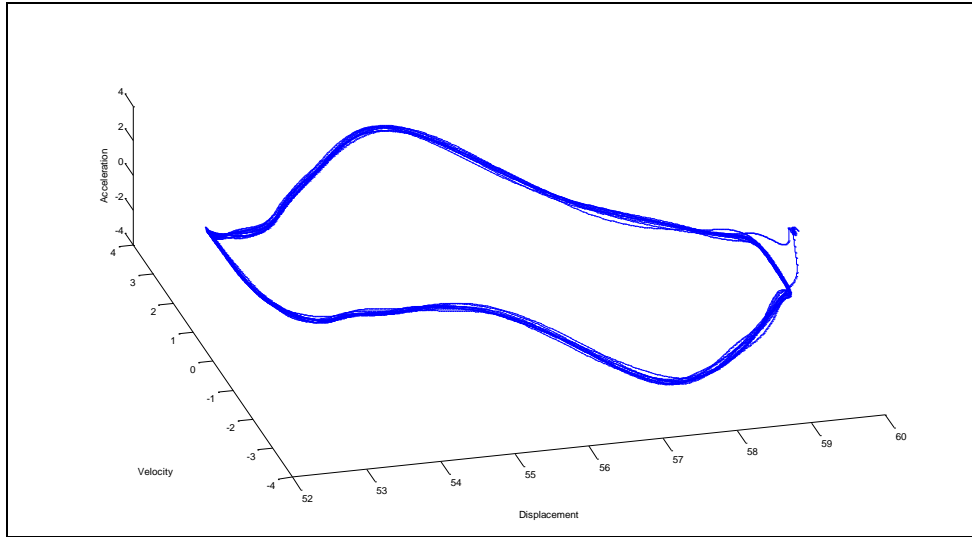


Figure 5. 85 3-D phase Plane Plot

The phase plane plots show peculiar patterns without much divergence in trajectories.

**Cadaver Disc Cut at Higher Speed:**

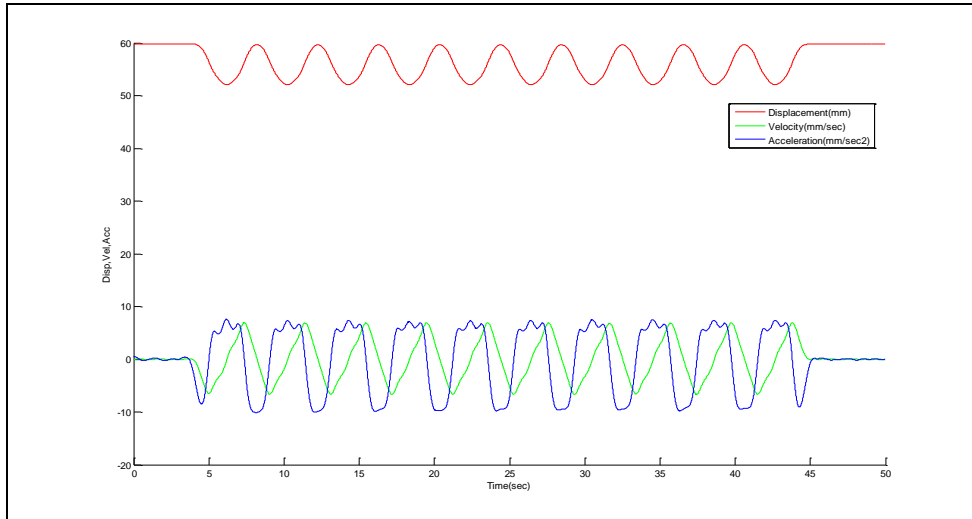


Figure 5. 86 Displacement Time Series with Velocity and Acceleration

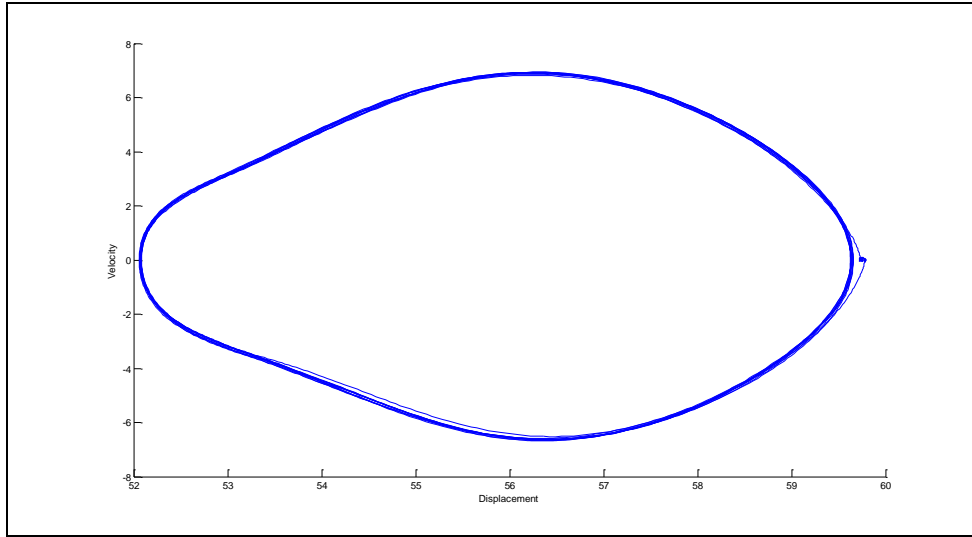


Figure 5. 87 Phase Plane Plot

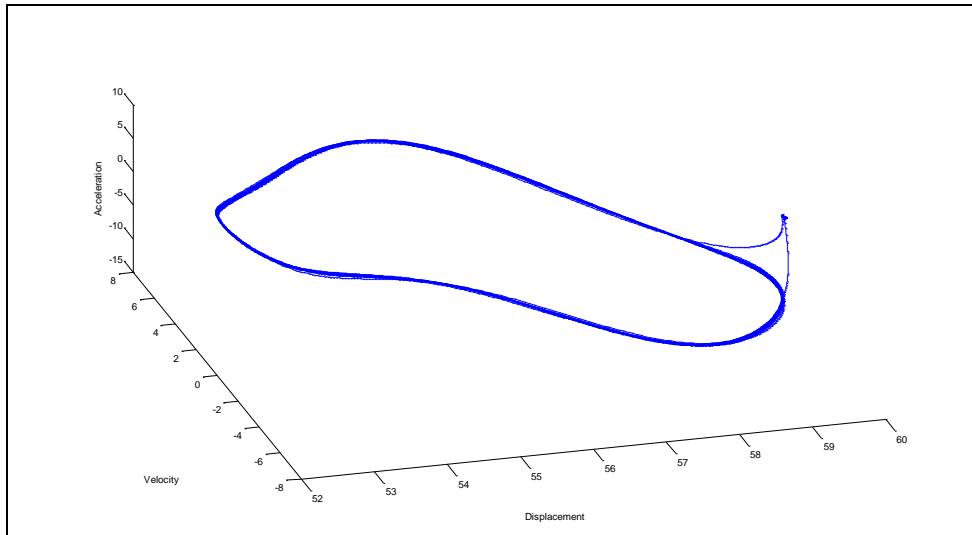


Figure 5. 88 3-D Phase Plane Plot

Similar to the slower speed phase plane plots, the higher speed phase plane plots depict less separation of trajectories and more of the system's periodicity.



### Cadaver Right Capsule Cut at Slower Speed:

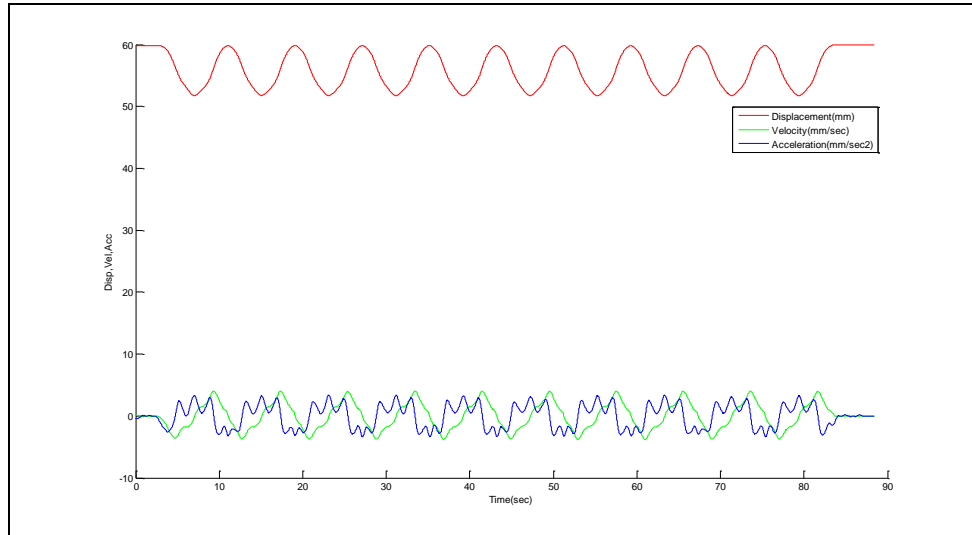


Figure 5. 89 Displacement Time Series with Velocity and Acceleration

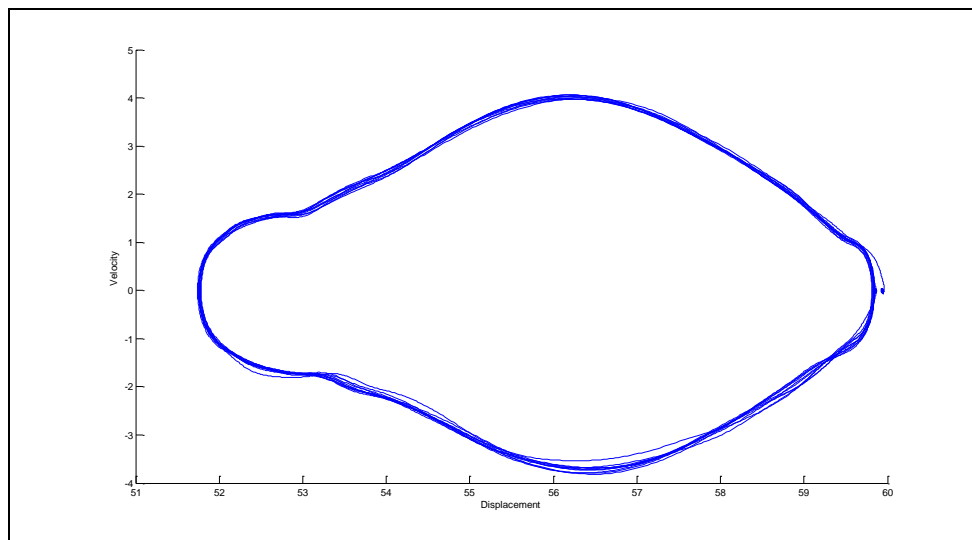


Figure 5. 90 Phase Plane Plot

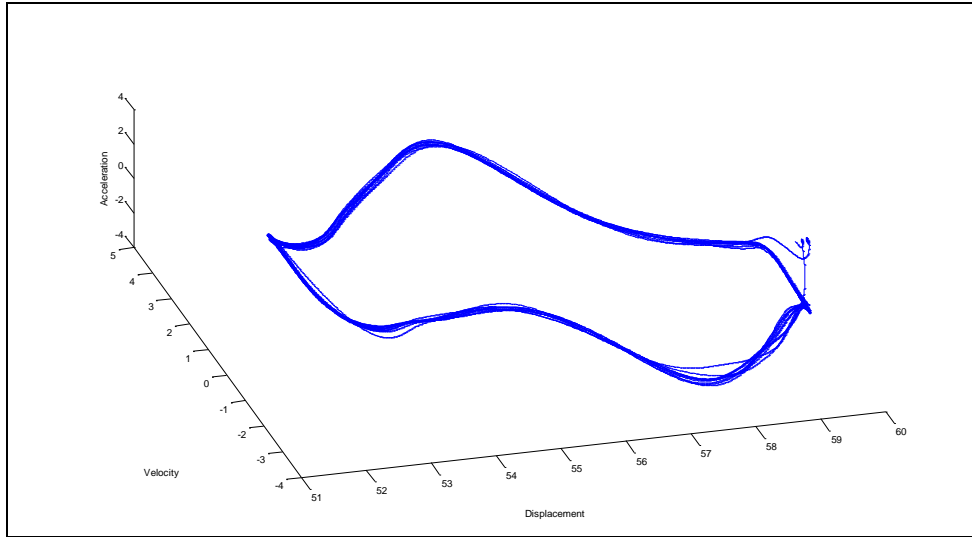


Figure 5. 91 3-D Phase Plane Plot

Figures 5.55 and 5.56 show phase plane plots for intervertebral spine movement when injured on the right capsule at L4-L5 level. The plot shows some elegant pattern depicting the periodicity of the system.

**Cadaver Right Capsule Cut at Higher Speed:**

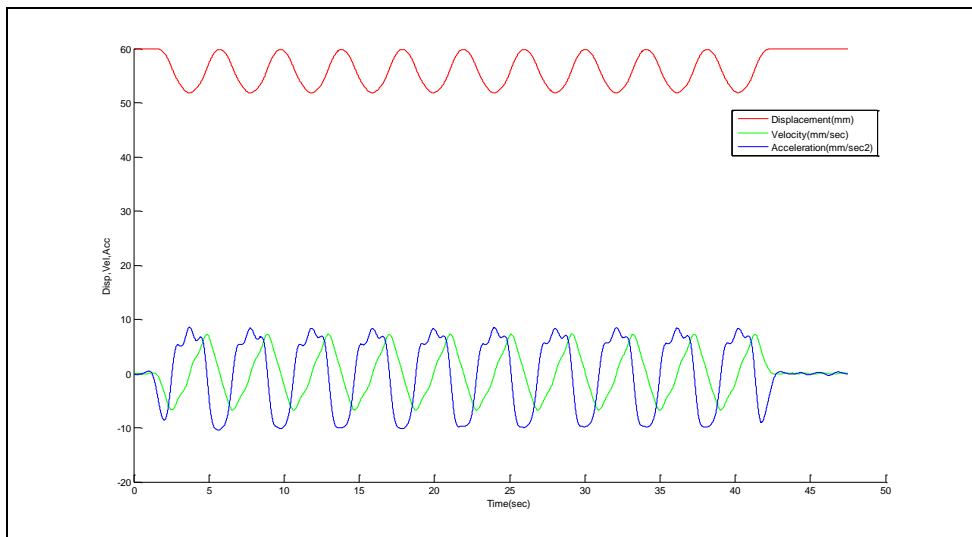


Figure 5. 92 Displacement Time Series with Velocity and Acceleration

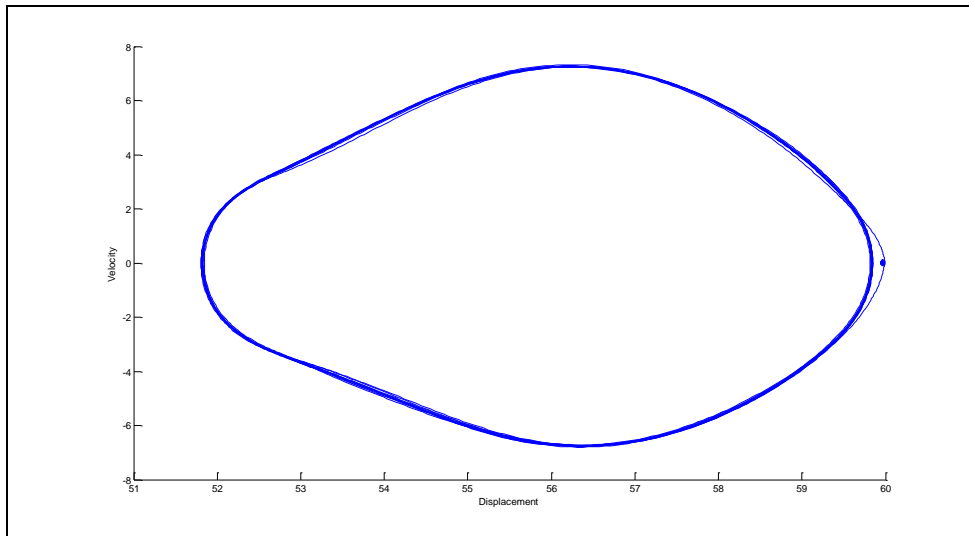


Figure 5. 93 Phase Plane Plot

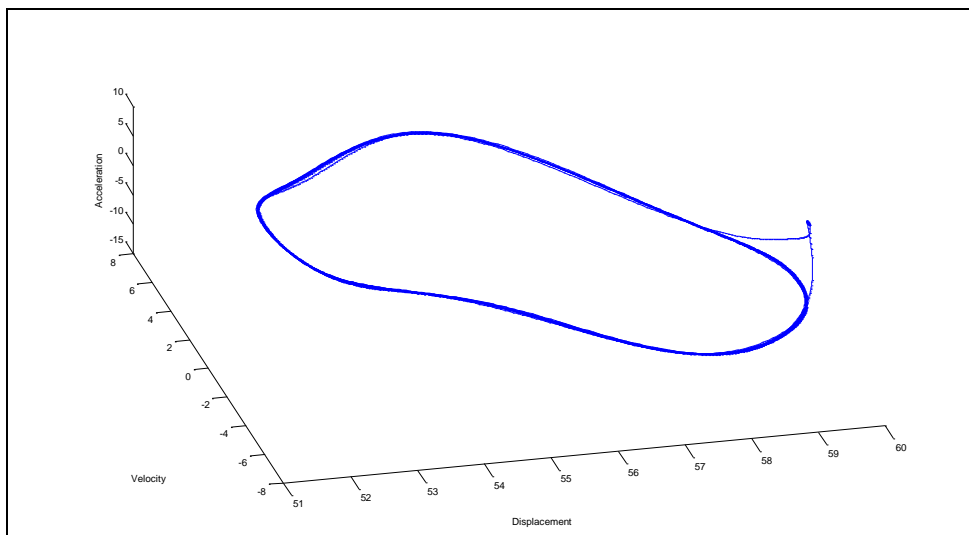


Figure 5. 94 3-D Phase Plane Plot

Phase plane plots of this test show similar patterns as seen in the above test. In this case, the speed and injuries to the cadaveric spine had a minimal effect on intersegmental stability.

Mean, standard deviation, coefficient of variation, and approximate entropy were computed for each of the time series data. Below, Table 5.1 shows the values for each of the tests performed on a cadaveric specimen.

Table 5. 6 Linear and Nonlinear Measures

<b>Test Condition</b>		<b>Mean</b>	<b>SD</b>	<b>CV (%)</b>	<b>ApEn</b>
Cadaver without Cut Slower Speed	Total ROM	6.468531	0.039696	0.613672	0.0477
	Velocity Forward (V1)	-1.76277	0.062718	-3.55792	
	Velocity Backward (V2)	1.773309	0.064234	3.622261	
	Velocity Backward (V3)	2.152	0.114584	5.32452	
	Velocity Forward (V4)	-2.14217	0.133844	-6.24804	
Cadaver without Cut Higher Speed	Total ROM	6.483916	0.036232	0.558797	0.065
	Velocity Forward (V1)	-3.53525	0.113045	-3.19766	
	Velocity Backward (V2)	3.669537	0.141752	3.862946	
	Velocity Backward (V3)	4.204689	0.151203	3.596049	
	Velocity Forward (V4)	-4.03208	0.372195	-9.23084	
Cadaver Disc Cut at Slower Speed	Total ROM	7.79021	0.050265	0.645238	0.0641
	Velocity Forward (V1)	-2.11924	0.081573	-3.84915	
	Velocity Backward (V2)	2.154336	0.066777	3.099663	

	Velocity Backward (V3)	2.633066	0.20561	7.808761	
	Velocity Forward (V4)	-2.4881	0.228225	-9.17269	
Cadaver Disc Cut at Higher Speed	Total ROM	7.744406	0.067084	0.866221	0.0615
	Velocity Forward (V1)	-4.34084	0.102533	-2.36206	
	Velocity Backward (V2)	4.23037	0.165887	3.921328	
	Velocity Backward (V3)	4.897316	0.265935	5.43021	
	Velocity Forward (V4)	-5.16134	0.282337	-5.47022	
Cadaver Right Capsule Cut at Slower Speed	Total ROM	8.206294	0.054791	0.66767	0.061
	Velocity Forward (V1)	-2.20426	0.085847	-3.89461	
	Velocity Backward (V2)	2.352996	0.108934	4.629577	
	Velocity Backward (V3)	2.686655	0.047786	1.778625	
	Velocity Forward (V4)	-2.63781	0.211405	-8.01443	
Cadaver Right Capsule Cut at Higher Speed	Total ROM	8.25	0.045477	0.551236	0.0771
	Velocity Forward (V1)	-4.45809	0.146835	-3.29367	
	Velocity Backward (V2)	4.692214	0.160693	3.424669	
	Velocity	5.24866	0.239875	4.570218	

	Backward (V3)				
	Velocity Forward (V4)	-5.22231	0.377887	-7.23602	

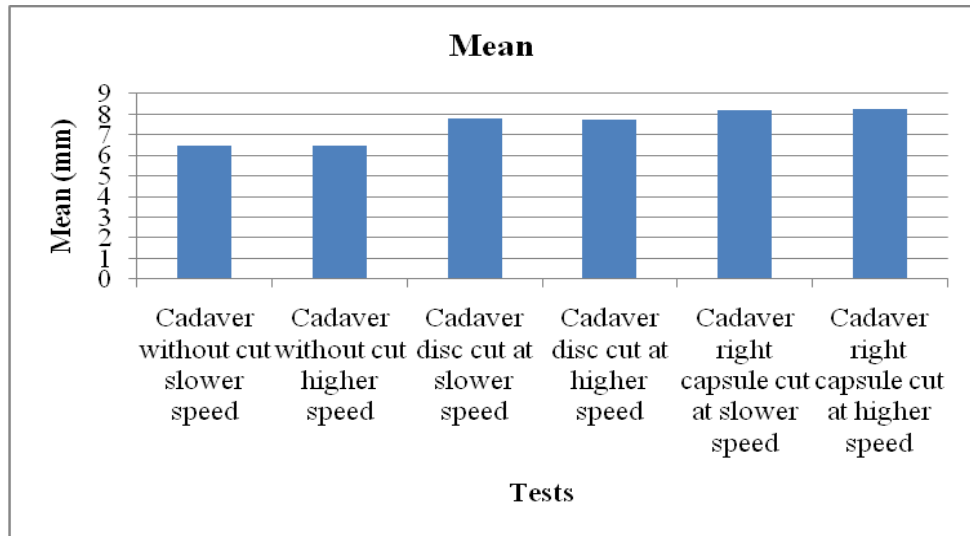


Figure 5. 95 Mean for Tests

As seen in Figure 5.95, the mean values show uniform values throughout the tests irrespective of speed and injuries made to the specimen.

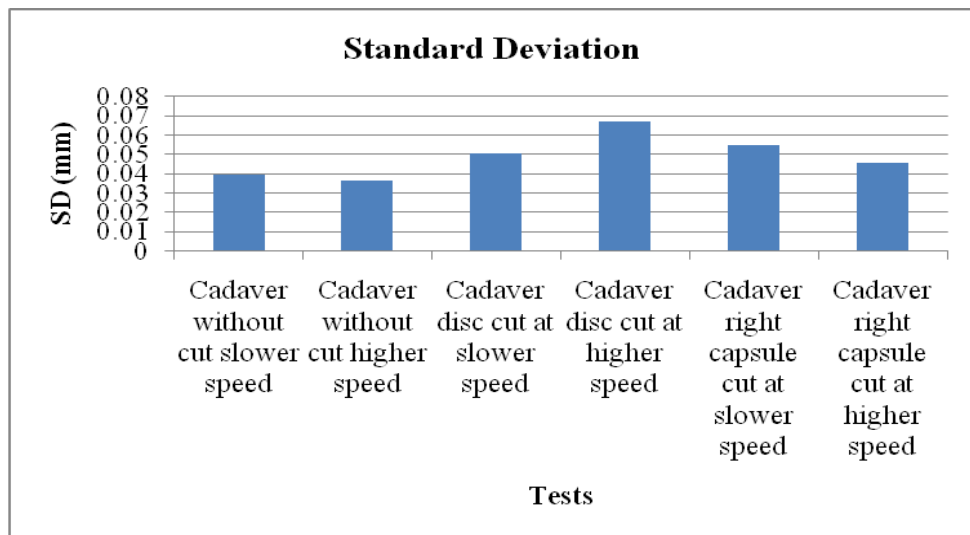


Figure 5. 96 Standard Deviation for Tests

Although SD shows some increase in value for the disc cut and tested at higher speed, it remains more or less uniform throughout the tests.

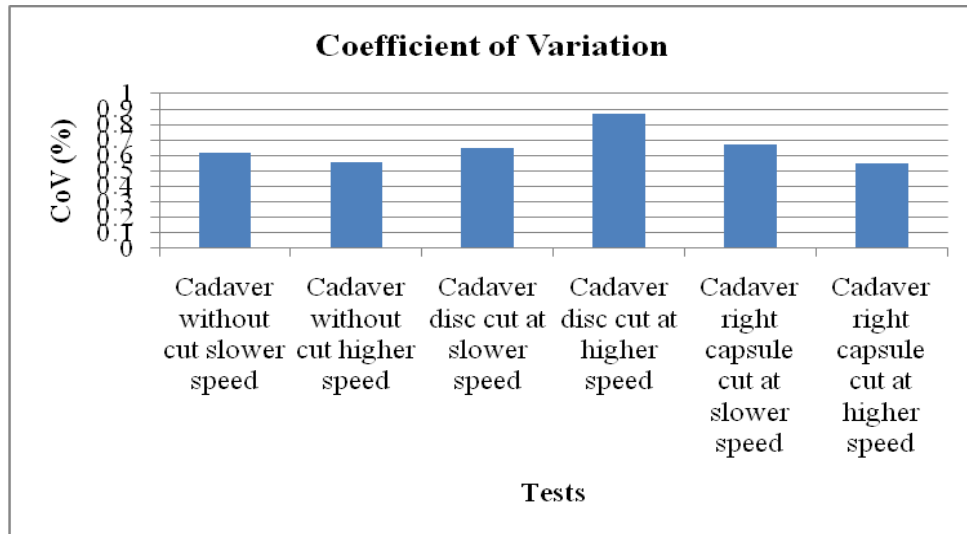


Figure 5. 97 Coefficient of Variation for Tests

Similarly to the SD graph, CV shows maximum variability for the cadaver tested at the higher speed and injured at the disc. However, the values are more or less uniform for all other tests.

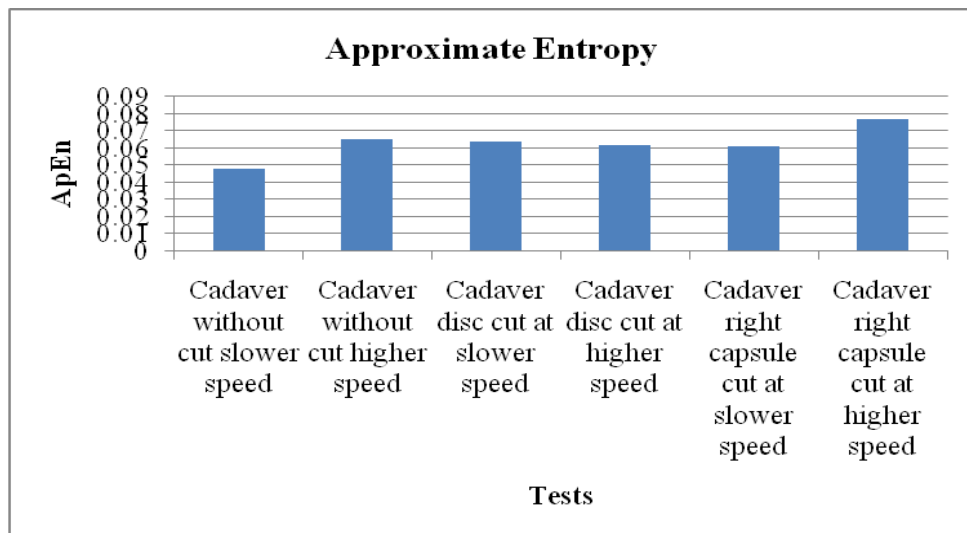


Figure 5. 98 Approximate Entropy for Tests

As seen from the linear techniques, ApEn shows a similar trend. It shows a small rise and then the values remain constant thereafter. Its values are more or less uniform across the tests irrespective of speed and injuries made to the specimen.

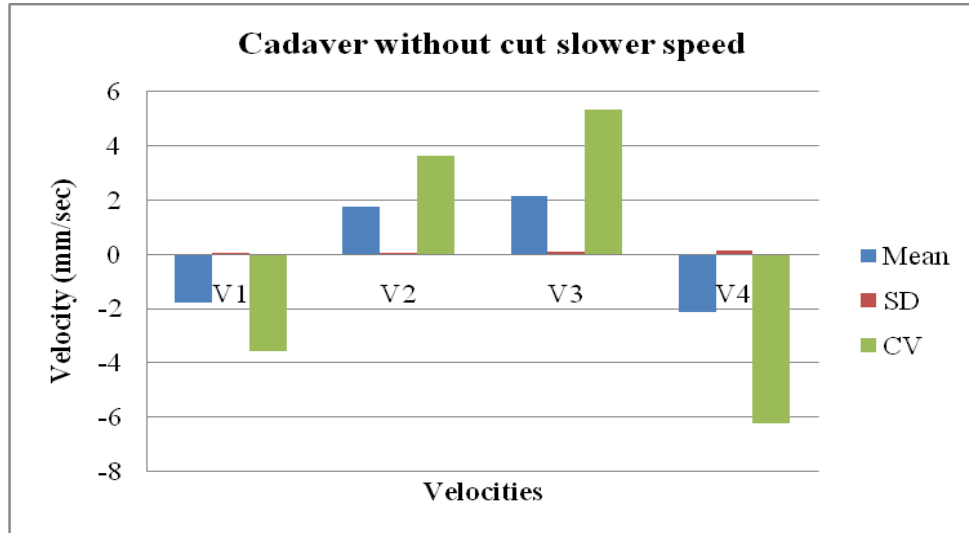


Figure 5. 99 Variations in Velocity

The mean and the SD of velocity remain uniform across four sections, while CV is maximum for backward-to-neutral movement.

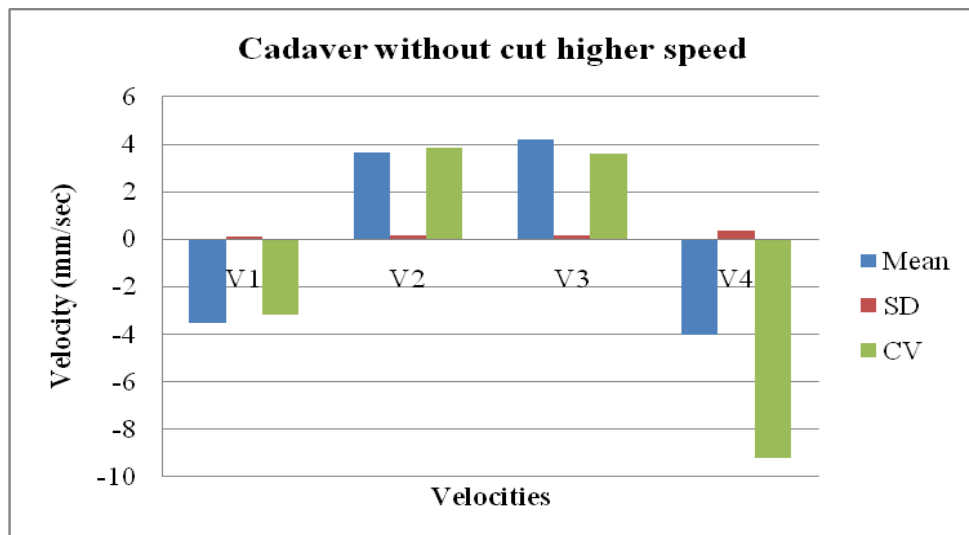


Figure 5. 100 Variations in Velocity



Similarly to the previous test, the mean and SD of velocity remains uniform throughout the tests, while CV is maximum for backward-to-neutral movement.

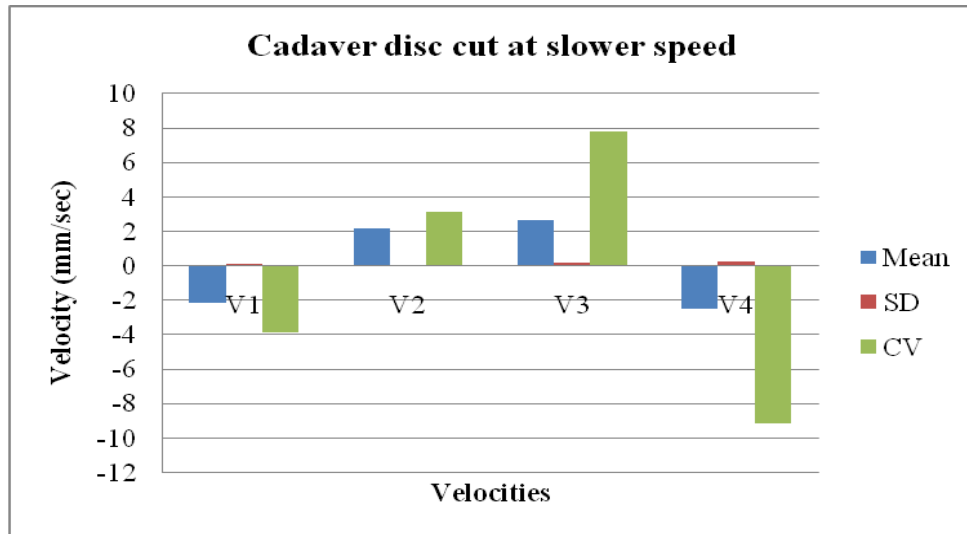


Figure 5. 101 Variations in Velocity

Figure 5.101 shows uniform values for mean and SD throughout the test, while the CV is maximum for backward-to-neutral motion of L4-L5 level.

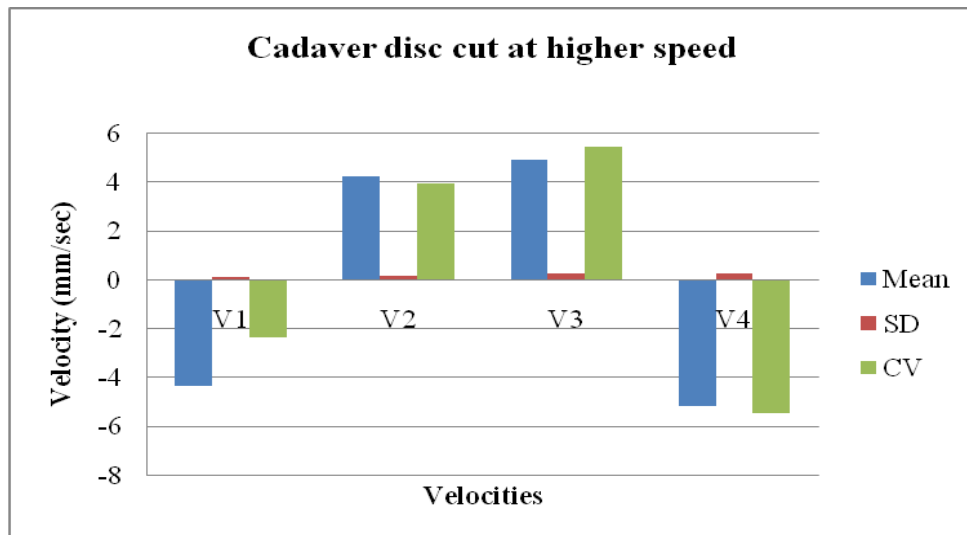


Figure 5. 102 Variations in Velocity

As above, the mean and SD are uniform throughout the tests, while CV of velocity is higher for backward-to-neutral movement.

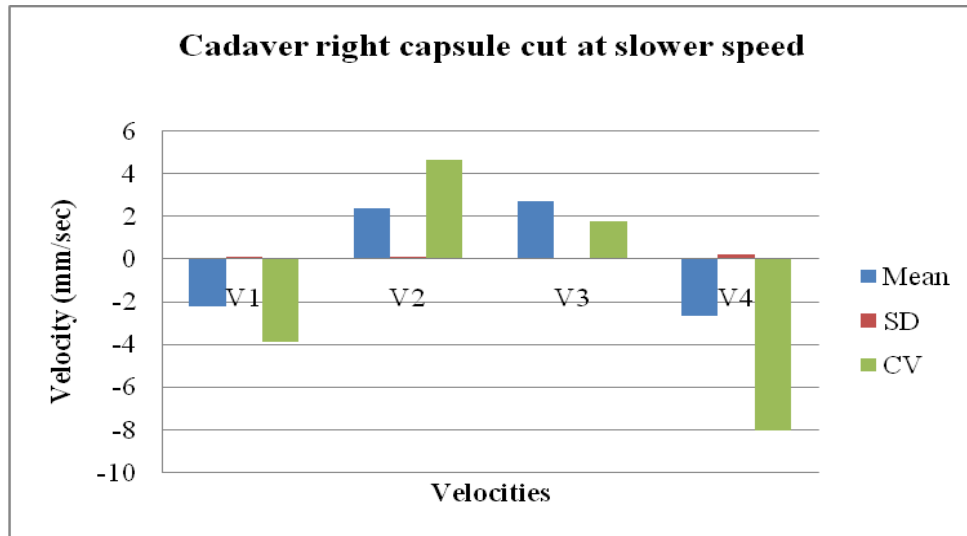


Figure 5. 103 Variations in Velocity

Even after injuring the specimen at several positions, the mean and SD of velocity remain uniform across the tests, while CV is greater for backward-to-neutral position.

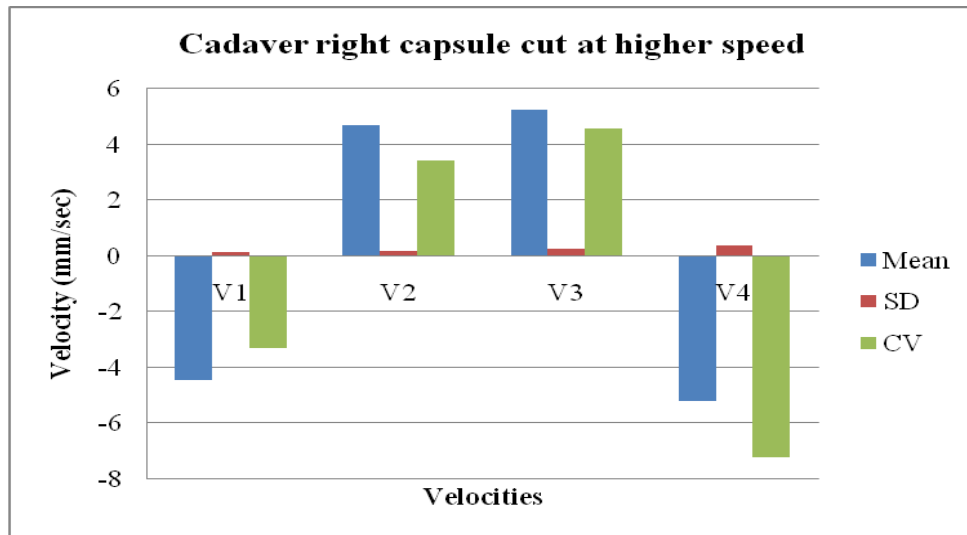


Figure 5. 104 Variations in Velocity

Figure 5.104 shows similar trends as before. The mean and SD are uniform throughout, while CV is maximum for backward-to-neutral movement.

For this particular cadaveric test, the linear and nonlinear techniques show good correlation with each other. Their values are more or less uniform throughout the test irrespective of the injuries made and the speed of the flexion-extension.

## **6. Discussions**

Musculoskeletal pathologies and injuries may result in non-periodic kinematic and kinetic quantities due to increase in instability. Studies show that both linear and nonlinear techniques have been applied toward understanding this condition in various movement analyses. Although spinal stability has been estimated using linear and nonlinear techniques, few previous studies aimed to compare these quantities for the control of stability during dynamic trunk movements in human subjects and cadaveric specimens. The present study is one of the few studies that were conducted using linear and nonlinear techniques.

The phase plane plot is a tool that provides a perspective on some of the phenomena that can be found in nonlinear systems. There are many phenomena that are peculiar to nonlinear systems, and these plots can be helpful to understanding and visualizing what might happen in a nonlinear system. In this study, these plots provide information regarding how flexion-extension time series data were organized within a state space. Results show that they can distinguish between the periodic and chaotic movements, and can be used as a reference to determine variability involved in human movements. Although these plots are useful, they do not quantify the variability and fail to reveal the underlying dynamic structure of the system. It is difficult to distinguish between two subtests with almost the same variability, and the interpretation of results is very subjective. These findings are in agreement with previous studies (Yamada, 1995;

Buzzi et al., 2003) that used phase plane plots to analyze human movements. Those studies concluded that although phase plane plots were effective in distinguishing the human motion under analysis, linear and nonlinear techniques were important to completely understand and quantify these motions.

In order to quantify motor variability during lumbar flexion-extension movement, stability was examined. Stability is defined as the sensitivity of the system to small perturbations (Dingwell and Cusumano, 2000). If motor variability is related to stability, then the increased variability should result in increased instability (Buzzi et al, 2003). Stability can be estimated using linear and nonlinear tools.

In case of human subject testing, the traditional linear measures of variability, which generally provide estimates of the average magnitude of variations across the subtests, demonstrate significant differences among the subtests. However, from these results we cannot conclude that the starting direction and position had any effect on the stability of the lumbar spine. The linear methods for a particular subject subtest do not correlate well with each other. For example, the mean graph diagram for the first subject shows minimum variability for the RD subtest, while the variability was lower for the RC subtest in case of standard deviation and coefficient of variation. Moreover, from these results we cannot distinguish between inherent variability and increases in noise within the system. This observation is also supported by previous studies in human movement analysis in which linear measure failed to reveal the underlying structure of the human motion under analysis. Specifically, Dingwell et al. (2001) found that traditional measures of variability poorly predicted the stability in human movement analysis as compared to nonlinear techniques. Buzzi et al. (2003) concluded that traditional linear

tools cannot distinguish between inherent variability and increases in noise within the system.

Estimating the nonlinear dynamics of the system may help us to understand changes in actual motor control mechanisms that result from change in starting position and direction. The nonlinear analysis depicts an increase in musculoskeletal stability as the complexity of the system decreases with the subtests. The ApEn values, irrespective of starting directions and position, increase for first couple of subtests and then show a gradual decline for most of the subjects. This may be due to the adaptation of the human body system to the flexion-extension tasks as the test progressed. During the final stages of the test, subjects may have discovered strategies for stable trunk movement. Furthermore, the ApEn and linear techniques do not correlate. This conclusion is also supported by previous studies using linear and nonlinear techniques to quantify variability. Specifically, Vaillancourt and colleagues (2001) used standard deviation and ApEn to quantify regularity of tremor in healthy and Parkinson's disease patients. The result showed standard deviation values were very similar across the healthy subjects and the Parkinson's subjects. However, the ApEn values differed significantly and the authors were able to distinguish between the two groups based on the complexity in the system. In another study (Slifkin and Newell, 2000), determining the effect of increases in continuous isometric force production on the variability of motor responses, the results showed standard deviation values increased exponentially as a function of force level production. However, the ApEn values showed completely different results, revealing an inverted U-shaped function. A similar kind of study (Stergiou, 2004), used tibial accelerometer data from 17 healthy subjects who walked on motorized treadmills at 5

different speeds. The author found that the standard deviation values increased with speed, while the ApEn values showed a U-shaped function. In another study by Karmarkar et al. (2006), the authors tried to determine the relationship between ApEn and standard deviation. The results showed no correlation between ApEn and standard deviation for minimum toe clearance data of healthy elderly and healthy young group. On the basis of these studies and the present study findings it would be fair to conclude that ApEn and linear methods do not correlate well and extreme care should be taken when interpreting the results.

An in vitro biomechanical model of the lumbar spine was analyzed for variability. The cadaveric lumbar spinal unit was loaded in flexion and extension, and the anatomic elements were transected from the posterior direction. The phase plane graphs were plotted for different tests and reveal similar patterns and periodicity. The trajectories of the plot show minimal separation, showing that all the tests exhibited similar variability. The incisions at various positions and speeds had very little effect on intervertebral movement of cadaveric spine. These results are also conformed from the linear and nonlinear analysis, as their values are similar throughout the tests. Several factors may contribute to this lack of variation in observed intervertebral variability. First, the use of an electric motor to control the specimen's movement may have resulted in the specimen to move with strict constrain. Second, the incision made on the capsule and disc may have minimum effect on the intervertebral stability of the cadaveric spine. The results show a slight increase in variability values as the cadaver specimen was transected at different positions and flexed at different speeds, but they are statistically insignificant. This study shows a positive correlation between linear and nonlinear techniques.

Angular velocity and acceleration charts for human subjects and cadavers were also estimated. These charts are used to understand the variations in speed as the subject or cadaveric specimen flexed and extended the lumbar spine. The angular velocity charts for the cadaveric specimen show a more or less uniform pattern. On other hand, all of the remaining charts show different patterns from which we cannot get any conclusive results.

In order to remove the unwanted contamination from the original signal, filter is used. The present study used a second-order Butterworth filter with a cut-off frequency of 10 Hz. Applying this filter to data from human subjects yielded the desired results, but the same filter failed to remove noise in the signal when applied to data from the cadaveric specimen. This may be due to the signal's low power. In order for filter to be more effective, the cut-off frequency was changed to 1 Hz.



## 7. Conclusions

The results of this study were examined from a dynamic perspective. Linear and nonlinear techniques were used to analyze and interpret the variability in human trunk movements. Results demonstrate that ApEn values computed in this study fundamentally quantify different aspects of locomotor behavior than traditional measures of variability. Mean of variability was minimum for RD subtest for all five subjects. All graphs showed initial rise then a gradual decline followed by rise revealing 'M' shape; more variability at the beginning and end part of the test. The standard deviation in human study was lower for RG subtest. SD showed higher variability in motion after and before initial and final subtests respectively. This may be due to fatigue each participant experienced as the test progressed. Similar to SD, CV values showed lower variability for first and last subtests in most of the cases. RD subtest was higher in most subjects, while RG showed lower values. On other hand in case of angular velocity graph for subtest (NF), mean of variability was higher while moving backwards. SD remained uniform for most subjects and CV was higher for second part of test (moving neutral to backward and neutral to forward). Subtest (FF) showed greater mean going backwards while SD was constant throughout. CV showed minimum variability while moving backward to neutral position. In case of subtest (FB) the mean and SD was higher for moving neutral to backward in most cases. CV had higher values for second part of test (neutral to forward and forward to neutral position). (BF) subtest showed mean was higher while moving from forward to

neutral in most cases. SD was higher initially and decreased gradually. CV on other hand was higher for neutral to backward motion and backward to neutral motion. For (BB) subtest mean was seen to be higher for second part of the test (i.e. movement from neutral to forward and forward to neutral). In contrast to that, SD and CV were seen to be on higher side for neutral to backwards and backwards to neutral movement. (NF) subtest had greater mean of variability for neutral to backward and backward to neutral movement. SD was uniform for most of the subtests. CV was higher for neutral to forward and forward to neutral movement. For (NB) subtest mean and SD were higher moving neutral to backward for most subjects. CV was higher for neutral to backward movement and backward to neutral movement.

The mean of variability for cadaver study indicated higher variability when the disc was cut. The variability increased marginally as the specimen was injured on capsule. SD and CV on other hand, showed higher variability for cadaver disc cut at higher speed and decreased gradually. These techniques failed to give good results as they did not show increase in variability as one would expect after injuring the specimen. Thus it is seen SD and CV was not the technique to understand variability in cadaveric specimen. ApEn on other hand showed increased in variability as the specimen was injured and pushed and pulled at higher speed. The angular velocity was higher for the neutral to backward and backward to neutral movements in most of the cases.

As seen from above linear and nonlinear analysis, each of them had different aspect of variability. Linear techniques were good in most cases but did not show good results in other case, while ApEn on other hand showed better results in both human and cadaveric experiments.

They concentrated on understanding how variations in these movement patterns change over time. It is proposed that because these measures specifically quantify the variability of the locomotor system, they are more relevant for examining the neuromuscular control during flexion-extension tests. Based on the results of this investigation, both linear and nonlinear measures can quantify variability during human bodily movement, but it's the nonlinear measures that provide insightful understanding of the system.

To the best of the author's knowledge this is the first study to determine the variability of sitting motions on an unstable surface using approximate entropy. Linear and nonlinear dynamic systems analyses were successfully applied to trunk flexion-extension data, which can serve as control data for further studies and understanding kinematics and kinetics of low back pain patients. This study is restricted to collecting and describing normative data on 5 healthy volunteer subjects. Such information can be useful in establishing the baseline data on the stability of the lumbar spine on healthy subjects. We need to gather more data on several healthy volunteer subjects with different age, gender, race, and ethnicity to establish a database on the variability of healthy population. Further research should incorporate other nonlinear measures to understand the influence of direction, speed, etc., during flexion-extension tests on the human lumbar spine. Future research should undertake in quantifying the variability in low back pain patients and changes in these as a function of low back pain treatments.

## References

1. eMedicine Mechanical Low Back Pain Hills, Everett C. MD Penn State Hershey Rehabilitation Hospital Nov 2009.  
<http://emedicine.medscape.com/article/310353-overview>
2. Luo, X., Pietrobon, R., Sun, S.X., Liu, G.G. & Hey, L. 2004 “Estimates and patterns of direct health care expenditures among individuals with back pain in the United States.” *Spine*, 29 (1):79-86.
3. Andersson, G.B. 1999. “Epidemiological features of chronic low-back pain.” *Lancet*, 354 (9178):581-5.
4. Hoogendoorn, W.E., van Poppel, M.N., Bongers, P.M., Koes, B.W., & Bouter, L.M. 2000. “Systematic review of psychosocial factors at work and private life as risk factors for back pain.” *Spine*, 25 (16):2114-25.
5. Hartvigsen J., Lings S., Leboeuf-Yde C., & Bakketeig L. 2003. “Psychosocial factors at work in relation to low back pain and consequences of low back pain; a systematic, critical review of prospective cohort studies” *Occupational Environmental Medicine*, 61 (1): e2.
6. Mulholland, R.C. 2008. “The myth of lumbar instability: the importance of abnormal loading as a cause of low back pain.” *European Spine Journal*, 17:619–625.
7. Melloh M., Elfering A., Egli Presland C., Roeder C., Barz T., Rolli Salathe C., Tamcan O., Mueller U., & Theis J.C. 2009. “Identification of prognostic

- factors for chronicity in patients with low back pain: a review of screening instruments.” *International Orthopaedics*, 33 (2): 301–313.
8. Bergman, S. 2007. “Management of musculoskeletal pain.” *Best Practice & Research Clinical Rheumatology*, 21 (1): 153-166.
  9. Papadakis, N.C., Christakis, D.G., Tzagarakis, G.N., Chlouverakis, G.I., Kampanis, N.A., Stergiopoulos, K.N., & Katonis, P.G. 2009. “Gait variability measurements in lumbar spinal stenosis patients: part A. Comparison with healthy subjects.” *Physiological Measurement*, 30: 1171–1186.
  10. Hausdorff, J.M. 2007. “Gait dynamics, fractals, and falls: Finding meaning in the stride-to-stride fluctuations of human walking.” *Human Movement Science*, 26:555–589.
  11. Goldberger, A.L., Amaral, L., Hausdorff, J.M., Ivanov, P., Peng, C.K. & Stanley, H.E. 2002 “Fractal dynamics in physiology: Alterations with disease and aging.” *Proceedings of the National Academy of Sciences*, 99:2466–2472.
  12. Ho, K.K., Moody, G.B., Peng, C.K., Mietus, J.E., Larson, M.G. & Levy, D. 1997. “Predicting survival in heart failure case and control subjects by use of fully automated methods for deriving nonlinear and conventional indices of heart rate dynamics.” *Circulation*, 96:842–848.
  13. Hausdorff, J.M., Herman, T., Baltadjieva, R., Gurevich, T., & Giladi, N. 2003. “Balance and gait in older adults with systemic hypertension.” *American Journal of Cardiology*, 91:643–645.
  14. Stergiou, N. 2004. “Innovative Analysis of Human Movement.” *Human Kinetics*.

15. Fitzgerald, G.K., Wynveen, K.J., Rheault, W. & Rothchild, B. 1983. "Objective assessment with establishment of normal values for lumbar spinal range of motion." *Physical Therapy*, 63:1776-1781.
16. Buzzi, U.H., Stergiou, N., Kurz, M.J., Hageman, P.A., & Heidel, J. 2003. "Nonlinear dynamics indicates aging affects variability during gait." *Clinical Biomechanics*, 18:435–443.
17. Trudelle-Jackson, E., Fleisher, L.A., Borman, N., Morrow, J.R., & Frierson, G.M. 2010. "Lumbar spine flexion and extension extremes of motion in women of different age and racial groups" *Spine*, 35 (16):1539–1544.
18. Van Herp, G., Rowe, P., Salter, P. & Paul, J.P. 2000. "Three-dimensional lumbar spinal kinematics: A study of range of movement in 100 healthy subjects aged 20 to 60+ years." *Rheumatology*, 39:1337-1340.
19. Hausdorff, J.M., Zemani, L., Peng, C.K., & Goldeberger, A.L. 1999. "Maturation of gait dynamics: stride-to-stride variability and its temporal organization in children." *Journal of Applied Physiology*, 36(3): 1040–1047.
20. Dingwell, J.B., Cusumano, J.P., Cavanagh, P.R., & Sternad, D. 2001 "Local dynamic stability versus kinematic variability of continuous overground and treadmill walking." *Journal of Biomechanical Engineering*, 123:27-32.
21. Garcia-Alsina, J., Garcia Almazan, C., Moranta Mesquida, J., & Pleguezuelos Cobo, E. 2005. "Angular position, range of motion and velocity of arm elevation: A study of consistency of performance." *Clinical Biomechanics*, 20: 932–938.
22. Brown, M. D., Holmes, D.C., & Heiner, A.D. 2002. "Measurement of cadaver lumbar spine motion segment stiffness." *Spine*, 27(9): 918 – 922.

23. Hitchon, P.W., Eichholz, K., Barry, C., Rubenbauer, P., Ingalhalikar, A., Nakamura, S., Follett, K., Lim, T.H., & Torner, J. 2005. "Biomechanical studies of an artificial disc implant in the human cadaveric spine." *Journal of Neurosurgery: Spine*, 2:339–343.
24. Stergiou, N., Harbourne, R.T., Cavanaugh, J.T. 2006. "Optimal movement variability: A new theoretical perspective for neurologic physical therapy." *Journal of Neurologic Physical Therapy*, 30 (3): 120-129.
25. Hadders-Algra, M. 2007. "Putative neural substrate of normal and abnormal general movements." *Neuroscience and Biobehavioral Reviews*, 31:1181–1190.
26. Karmakar, C.K., Khandoker, A.H., Begg, R.K., Palaniswami, M., & Taylor, S. 2006. "Understanding ageing effects by approximate entropy analysis of gait variability." *Conf Proc IEEE Eng Med Biol Soc*. 2007:1965-1968.
27. Khandoker, A.H., Palaniswami, M., Begg, R.K. 2008. "A comparative study on approximate entropy measure and poincaré plot indexes of minimum foot clearance variability in the elderly during walking." *Journal of NeuroEngineering and Rehabilitation*, 5:4.
28. Pincus, S. 1994 "Approximate entropy (ApEn) as a complexity measure." *Chaos*, 5(1):110-117.
29. Pincus, S. & Golberger, A.L. 1994. "Physiological time-series analysis: What does regularity quantify?" *American Journal of Physiology*, 266(4):H1643-1656.
30. Grassberger, P. & Procaccia, I. 1983. "Characterization of strange attractors." *Physical Review Letters*, 50(5):346-349.

31. Harbourne, R.T. & Stergiou, N. 2009. "Movement variability and use of nonlinear tools: Principles to Guide Physical Therapist Practice." *Physical Therapy*, 89(3): 267–282.
32. Deng, K., Moore, A.W., & Nechyba, M.C. 1997. "Learning to recognize time series: Combining ARMA models with Memory-based Learning." *Computational Intelligence in Robotics and Automation* 246–250.
33. Smith, S.W. 1999. "The Scientist and Engineer's Guide to Digital Signal Processing." <http://dspguide.com/pdfbook.htm>.
34. Wachowiak M.P., Rash G.S., Quesada P.M., & Desoky A.H. 2000. "Wavelet based noise removal for biomechanical signals: a comparative study." *IEEE Transactions on Biomedical Engineering*, 47(3):360-368.
35. Winter, D.A., Patla, A.E., Prince, F., Ishac, M., Gielo-Perczak, K. 1998. "Stiffness control of balance in quiet standing." *Journal of Neurophysiology*, 80:1211-1221.
36. Moorhouse, K.M., & Granata, K.P. 2005. "Trunk stiffness and dynamics during active extension exertions." *Journal of Biomechanics*, 38:2000–2007.
37. Lenth, R.V. 2001. "Some practical guidelines for effective sample-size determination." *The American Statistician*, 55:187-193.
38. Sekiya, N., Nagasaki, H., Ito, H., & Furuna, T. 1997. "Optimal walking in terms of variability in step length." *Journal of Orthopedic and Sports Physical Therapy*, 26(5):266-272.



39. Buzzi, U.H., Stergiou, N., Kurz, M.J., Hageman, P.A., & Heidel, J. 2003. "Nonlinear dynamics indicates aging affects variability during gait." *Clinical Biomechanics*, 18:435–443.
40. Slifkin, A.B., & Newell, K.M. 2000. "Variability and noise in continuous force production." *Journal of Motor Behavior*, 32(2): 141–150.
41. Vaillancourt, D.E., Slifkin, A.B., & Newell, K.M. 2001. "Regularity of force tremor in Parkinson's disease." *Clinical Neurophysiology*, 112:1594–1603.
42. Harbourne, R.T. & Stergiou, N. 2009. "Movement variability and the use of nonlinear tools: Principles to guide physical therapist practice." *Physical Therapy*, 89(3): 267–282.
43. Granata, K.P. & England, S.A. 2006. "Stability of dynamic trunk movement." *Spine*, 31(10):E271-276.
44. Pincus, S.M., Gladstone, I.M., Ehrenkranz, R.A. 1991. "A regularity statistic for medical data analysis." *Journal of Clinical Monitoring and Computing*, 7:335–345.
45. University of Maryland Spine Center <http://www.umm.edu/spinecenter/education/>
46. Henry Gray. 1918. "Anatomy of Human Body" <http://www.bartleby.com/107/>
47. John J. Buchanan Fay B. Horak. 2001 "Transitions in a postural task: do the recruitment and suppression of degrees of freedom stabilize posture?" *Exp Brain Res* 139:482–494
48. Jonathan B. Dingwell, Laura C. Marin. 2006. "Kinematic variability and local dynamic stability of upper body motions when walking at different speeds." *Journal of Biomechanics* 39:444–452

49. Regina T. Harbourne, Nicholas Stergiou. 2003. "Nonlinear Analysis of the Development of sitting Postural Control." *Dev Psychobiol.* 42(4):368-77
50. Pincus SM. 1990. "Approximate entropy as a measure of system complexity." *Proc. Nati. Acad. Sci.* 88: 2297-2301
51. Pincus SM. 1995. "Approximate entropy (ApEn) as a complexity measure." *Chaos* 5(1):110-117
52. Johannes D Veldhuis and Steven M Pincus. 1998. "Orderliness of hormone release patterns: a complementary measure to conventional pulsatile and circadian analyses." *European Journal of Endocrinology* 138: 358–362
53. Justin J Kavanagh. 2009. "Lower trunk motion and speed-dependence during walking." *Journal of NeuroEngineering and Rehabilitation* 6: 9
54. Kaplan, D.T., Glass, L., 1995. "Understanding Nonlinear Dynamics." *Springer-Verlag, New York, NY.*
55. OrthoIndy, (image on internet)  
Available from: <http://www.indyspinemd.com/Normal/index.asp>
56. Inition, (image on internet)  
Available from: <http://www.inition.co.uk>
57. Liberty user manual, 2008 (image on internet)  
Available from:  
[http://www.polhemus.com/polhemus\\_editor/assets/LIBERTY%20Rev%20F%20URM03PH156.pdf](http://www.polhemus.com/polhemus_editor/assets/LIBERTY%20Rev%20F%20URM03PH156.pdf)

## Appendices

### A. Technical Specifications

#### A.1 Liberty Polhemus Specifications



Figure A. 1 Liberty Polhemus Unit

Table A. 1 Technical Specification of Polhemus Unit

Degrees-of-Freedom	6DOF
Number of Sensors	1-16
Update Rate	240 Hz per sensor)
Static Accuracy Position	0.03in
Static Accuracy Orientation	0.15° RMS
Latency	3.5ms
Resolution Position at 30cm range	0.00015in 0.0004cm
Resolution Orientation	0.0012°
Range from Standard TX2 Source	Up to 5 feet or 1.52 meters

Extended Range Source	Up to 15 feet or 4.6 meters
Interface	RS-232 or USB (both included)
Host OS compatability	GUI/SDK 2000/XP

## A.2 Magnetic Source

The source is the device which produces the electromagnetic field and is normally the reference for the position and orientation measurements of the sensors. It is usually mounted in a fixed position to a non-metallic surface or stand that is located in close proximity to the sensors. The standard source is the 2" cube.

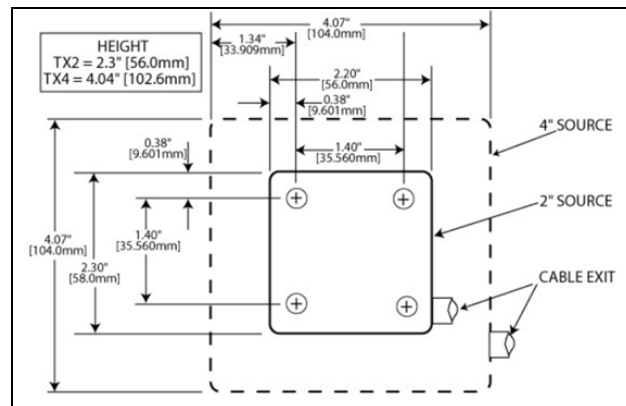


Figure A. 2 Magnetic Source Diagram

## A.3 Sensors

The sensor is the smaller device whose position and orientation is measured relative to the source. The sensor is dimensionally shown in Figure A.3, including the position of the electrical center. The sensor package provides two mounting holes for #4 nylon screws in the event that sensor mounting is required.

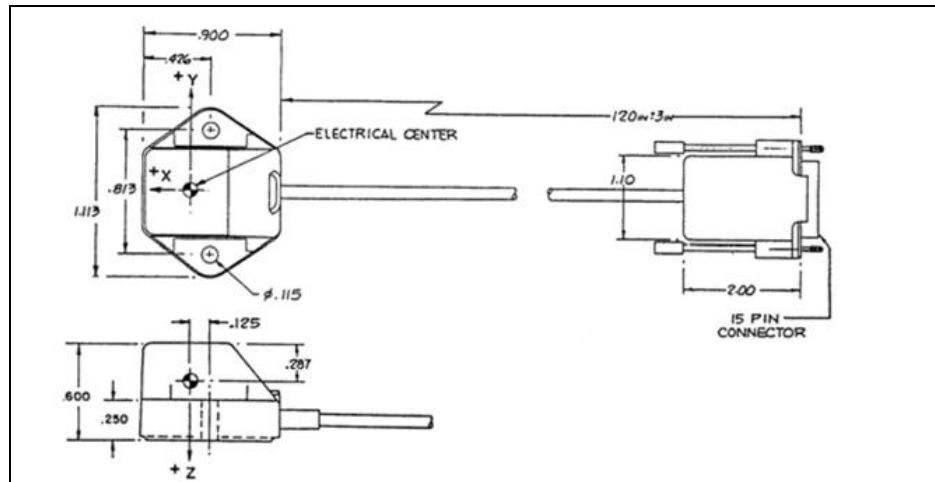


Figure A. 3 Sensor Diagram

Table A. 2 Technical Specifications of Optotrak 3020 Unit

#### A.4 Optotrak 3020

Dimensions	1110 mm × 315 mm × 215 mm
Weight	40 kg
Bracket Weight	5 kg
Power Requirements	100/120 VAC, 60 Hz or 220/240 VAC, 50 Hz
Maximum Marker Rate	3500 Hz
Frame Rate	(raw) 750 Hz ( 3D) 450 Hz (3D with optional hardware) 750 Hz (6D with optional hardware) 145 Hz
RMS Accuracy at 2.25 m distance	0.1 mm for x, y coordinates 0.15 mm for z coordinate
3-D Resolution at 2.25 m distance	0.01 mm

Sensor Resolution	1:200,000
Supported Platforms	
Pentium Class PC	MS Windows 95/98/NT/2000
SGI (requires SCSI)	Irix 5.x or higher (o32-bit), Irix 6.x (n32-bit, n64-bit)
HP (requires SCSI)	HP-UX 9.x or higher
SUN (requires SCSI)	Solaris 2.x or higher
Linux support also available for Linux 2.x or higher	

Table A. 3 Technical Specifications of System Control Unit

#### A.5 System Control Unit (SCU)

Dimensions	297mm ×236mm ×91 mm
Weight	3.4 kg
Power Requirements	100-240 VAC 50/60 Hz, 1.25 A
Connections for Host computer	PCI card, SCSI Ethernet
Number of Strober Ports	3

## A.6 Optotrak Data Acquisition Unit II

The Optotrak Data Acquisition Unit II (ODAU II) is an optional component to the Optotrak system. The ODAU II allows you to collect analog and digital data that is synchronized with the Optotrak position data. Pre-conditioned signals from devices such as EMG sensors, force plates, accelerometers, and strain gauges may be viewed in real-time and stored to data files for later analysis. You have feedback control to the subject/object of study through 8 digital I/O channels or 2 analog output channels.



Figure A. 4 Optotrak Data Acquisition Unit II

## B. MATLAB Programs

### B.1 MATLAB Program for Filtering Data

```
clear all;
clc;
A=xlsread('Timeseries')/1000;
framerate=100;
Q=((length(A)/framerate));
W=(Q/length(A));
t=(0:W:Q-W)';
[m,w]=butter(1,10/50);
disp=filtfilt(m,w,A);
f = fittype('smoothingspline');
fit1 = fit(t,disp,f);
[vel,accel] = differentiate(fit1,t);
figure(1)
hold on;
plot(t,disp,'r');
plot(t,vel,'g');
plot(t,accel,'b');
legend('Displacement(deg)','Velocity(deg/sec)','Acceleration(deg/sec2)')
xlabel('Time(sec)')
ylabel('Disp, Vel, Acc')
figure(2)
hold on
plot(disp,vel)
xlabel('Displacement')
ylabel('Velocity')
figure(3)
hold on
plot3(disp,vel,accel)
xlabel('Displacement')
ylabel('Velocity')
zlabel('Acceleration')
```



## B.2 MATLAB Program to Calculate Range of Motion and Velocity

```
clear all
clc
A=xlsread('smooth',-1);
plot(A)
[x,y]=ginput(45);
for i=1:length(x)-1
    T(i)=x(i+1)-x(i);
    R(i)=((y(i+1))-y(i)));
    len(i)=sqrt(1+(R(i)/T(i))^2);
    clength(i)=((len(i)*y(i+1))-(len(i)*y(i)));
end
curvelength=((clength)');
ROM=(curvelength(1:2:end));
for k=1:length(T)
    Time(k)=T(k)/120;
end
for e=1:length(x)-1
    Velo(e)=curvelength(e)/Time(e);
end
Velocity=Velo';
for y=2:length(x)-1
    vel(y)=(Velo(y)-Velo(y-1));

end
vel(1)=Velo(1);
for u=1:length(x)-1
    Accel(u)=vel(u)/Time(u);
end
Acceleration=Accel';
```

### B.3 MATLAB Program to Calculate Approximate Entropy (ApEn)

```
clear all;
clc;
a=0;
S=xlsread('Timeseries');
r=2;
g=5;
N=length(S);
for m=g:g+1
a=a+1;
pen=N-m+1;
[row, cols] = size(S);
p = zeros(cols-(m-1), m);
for i = 1:cols -(m-1);
    p(i, :) = S(i:i+(m-1));
end
P = num2cell(p, 2);
Y=cell((length(P))*(length(P)),1);
n=0;
for j=1:size(P);
for k=1:size(P);
    for s=n;
        n=s+1;
        Y{n}=P{j}-P{k};
    end
end
end
e=0;
u=0;
while u<((length(P)*length(P))-(length(P)-1));
v=u+1;
count=0;
e=e+1;
for u=v:v+(length(P)-1);
if (abs(Y{u})<r);
    B{u}=Y{u};
    if prod(B{u})<1;
        count=count+1;
    end
end
end



end
C(e)=count/pen;
end
Cal(a)=mean(C);
```

```
clearvars -except Cal a N S r  
end
```

```
ApEn=log(Cal(1)/Cal(2))
```

## C. Documentation

### C1. Auburn IRB

<i>Office of Research Compliance 307 Sanford Hall Auburn University, AL 36849</i>	 <b>AUBURN</b> UNIVERSITY	<i>Telephone: 334-844-5966 Fax: 334-844-4391 lrubac@auburn.edu</i>
March 16, 2010		
MEMORANDUM TO:	Dr. P.K. Raju Department of Mechanical Engineering	
PROTOCOL TITLE:	"Development of Protocols for Biomechanical Tests and Measurement of Spinal Manipulative Procedures for Training of Research Personnel"	
IRB AUTHORIZATION NO.:	09-344 MR 1001	
APPROVAL DATE:	January 20, 2010	
EXPIRATION DATE:	January 19, 2011	
<p>The referenced protocol was approved "Minimum Risk" at the IRB Meeting on January 20, 2010, pending revisions. (Final revisions were received on March 4, 2010.) Please reference the IRB authorization number in any correspondence regarding your project.</p> <p>Please remember that any anticipated change in the approved procedures must be submitted to and approved by the IRB prior to implementation of the planned activity. Any unanticipated problems involving risk to subjects or others require immediate suspension of the activity and an immediate written report to the IRB.</p> <p>If you will be unable to file a Final Report on your project before January 19, 2011, you must submit a request for an extension of approval to the IRB no later than January 5, 2011 to be included on the agenda for the January 2011 IRB meeting. If your IRB authorization expires and/or you have not received written notice that a request for an extension has been approved prior to January 19, 2011, you must suspend the project immediately and contact the Office of Research Compliance.</p> <p><u>A Final Report will be required to close your IRB project file.</u></p> <p>If you have any questions concerning this Board action, please contact the Office of Research Compliance.</p>		
<p>Sincerely,</p>  Kathy Jo Ellison, RN, DSN, CIP Chair of the Institutional Review Board for the Use of Human Subjects in Research		
cc: Dr. Jeffrey Suhling		

## C2. Biomechanics Test Log Form

<b>BIOMECHANICS TEST LOG</b>	<b>OFFICE USE ONLY</b>
Verify1: _____ / ____ / 20__	Project ID: D2P3                      Date: ____ / ____ / 20__
	Participant ID: _____      Web Log Complete: <input type="checkbox"/>
	User ID: _____                File: ODM

Do you have any non-removable metals either in or on your body? .....  No     Yes

---

**Postural Sway**

Foot Position:.... <input type="checkbox"/> 1 <input type="checkbox"/> 2 <input type="checkbox"/> 3 <input type="checkbox"/> 4	<u>PRE</u>	<u>PST</u>
Plate 1 (P1) Performed? .....	<input type="checkbox"/> No <input type="checkbox"/> Yes	<input type="checkbox"/> No <input type="checkbox"/> Yes
Foam 1 (F1) Performed? .....	<input type="checkbox"/> No <input type="checkbox"/> Yes	<input type="checkbox"/> No <input type="checkbox"/> Yes
Plate 2 (P2) Performed? .....	<input type="checkbox"/> No <input type="checkbox"/> Yes	<input type="checkbox"/> No <input type="checkbox"/> Yes
Foam 2 (F2) Performed? .....	<input type="checkbox"/> No <input type="checkbox"/> Yes	<input type="checkbox"/> No <input type="checkbox"/> Yes
Foot Length-Plate:.....	Right: ____ cm	Right: ____ cm
	Left: ____ cm	Left: ____ cm
Foot Flare Angles-Plate:.....	Right: ____ °	Right: ____ °
	Left: ____ °	Left: ____ °
Foot Flare Angles-Foam:.....	Right: ____ °	Right: ____ °
	Left: ____ °	Left: ____ °

Notes:

Biomechanics Test Log.doc
20 May 2009

**Repositioning**

Sensor Height (from seat to sensor bottom): S1: \_\_\_\_\_ L3: \_\_\_\_\_ L1: \_\_\_\_\_ T1: \_\_\_\_\_

Body Measurements: Chair Height: .....  0  1  2  3  4  5

Riser: .....  0  1  2  3  4

Tendon to Board: \_\_\_\_\_ cm

Participant performed:  1 Both  2 Forward Only (Backward Pain)  3 Backward Only (Forward Pain)  4 None

Seq	Dir		PRE	PST
RA	<u>1</u> Range (NF-R) [All] .....	Performed?.....	<input type="checkbox"/> 1 No <input type="checkbox"/> 2 Yes	<input type="checkbox"/> 1 No <input type="checkbox"/> 2 Yes
RB	FF (Both & Forw) .....	Performed?.....	<input type="checkbox"/> 1 No <input type="checkbox"/> 2 Yes	<input type="checkbox"/> 1 No <input type="checkbox"/> 2 Yes
RC	FB (Both & Forw) .....	Performed?.....	<input type="checkbox"/> 1 No <input type="checkbox"/> 2 Yes	<input type="checkbox"/> 1 No <input type="checkbox"/> 2 Yes
RD	BF (Both & Backw) .....	Performed?.....	<input type="checkbox"/> 1 No <input type="checkbox"/> 2 Yes	<input type="checkbox"/> 1 No <input type="checkbox"/> 2 Yes
RE	BB (Both & Backw) .....	Performed?.....	<input type="checkbox"/> 1 No <input type="checkbox"/> 2 Yes	<input type="checkbox"/> 1 No <input type="checkbox"/> 2 Yes
RF	NF (Both & Forw) .....	Performed?.....	<input type="checkbox"/> 1 No <input type="checkbox"/> 2 Yes	<input type="checkbox"/> 1 No <input type="checkbox"/> 2 Yes
RG	NB (Both & Backw) .....	Performed?.....	<input type="checkbox"/> 1 No <input type="checkbox"/> 2 Yes	<input type="checkbox"/> 1 No <input type="checkbox"/> 2 Yes

Notes:

**Sudden Load**

Drop Distance: \_\_\_\_\_ cm Pulley Height: \_\_\_\_\_ cm Floor to Harness: \_\_\_\_\_ cm

Floor to ASIS: \_\_\_\_\_ cm Floor to L3: \_\_\_\_\_ cm

SL (U1) Performed? .....  1 No  2 Yes |  1 No  2 Yes


Notes:

**EMG Normalization**

EN Performed? .....  1 No  2 Yes |  1 No  2 Yes

Notes:

### C3. Accelerometer Calibration Sheet

<b>Certificate of Conformance</b>	 2.00	<b>calibration date</b> <b>04/08/2005</b>	
<b>Calibration Data: Room Temperature</b>			
	<b>X Axis</b>	<b>Y Axis</b>	<b>Z Axis</b>
<b>Zero-G Voltage</b>	2.480	2.500	2.410
<b>Sensitivity</b>	0.099	0.105	0.105
<b>Part Number</b>	CXL10HF3		
<b>Serial Number</b>	5010875		
<b>Options:</b>	AC Coupled, min freq: 0.3 Hz		
	<b>Wiring Diagram:</b>		
	<b>Color</b>	<b>Pin</b>	<b>Function</b>
	Red	1	6 - 30 Vdc
	Black	2	Ground
	White	3	X-axis
	Yellow	4	Y-axis
	Green	5	Z-axis

Thank you for choosing a Crossbow sensor. This worksheet is designed to help you get started. Refer to the product data sheet for more complete information.

**Definitions**  
**Zero-G Voltage** : This number is the output voltage of the sensor with zero applied acceleration measured at the factory on the day of the calibration.  
**Sensitivity** : This number is the sensor's sensitivity in Volts per G.

**Calibration**  
 The simplest method of field calibration is to record the sensor's output voltage when exposed to the Earth's gravitational field. Expose the sensor to +1G to obtain a more positive reading than the zero-G voltage. Expose the sensor to -1G to obtain a more negative reading than the zero-G voltage. The offset is defined as the average of the +1G and -1G voltages. The sensitivity in Volts per G is one-half the difference of the +1G and -1G voltages. Please note that this technique only works on DC coupled sensors. If your sensor is AC coupled, a shaker is required for proper calibration.

**Technical Support**  
 For further technical assistance, contact Crossbow Technology.

Crossbow Technology, Inc.  
 41 East Daggett Drive  
 San Jose, CA 95134

Phone : 408.965.3300  
 Fax : 408.324.4840  
 URL : <http://www.xbow.com>  
 Email : [info@xbow.com](mailto:info@xbow.com)